

University of Kasdi Merbah Ouargla
Faculty of Hydrocarbons, Renewable Energy, Earth, and Universe
Science
Department of Hydrocarbons Production



dissertation

To obtain the master's degree
Option: Professional production

Presented by:

BAHLALI Aya

YAGOUB Daka

Theme

Applying silica nanoparticles and nanoclay in nanoflooding to improve the efficiency of enhanced oil recovery(EOR): experimental investigation

Date of graduation:26/06/2024

Jury Members :

Mr. khelifa Cherif	MA (A)	President	UKM Ouargla
Ms. BOUFADES Djamila	MC (A)	Examiner	UKM Ouargla
Mr. CHETTI DJAMEL Eddine	MA (A)	Supervisor	UKM Ouargla
Ms. Mahdadi Naouia	MC (A)	Co-Supervisor	UKM Ouargla

2023/2024

بِسْمِ اللّٰهِ الرَّحْمٰنِ الرَّحِیْمِ

شكر و عرفان

إلى جميع الأساتذة الكرام والمشرفين والإداريين الأعزاء في مسيرتي الجامعية
بمزيد من الامتنان والاحترام، أود أن أعبر عن شكري العميق وامتناني البالغ لكل من ساهم وشارك في رحلتي الأكاديمية. كانت هذه الرحلة
ملينة بالتحديات والإنجازات، ولكن بفضل دعمكم اللا متناهي وتوجيهاتكم الحكيمة، استطعت تحقيق الكثير من النجاحات والتطور.
أريد أن أخص بالذكر الأساتذة:

-الأستاذ لبطاحي, الأستاذ عجو زكرياء, الأستاذة شاوش وفاء, الأستاذة بوفادس جميلة
كل منكم كان مصدر إلهام لي، وقدمتم لي التوجيه والنصائح القيمة التي ساعدتني على التفوق في مساري . بفضل تفانيكم ومساعدتكم،
أصبحت أقدر على تحقيق أحلامي وتحقيق أهدافي.
وإلى مشرفي الأستاذ شطي جمال الدين ، أود أن أعبر عن امتناني العميق لكما على دعمكم اللا متناهي وتوجيهاتكم الحكيمة خلال إعدادي
لمذكرة التخرج. لقد كانت توجيهاتكم ونصائحكم القيمة عاملاً رئيسياً في نجاح هذا العمل البحثي.
وأخيراً، لا يمكنني نسيان الشكر للسيد سليم، الإداري الخاص بشؤون الطلبة، على حسن استقباله ومساعدته المستمرة طوال فترة
دراستي.
أتم جميعاً رمز للتفاني والاحترافية، ولقد أثرتم بشكل كبير في حياتي الأكاديمية والمهنية. أتمنى لكم دوام النجاح والتقدم في مسيرتكم المهنية
والأكاديمية.
مع خالص الشكر والامتنان،

إهداء

قال تعالى (قل اعملوا فسيرى الله عملكم ورسوله و المؤمنون)

بسم الله الرحيم الرحمان الرحيم و الصلاة و السلام على اشرف المرسلين إلهي لا يطيب الليل إلا بشكرك ولا يطيب النهار إلا بطاعتك ..

ولا تطيب اللحظات إلا بذكرك..ولا تطيب الآخرة إلا بعفوك ..

ولا تطيب الجنة إلا برؤيتك، الحمد لله الذي بنعمته تم الصالحات ،الحمد لله الذي بنعمته وفقنا لانجاز هذا العمل العلمي المتواضع

إلى من بلغ الرسالة و أدى الأمانة ..ونصح الأمة ..إلى نبي الرحمة و نور العالمين سيدنا محمد صلى الله عليه و سلم

إلى صاحبي الفضل العظيم امي الحبيبة و والدي العزيز

إلى اخي رائد او كما اسميه بطلي الصغير الذي كانت صورته تأتي بين عيني كلما اتابني شعور بالفشل فكان حافزي لان لا استسلم

إلى أخواتي الرائعات كل باسمها

إلى كل افراد عائلتي و اخص فيهم ذلك الشخص الغالي العم نبيل حفظه الله ،ولا انسى اصدقائي و على رأسهم زميلتي في هذا العمل يعقوب ذكاء و

ايضا زملائي في الخبر ؛زحاف معمر ، بلحلو ناريمان ،بوشوارب ملاك و شيخي نجوى

إلى الاستاذين الشابين اللذان حلا محل الاخوة ؛شاوش وفاء و عجو زكرياء لمساندتهما و دعمهما المستمر

و إلى الزميل بلعيد ياسين و لا انسى اي شخص كان نقطة ايجابية في حياتي و قبل ان اهدي لنفسي التي قاومت في سبيل الوصول اقدم اهداء

خاصا لأطفال،نساء،شيوخ و رجال فلسطين الاحرار اتم في قلوبنا.

آية

إهداء

(و آخر دعواهم أن الحمد لله رب العالمين)

الحمد لله الذي ما تم حمد ولا ختم سعي الا بفضله

من قال "أنا لها" نالها وأنا لها و ان أبت رغبا عنها أتيت بها، إنتهت رحلتي الجامعية بجلوها و مزها، انا اليوم انظر الى حلم طال انتظاره و أصبح واقعا افتخر به، لم يكن الحلم قريبا و لا النجاح سهلا، لكنني فعلتها، ولم أكن لافعل لولا فضل الله فالحمد لله الذي يسر البدايات و بلغنا النهايات الحمد لله عند البدء و الختام

إلى الذي زين اسمي بأفضل الالتقاب، من دعمني بلا حدود و اعطاني بلا مقابل، إلى من سعى إلى راحتي و نجاحي، إلى من علمني أن الحياة كفاح سلاحها العلم و المعرفة، داعمي الاول في مسيرتي، سندي، قوتي، وملاذي بعد الله إلى فخري و اعترازي، تاج راسي أي الغالي "محمد ياسين"

إلى الصوت الذي يساعه بظمن قلبي و تسكن جوارحي الى من كافحت اياما و ليالي لتري البسمة على وجوهنا، الى من نذرت حياتها لنا فنسيت بذلك نفسها الى التي جاورت قلبها قبل ان تراني عيناها، الى التي اتلمس خطواتي برضاها الى ملاكي الطاهر، قدوتي الاول الى اعذب لفظ تلفظت به البشرية الى من هي في الحياة حياة، ينحني الحرف حبا و امتنانا اليك يا ضياء حياتي ابي الغالية "مسعودي عفاف" الحمد لله الذي اصطفاك بين البشر اما لي يا خير سند و عوض

إلى من قيل فيهم: "سنشد عضدك بأخيك" الى من كانوا حافزا لاكون الافضل اخي "محمد تقي الدين" ادامك الله ضلعا ثابتا لي و امانا لأيامي اختي "اية الرحان" و صغيرتي "بيان"

إلى الاموات الاحياء في قلوبنا و لكن... لو يشعرون

إلى ذلك الحبيب النائم تحت التراب اعتدت على جميع الغائبين إلا غيابك خالي "خالد مسعودي" طاب حالك و جعلك الله في نعيم حتى يبعثون

إلى الايادي الطاهرة التي تمد لي العون "على مسعودي" "سفيان مسعودي" "كمال مسعودي" الى من ساندني بكل حب عممي "بريزة" شفاك الله شفاء لا يغادره سقما

إلى كل من كان عون و سند في هذا طريق الى كل عائلتي جددي، جدتاي، عمي، عممتاي، احوالي كل باسمه لرفقاء السنين و اصحاب الشدائد اهديك هذا الانجاز

و أهديه الى نفسي نفسي الطموحة العظيمة التوية الى شريكة عملي "بهلاي آية"

إلى من تعلمنا منه ان للنجاح قيمة و معنى و منه تعلمنا كيف يكون التفاني في الاخلاص و العمل، و منه آمنا ان لا مستحيل في سبيل الإبداع و الرقي

إلى رجل المواقف الدكتور "عجو زكرياء" دمت منارة للعلم و مشعلا يضيء دروب الخير الى من تقاسمتنا معهم مقاعد الدراسة فكانوا خير جليس الى زملاء المخبر "بلطو نريمان"، "زحاف معمر"، "رحباني ثابت"، "بوشوارب ملاك"، "شبيخي نجوة" تمنياتي لكم بالتوفيق شكرا من القلب لكل شخص يجعل الحياة الطف بكلماته، بأفعاله الصغيرة، بمبادراته

اللامتوقعة، شكرا لصانعي ايماننا بلطفهم شكرا الى من ارادوا بي كسرا فحبيب الله ظنهم فردت قوة و جبرا

شكرا للجميع

فكاه

Abstract

Abstract:

Nanoflooding is a novel chemical enhanced oil recovery (EOR) technique, has the potential to increase the oil production. This study investigates the synergistic effects of nanosilica, nanoclay and their combinations in nanoflooding to enhance oil recovery efficiency and mitigate asphaltene deposition. Two micromodel cases were studied: a cylindrical sand model and a cylindrical asphaltenic sand model. Various formulations including silica nanoparticles with different concentrations (0.01%, 0.05%, 0.1%, 0.5%), nanoclay concentrations (0.001%, 0.005%, 0.01%) to stabilize the nanomaterials and enhance the displacement efficiency we did add a biopolymer with the concentration of 0.1/100ml, also we added a surfactant to the injected solution to keep the dispersion of nanomaterials and reduce the interfacial tension. Experimental setups simulated reservoir conditions, focusing on nanoparticle interactions with reservoir fluids and rock surfaces. Core flood experiments revealed that silica nanoparticles alone increased the recovery factor, with further enhancements observed at higher concentrations (0.1% optimal) and with the addition of biopolymer. Nanoclay also improved recovery, with optimal performance observed at a concentration of 0.005%, and its combination with biopolymer further enhanced the recovery factor. The highest recovery factors were achieved using nanocomposite (nanosilica + nanoclay) and biopolymer combinations, supplemented with surfactant to reduce interfacial tension (IFT).

key words : Nanosilica, Nanoclay, Nanoflooding , EOR, biopolymer, Micromodel, asphaltene deposition ,interfacial tension.

ملخص:

الفيضانات النانوية هي تقنية جديدة لاستعادة النفط المعزز كيميائياً (EOR) ، ولديها القدرة على زيادة إنتاج النفط. تبحث هذه الدراسة في التأثيرات التآزرية للنانوسيليكا والنانوكلاي وتركيباتها في غابات النانو لتعزيز كفاءة استعادة النفط والتخفيف من ترسب الأسفلتين. تمت دراسة حالتين من النماذج: نموذج رملي أسطواني ونموذج رملي أسفلتني أسطواني. تركيبات مختلفة بما في ذلك جسيمات السيليكا النانوية بتركيزات مختلفة (0.01%، 0.05%، 0.1%، 0.5%)، تركيزات الكلاي النانوي (0.001%، 0.005%، 0.01%) لتثبيت المواد النانوية وتعزيز كفاءة الإزاحة التي قمنا بها لإضافة بوليمر حيوي مع تركيز محلول المضاف 100/0.1 مل أيضاً، تحاكي الإعدادات التجريبية ظروف الخزان، مع التركيز على تفاعلات الجسيمات النانوية مع سوائل الخزان والأسطح الصخرية. كشفت تجارب الفيضانات الأساسية أن جسيمات السيليكا النانوية وحدها زادت من عامل الاسترداد، مع ملاحظة المزيد من التحسينات بتركيزات أعلى (0.1% مثالية) ومع إضافة البوليمر الحيوي. كما قام نانوكلاي بتحسين التعافي، حيث لوحظ الأداء الأمثل بتركيز 0.005%، كما أدى دمج مع البوليمر الحيوي إلى زيادة تعزيز عامل الاسترداد. تم تحقيق أعلى عوامل الاسترداد باستخدام نانوكوموزيت (نانوسيليكا + نانوكلاي) وتركيبات البوليمر الحيوي، مكملة بخافض للتوتر السطحي لتقليل التوتر البيني (IFT).

كلمات مفتاحية: نانوسيليكا، نانوكلاي، الفيضانات النانوية، النماذج، ترسب الأسفلتين، توتر بيني.

Résumé :

Nanoflooding est une nouvelle technique chimique améliorée de récupération de pétrole (EOR), a le potentiel d'augmenter la production de pétrole. Cette étude examine les effets synergiques de nanosilica, de nanoclay et de leurs combinaisons dans le nanoflooding pour augmenter l'efficacité de récupération d'huile et pour atténuer le dépôt d'asphaltène. Deux cas de micromodèles ont été étudiés : un modèle cylindrique de sable et un modèle cylindrique de sable asphalténique. Diverses formulations comprenant des nanoparticules de silice avec différentes concentrations (0.01%, 0.05%, 0.1%, 0.5%), concentrations de nanoclay (0.001%, 0.005%, 0.01%) pour stabiliser les nanomatériaux et améliorer l'efficacité de déplacement, nous avons ajouté un biopolymère avec une concentration de 0,1/100ml, nous avons également ajouté un tensioactif à la solution injectée pour maintenir la dispersion des nanomatériaux et réduire la tension interfaciale. Les installations expérimentales ont simulé des conditions de réservoir, se concentrant sur des interactions de nanoparticule avec des fluides de réservoir et des surfaces de roche. Les expériences d'inondation du cœur ont révélé que les nanoparticules de silice à elles seules augmentaient le facteur de récupération, avec d'autres améliorations observées à des concentrations plus élevées (0,1% optimal) et avec l'ajout de biopolymère. Nanoclay a également amélioré la récupération, avec des performances optimales observées à une concentration de 0,005%, et sa combinaison avec le biopolymère a encore amélioré le facteur de récupération. Les facteurs de récupération les plus élevés ont été obtenus en

utilisant des combinaisons de nanocomposites (nanosilica + nanoclay) et de biopolymères, complétés avec un tensioactif pour réduire la tension interfaciale (IFT).

Mots clé: Nano inondation, RAH, nanoparticules de silice, nanoargile, micromodèle, biopolymère, surfactant, tension interfaciale.

Contents

Acknowledgement	I
المقدمة.....	II
Abstract	IV
Contents.....	VII
List of figures	X
List of tables.....	XII
Nomenclature, Symbols and Abbreviations.....	XIII
General introduction.....	1
Chapter I: Enhanced oil recovery (EOR).....	3
Introduction.....	4
I.1 Enhanced oil recovery(EOR)/improved oil recovery(IOR)definitions	4
I.2 Recovery factor.....	5
I.3 The conventional recovery methods	5
I.3.1 Primary recovery technique	5
I.3.2 Secondary recovery techniques	5
I.4 Enhanced Oil Recovery (EOR) processes.....	6
I.4.1 Thermal Recovery Technique	6
I.4.2 Gas Injection Techniques	7
I.4.3 Chemical Injection Technique	8
I.5 Mechanisms of EOR	10
I.6 factors affecting the efficiency of EOR process.....	10
I.7.1 Relative permeability	10
I.7.2 Wettability	11
I.7.3 Interfacial tension	12
I.7.4 Capillary pressure.....	12
conclusion	14
Chapter II :Nanomaterials in nanoflooding for EOR process	16
Introduction.....	17
II.1 Nanomaterials	17
II.1.1 Nanoparticles	17

II.1.1.1 Nanoparticles characteristics.....	18
II.1.1.2 Silica Nanoparticles (SiO ₂)(SiNPs).....	19
II.1.2 Nanoclays	21
II.2 nanoflooding	21
II.2.1 The Mechanisms of nanoparticles in EOR.....	22
II.2.1.1 Nanofluids	23
II.2.2 Factors controlling success of nanoflooding	29
II.2.2.1 NP size	29
II.2.2.2 NP concentration	30
II.2.2.3 Salinity.....	30
II.2.2.4 Reservoir temperature	31
II.2.2.5 Rock wettability	31
II.2.2.6 The rock grain size	31
II.2.2.7 Clay content	31
II.2.2.8 Reservoir permeability effect	31
II.2.2.9 Rate of injection.....	32
II.3 Enhancing the Stability of NPs	32
Chapter III : Analyses and experimental strategies	34
Introduction	35
III.1 Experimental Project	35
III.2 Materials	35
III.2.1 Sand.....	35
III.2.2 Brine.....	35
III.2.3 Diesel fuel.....	35
III.2.4 Silica powder	36
III.2.5 Clay powder.....	36
III.3 Samples characterization	37
III.3.1 Grain size analysis.....	37
III.3.2 X-ray diffraction image (XRD)	38
III.3.3 X-ray fluorescence (XRF).....	38
III.3.4 Scanning Electron Microscopy (SEM) / X-ray microanalysis (EDS)	38
III.4 Characteristics of Chemical product	38
III.4.1 Extraction of nanoparticles	38
III.4.2 Preparation of Nanofluid.....	39
III.4.3 Addition of polymer	39
III.5 Experimental apparatus and measurements.....	40
III.5.1 Experimental apparatus description and flow behavior in a porous medium.....	40
III.5.2 Porous media micromodels	41
➤ Sand micromodels.....	41
➤ Sand and asphaltene micromodels	41
III.6 Experimental procedure.....	42

III.7 Petrophysical properties Measurements	43
III.7.1 Porosity measurement	43
III.7.2 Permeability measurement.....	43
conclusion	44
Chapter IV : Experimental results and discussions	45
IV.1 Samples characterization results	46
IV.1.1 Grain size analysis results.....	46
IV.1.2 X-ray diffraction (XRD) results	47
IV.1.3 X-ray fluorescence (XRF) results.....	49
IV.1.4 Scanning Electron Microscopy (SEM) / X-ray microanalysis (EDS) results	50
IV.1.4.1 Silica sample	50
IV.1.4.2 Clay sample.....	52
IV.1.4.3 Biopolymer sample.....	53
IV.2 Effect of nanomaterials concentration in oil recovery	54
IV.2.1 Effect of Nanosilica concentration in recovery factor	54
IV.2.2 Effect of nanoclay concentration in recovery factor	55
IV.3 Displacements tests results and discussion	55
IV.3.1 Case 01: sand micromodel.....	55
IV.3.1.1 Silica Nanoflooding	56
IV.3.1.2 Nanoclay flooding.....	60
IV.3.1.3 silica+ clay nanofluid flooding:	62
IV.3.2 Case 02: sand and asphaltene micromodel:	67
IV.3.2.1 Silica Nanoflooding	68
IV.3.2.2 Nanoclay flooding.....	70
IV.3.2.3 Silica +clay nanofluid flooding.....	72
IV.4 Results of IFT measurement:	76
General Conclusion:	79
References	82
Appendices	LXXXVI
Appendix A	LXXXVI
Appendix B.....	LXXXVI
Appendix CError! Bookmark not defined.

List of figures

Figure 1 : Planning of the dissertation	2
Figure I.1 definition of EOR/IOR.....	4
Figure I.2: different categories of enhanced oil recovery	6
Figure I.3: steam flooding	7
Figure I.4: Simplified illustration of a thickened gas flooding	8
Figure I.5: Chemical flooding	9
Figure I.6: enhanced oil recovery methods (LPG = liquefied petroleum gas).	9
Figure I.7 : Illustration of wettability.....	12
Figure I.8 : Effect of capillary number on residual oil saturation.....	14
Figure I.19 : Effect of mobility ratio on displaceable oil.	14
Figure II.1: nanomaterials classes	17
Figure II.2: High surface area relative to volume of nanoparticles.....	19
Figure II.3 SEM of nano-silica.....	20
Figure II.4 : silica nanoparticle Dispersion (SiO ₂ , Purity: 99.9%)	20
Figure II.5: SEM images for nanoclay	21
Figure II.6: Schematic illustration of the main reported EOR methods.....	22
Figure II.7: Mechanisms of pore channels plugging	24
Figure II.8: Wettability-alteration-and-interfacial-tension-reduction-by-nanoparticles	25
Figure II.9: Mechanism of IFT reduction using NPs showing particle adsorption (contact angle) at the oil-water interface and formation of a monolayer which replaces the existing oil-water interface.....	27
Figure II.10: Disjoining pressure in porous medium for oil extraction mechanism	28
Figure II.11: Asphaltene adsorption mechanism on nanoparticles	29
Figure II.12: Effect of increasing salinity at constant silica NPs concentration on the wettability change of carbonate rocks.....	30
Figure II.13: Steric stabilization of nanoparticles using (a) polymer, (b)surfactant, and (c) polymer followed by a mixture of surfactant and polymer (Fiedot, Rac, Suchorska-Woźniak, Karbownik, & Teterycz, 2014).	33
Figure III.1:The sieve machine used in granulometric analysis.	37
Figure III.2: The installation of fluid displacement in a porous medium	40
Figure III.3: cylindrical sand micromodel.....	41
Figure III.4: asphaltenic sand micromodel.....	41
Figure III.5: weighing the wet sand sample, saturated sand sample and asphaltenic sand samble respectivement.....	43
Figure IV.1: distribution of grain size (mm) in the weighted sand sample (10,865kg)	46

Figure IV.2: SEM/EDS image of Silica powder.	51
Figure IV.3: SEM/EDS image of clay powder.....	52
Figure IV.4: SEM/EDS image of biopolymer.....	53
Figure IV.5: diagrams represented the effect of nanosilica concentration in recovery factor	54
Figure IV.6: diagrams represented effect of nanoclay concentration in recovery factor	55
Figure IV.7: Histogram represented the oil in place and the recoverd oil after brine flooding, nanosilica flooding and nanosilica flooding with polymer injection.....	58
Figure IV.8: diagram represented the results of RF after brine flooding, nanosilica flooding and nanosilica flooding with polymer injection.....	59
Figure IV.9: Histogram represented the oil in place and the recoverd oil after brine flooding, nanoclay flooding and nanoclay flooding with polymer injection.	61
Figure IV.10: diagram represented the results of RF after brine flooding, nanoclay flooding and nanoclay flooding with polymer injection.....	62
Figure IV.11: Histogram represented the oil in place and the recoverd oil after brine flooding, nanocomposite flooding and nanocomposite flooding with polymer injection.....	64
Figure IV.12: diagram represented the results of RF after brine flooding, nanocomposite flooding and nanocomposite flooding with polymer injection.....	65
Figure IV.13: Histograms represented the results of recovery factors in the case of sand micromodel.	65
Figure IV.14: samples of the recovered oil after brine flooding, nanosilica flooding and nanosilica flooding with polymer injection respectivement from right to left.....	69
Figure IV.15: Histogram represented the oil in place and the recoverd oil after brine flooding, nanosilica flooding and nanosilica flooding with polymer injection.....	69
Figure IV.16: diagram represented the results of RF after brine flooding, nanosilica flooding and nanosilica flooding with polymer injection.....	70
Figure IV.17: Histogram represented the oil in place and the recoverd oil after brine flooding, nanoclay flooding and nanoclay flooding with polymer injection.	71
Figure IV.18: diagram represented the results of RF after brine flooding, nanoclay flooding and nanoclay flooding with polymer injection.....	72
Figure IV.19: Histogram represented the oil in place and the recoverd oil after brine flooding, nanocomposite flooding and nanocomposite flooding with polymer injection.....	73
Figure IV.20: relative circle represented the result of RF after nanoflooding without injecting the polymer	74
Figure IV.21 : relative circle represented the result of RF after nanoflooding with the polymer injection	74
Figure IV.22: Histograms represented the results of recovery factors in the case of asphaltenic sand micromodel.....	75
Figure IV.23: IFT between diesel fuel and different fluid.....	76

List of tables

Table I -1 mechanisms and challenges of each EOR methods	10
Table II.1: Examples of different nanomaterials dimensions	18
Table III.1: Properties of diesel fuel.....	36
Table III.2: The Physical properties of silica fume (powder)	36
Table III.3: The Physical and chemical properties of clay (bentonite powder)	36
Table IV.1: The quantities and percentages of sand in each sieve in relation to the diameter of the sieves.....	46
Table IV.2: X-ray diffraction (XRD) results	47
Table VI.3: Result of X-ray fluorescence (XRF)	49
Table IV.4:results of porosity measurements.	56
Table IV.5: result of Absolute permeability measurement.	56
Table IV.6: results of brine flooding.	56
Table IV.7: results of silica nanoflooding	57
Table IV.8: results of silica nanofluid flooding and polymer injection.	57
Table IV.9: results of brine flooding.	60
Table IV.10: results of nanoclay flooding	60
Table IV.11: results of clay nanofluid and polymer injection.....	60
Table IV.12: results of brine flooding.	62
Table IV.13: result of silica+ clay flooding.	63
Table IV.14: results of Silica+ clay nanofluid flooding and polymer injection.	63
Table IV.15: The results of the porosity measurements.	67
Table IV.16: results of permeability measurement.....	67
Table IV.17: results of brine flooding.	68
Table IV.18: results of silica nanofluid flooding.....	68
Table IV. 19:results of silica nanofluid flooding and polymer injection.	68
Table IV.20: results of brine flooding.	70
Table IV.21: result of nanoclay flooding.....	70
Table IV.22: result of nanoclay flooding and polymer injection.	71
Table IV. 23: results of brine flooding.	72
Table IV. 24: results of silica+ clay flooding.....	73
Table IV.25: results of Silica+ clay nanofluid and polymer injection.	73

Nomenclature, Symbols and Abbreviations

EOR: Enhanced oil recovery

IOR: improved oil recovery

IOIP: initial oil in place

NPs: Nanoparticles

IFT: Interfacial tension

SiNPs: silica nanoparticles

PNP: Polymer NPs

RF: Recovery factor

PAMAM: polyamidoamide

TGA: thermogravimetric analysis

API: American Petroleum Institute(density API)

K_{ro}: relative permeability to oil

K_{rg}: relative permeability to gas

K_{rw}: relative permeability to water

K: absolute permeability

K_o: effective permeability to oil for a given oil saturation

K_g: effective permeability to gas for a given gas saturation

K_w: effective permeability to water at some given water saturation

S_{wi}: irreducible water saturation

S_{or}: residual oil saturation

θ : contact angle (degree)

P_c: capillary pressure

P_w: pressure of the nonwetting phase

P_{nw}: pressure of the wetting phase

N_c: capillary number

M: Mobility Ratio

v : Darcy velocity (m/s)

μ : fluid viscosity (Pa. s)

λ_{ing} : the mobility of the displacing fluid

λ_{ed} : is the mobility of the displaced fluid

Φ : Porosity (dimensionless)

v : Velocity of particles (m/s)
 σ_{12} : Interfacial tension (mN/m)
pH : Potential of hydrogen
ppm : Part per million
Psi : Pound force per square
Wt% : Weight percent
XRD : X-ray diffraction
EDX : Energy-dispersive X-ray
SEM : scanning electron microscope
EDS: Energy-dispersive X-ray spectroscopy
MEB: electron microscope scanning
FEI: field electron and ion (company)
GOR: gas oil ratio
 φ : diffraction angle (degree)



General introduction

General introduction

According to the International Energy Agency (IEA), the world's demand for fossil fuels is expected to increase by about one-third by the year 2035 (Oscar E. Medina 1, 2019).

To face this challenge, the oil and gas industry has chosen the implementation of new technologies capable of improving the efficiency in the enhanced oil recovery (EOR) processes. In this context, the incorporation of nanotechnology through the development of nanoparticles and nanofluids to increase the productivity of heavy and extra-heavy crude oils has taken significant importance (Oscar E. Medina 1, 2019).

The injection of nanofluids into oil reservoirs, a novel chemical enhanced oil recovery (EOR) technique, has the potential to produce a greater portion of the 50% of in-place oil reserves, which is currently not recoverable by conventional primary and secondary recovery methods (Davis, 2010), nor even by conventional EOR.

This dissertation embarks on a comprehensive exploration of nanoparticle-enabled nanoflooding. By delving into the pivotal role of EOR in petroleum production, elucidating the mechanisms of nanoflooding, enhancing nanoparticle stability. This study endeavors to unravel novel pathways towards enhanced oil recovery.

Problematic statement:

How can nanoparticle-enabled nanoflooding techniques be optimized to effectively enhance oil recovery from crude oil reservoirs, considering factors such as nanoparticle stability, interfacial interactions, and reservoir conditions?

Objectif of the study:

The primary objective is to experimentally investigate how nanofluids interact with reservoir conditions, focusing on their efficacy in displacing trapped oil.

Implementation of the dissertation:

- Chapter I: Enhanced oil recovery (EOR)
- Chapter II : Nanomaterials in nanoflooding for EOR process
- Chapter III: Analyses and experimental strategies
- Chapter VI : Experimental results and discussions

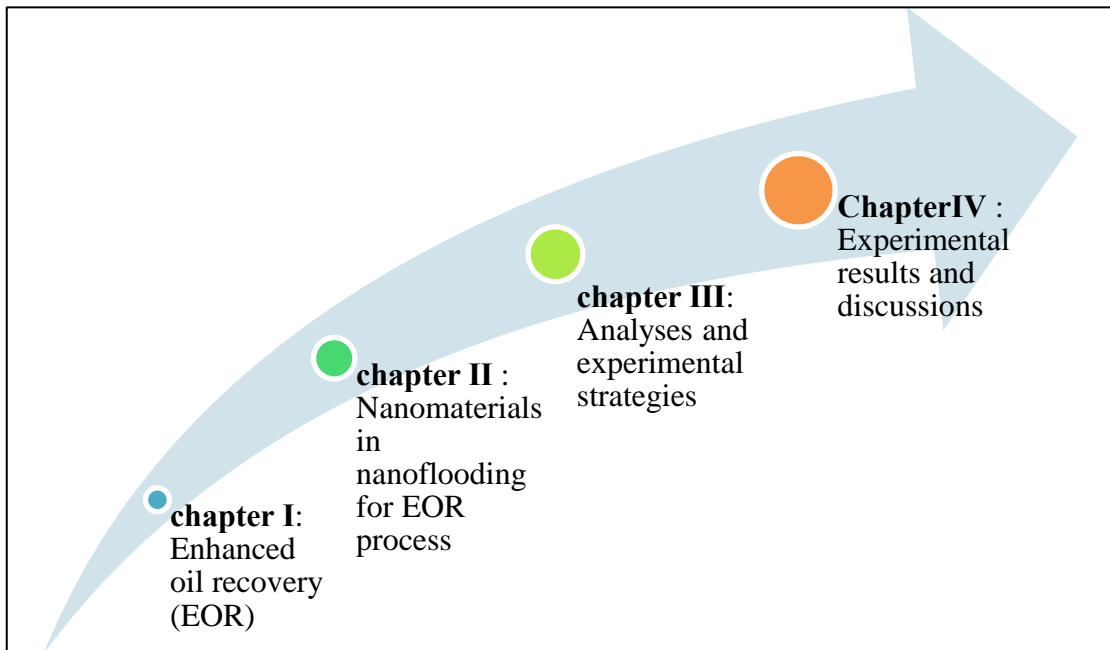
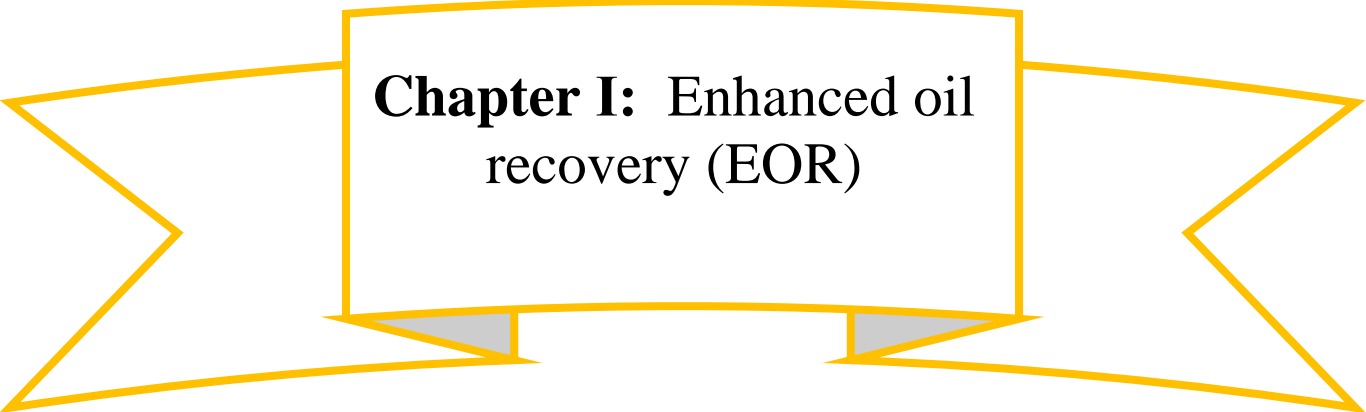


Figure 1 : Planning of the dissertation



**Chapter I: Enhanced oil
recovery (EOR)**

Introduction

After conventional recovery methods have been exhausted. Much of this oil would be recovered by Enhanced Oil Recovery (EOR) methods, which are part of the general scheme of Improved Oil Recovery (IOR). The choice of the method and the expected recovery depends on many considerations, economic as well as technological (Thomas, *Enhanced Oil Recovery – An Overview*, 2007) .

In This chapter we will mention the conventional recovery methods (primary and secondary) and provide a comprehensive exploration of Enhanced Oil Recovery (EOR), its techniques, mechanisms and the factors affecting the process.

I.1 Enhanced oil recovery(EOR)/improved oil recovery(IOR)definitions

At this stage, it is important to define EOR. There is a lot of confusion around the usage of the terms EOR and IOR. Figure 1 shows these in terms of oil recovery. Primary and secondary recovery (conventional recovery) targets mobile oil in the reservoir and tertiary recovery or EOR targets immobile oil (that oil which cannot be produced due to capillary and viscous forces) (AL-KAABI, 2010).

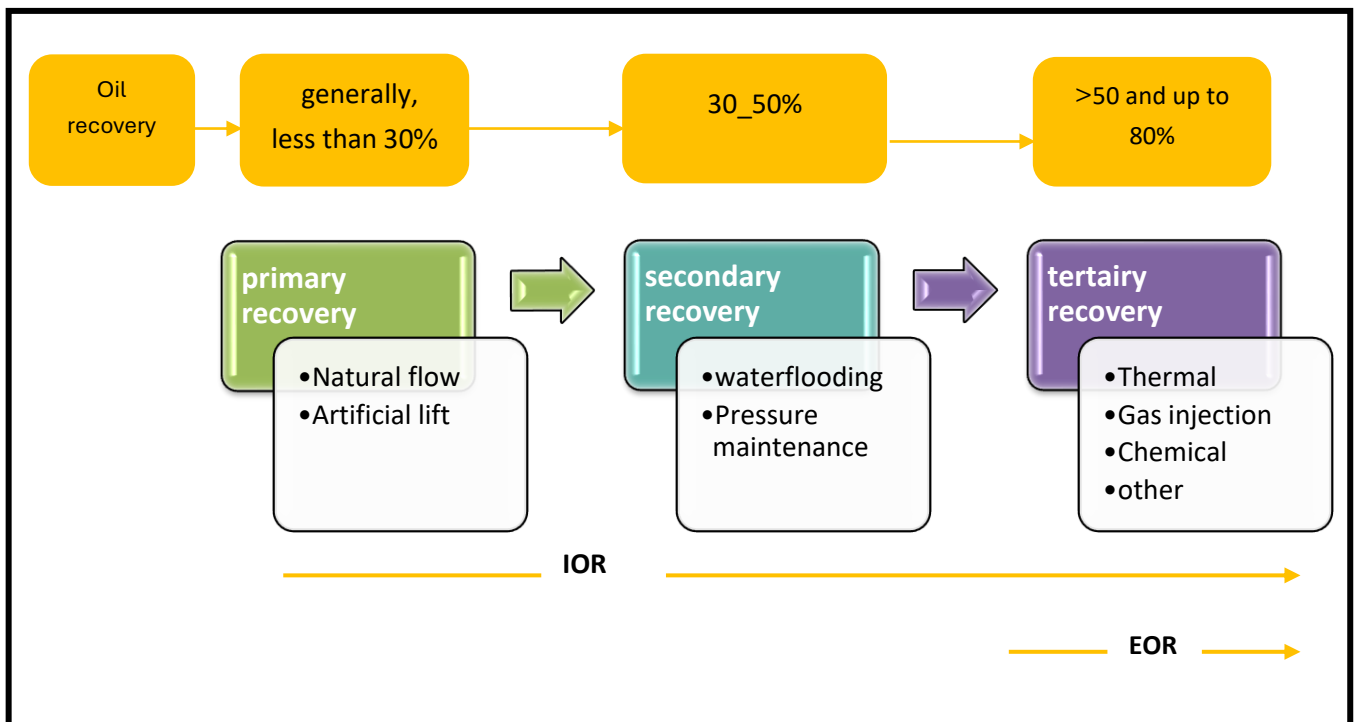


Figure I.1 definition of EOR/IOR

I.2 Recovery factor

Recovery factor (RF) is one of the most important parameters for economic justification in the petroleum industry (M.Prasad, 2011) . the RF is calculated from the ratio between expected ultimate recovery (EUR) and original oil in place (OOIP), see equation I.1:

$$RF = \frac{EUR}{OOIP} \quad (I.1)$$

I.3 The conventional recovery methods

I.3.1 Primary recovery technique

Primary recovery involves extracting the initial energy stored in the reservoir. found to be the only energy source for extracting oil and gas from a reservoir. Extraction of oil from reservoirs using only primary methods can vary in scope. from almost nothing to over 60%. Due to the frequent presence of a significant amount of oil that remains in a reservoir after primary recovery is completed , primary recovery pertains to the volume of hydrocarbons that can be retrieved using the reservoir's natural energy. When a new reservoir is first discovered, the reservoir rock and fluids experience significant pressure.

I.3.2 Secondary recovery techniques

Methods for enhancing oil recovery cannot be successful without secondary recovery techniques. These methods are implemented once the initial extraction method has been utilized to recover oil from the reservoir. Secondary recovery methods are imperative because they enable the extraction of additional oil from the reservoir that would not have been accessible using only primary recovery techniques.

Below are a few secondary recovery methods frequently utilized in the oil sector:

➤ **Waterflooding**

Waterflooding is the primary secondary recovery method typically employed in the oil sector. With this method, oil displacement is achieved by injecting water into the reservoir. Water assists in moving the oil towards the production wells, facilitating its extraction process. Waterflooding is a beneficial method because it aids in preserving reservoir pressure, which is crucial for oil extraction.

➤ Gas Injection

In this method, gas is pumped into the reservoir in order to drive the oil towards the production wells. The gas can be either natural gas or carbon dioxide. Injecting gas is a useful method because it assists in upkeeping reservoir pressure and decreasing the oil's viscosity, which simplifies extraction.

I.4 Enhanced Oil Recovery (EOR) processes

In every oil reserve, a considerable quantity of oil remains uncollected even after primary and secondary extraction techniques. This is when tertiary or advanced oil recovery techniques are utilized. Enhanced oil recovery methods strive to boost the total oil output from the reservoirs. The significance of EOR techniques is highly understood by oil companies and authorities. It is well known that there are three major categories of available EOR technologies as shown in bellow **figure I.2**.

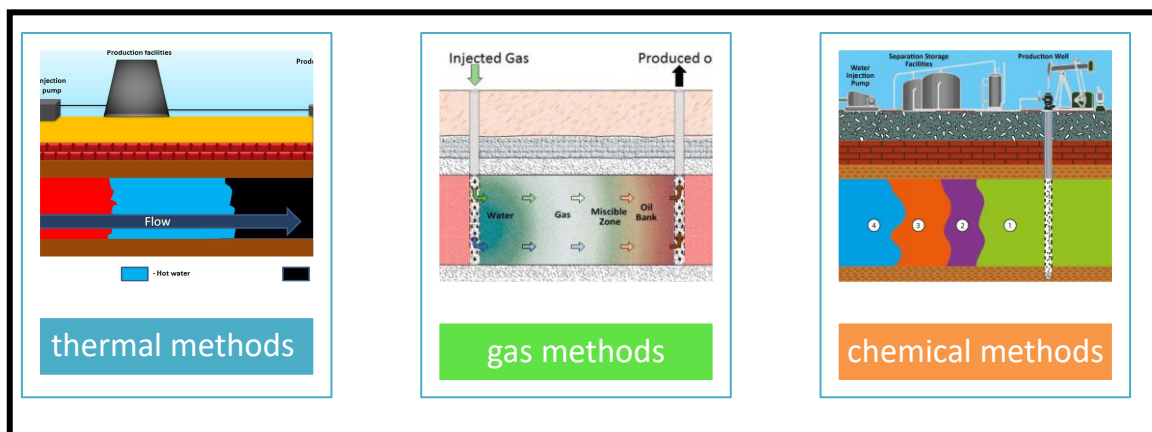


Figure I.2: different categories of enhanced oil recovery

Here are some insights into each category of tertiary recovery techniques:

I.4.1 Thermal Recovery Technique

Thermal EOR is used mainly in the production of high-viscosity paraffinic and resinous oils (Malozymov, et al., 2023). There are two basic techniques for heating the reservoir:

- Injecting steam or hot gases into the reservoir.
- Injecting either air or oxygen into the reservoir and burning some of the oil in the reservoir. This technique is called in situ combustion (Nabipour, 2007). the injection of

steam or hot water into reservoirs to lower the viscosity of oil, so the oils mobility is increased, and this makes it easier to extract from the reservoir. Steam injection is the most commonly used thermal recovery technique, and it has been successful in many oil fields worldwide. For example, the Kern River oil field in California has been using steam injection since the 1960s, and it has been able to produce over 2 billion barrels of oil to date.

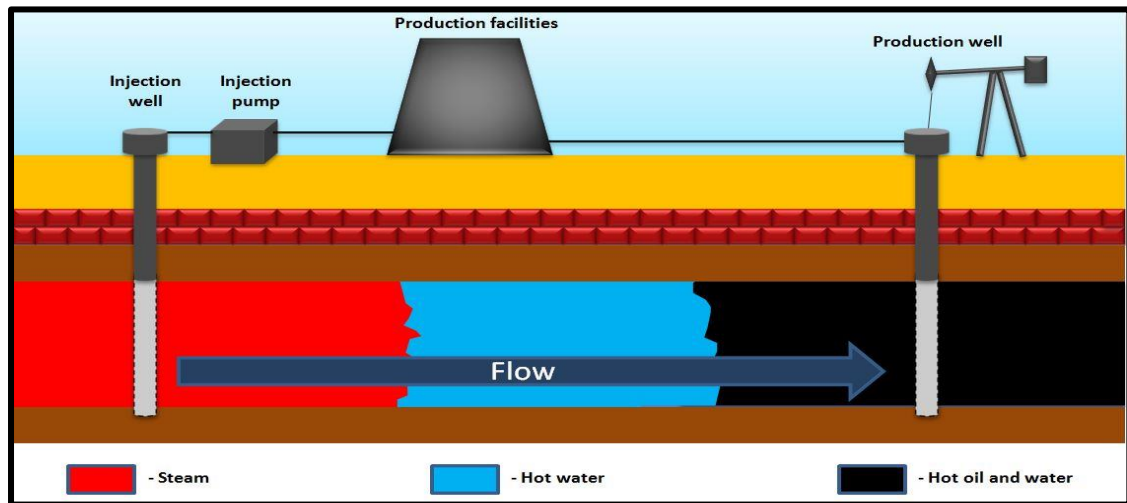


Figure I.3: steam flooding

I.4.2 Gas Injection Techniques

This category of tertiary recovery techniques involves injecting gas into the reservoir to increase the reservoir pressure and displace the remaining oil. The most commonly used gases for gas injection are nitrogen, carbon dioxide, and natural gas. Carbon dioxide injection is the most widely used gas injection technique globally, and it has been successful in many oil fields, such as the SACROC oil field in Texas. The SACROC oil field has been using carbon dioxide injection since the 1970s, and it has been able to produce over 2.5 billion barrels of oil to date.

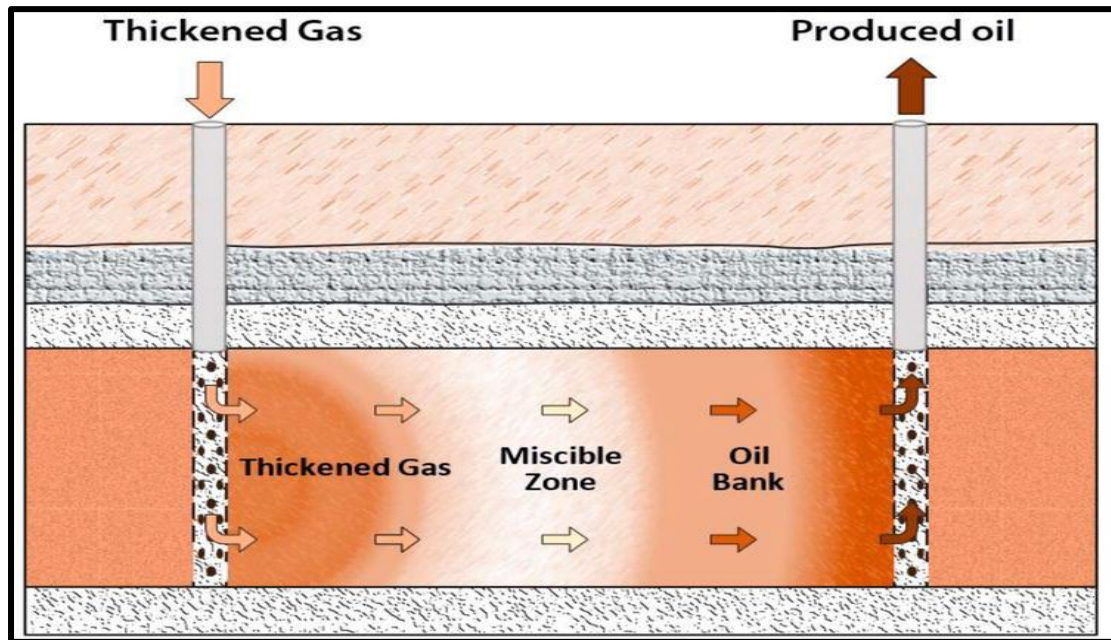


Figure I.4: Simplified illustration of a thickened gas flooding

I.4.3 Chemical Injection Technique

This category of tertiary recovery techniques involves injecting chemicals (alkaline, polymers, and surfactants) into the reservoir (figure I.5) to reduce the surface tension between the oil and the reservoir rock, making it easier to extract the oil. The most commonly used chemicals for chemical injection are surfactants and polymers. Surfactants are used to reduce the surface tension between the oil and the reservoir rock, whereas polymers are used to increase the viscosity of the water injected into the reservoir. Chemical injection techniques have been successfully used in many oil fields worldwide, such as the Prudhoe Bay oil field in Alaska, which has been able to produce over 13 billion barrels of oil using chemical injection techniques since its discovery in 1968.

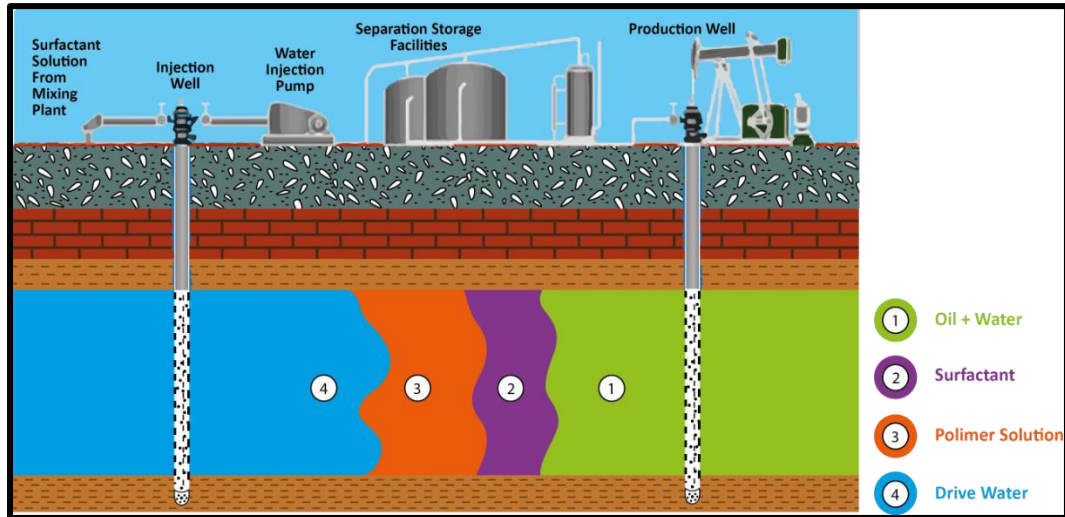


Figure I.5: Chemical flooding

Each EOR technique is typically suited to specific reservoir types, with no single method universally considered superior. The success of implementing these techniques hinges on the reservoir's rock and fluid properties, structural model, as well as geographic, logistical, and economic factors. Moreover, multiple EOR methods may be combined within a single oil field, presenting numerous possibilities for method integration.

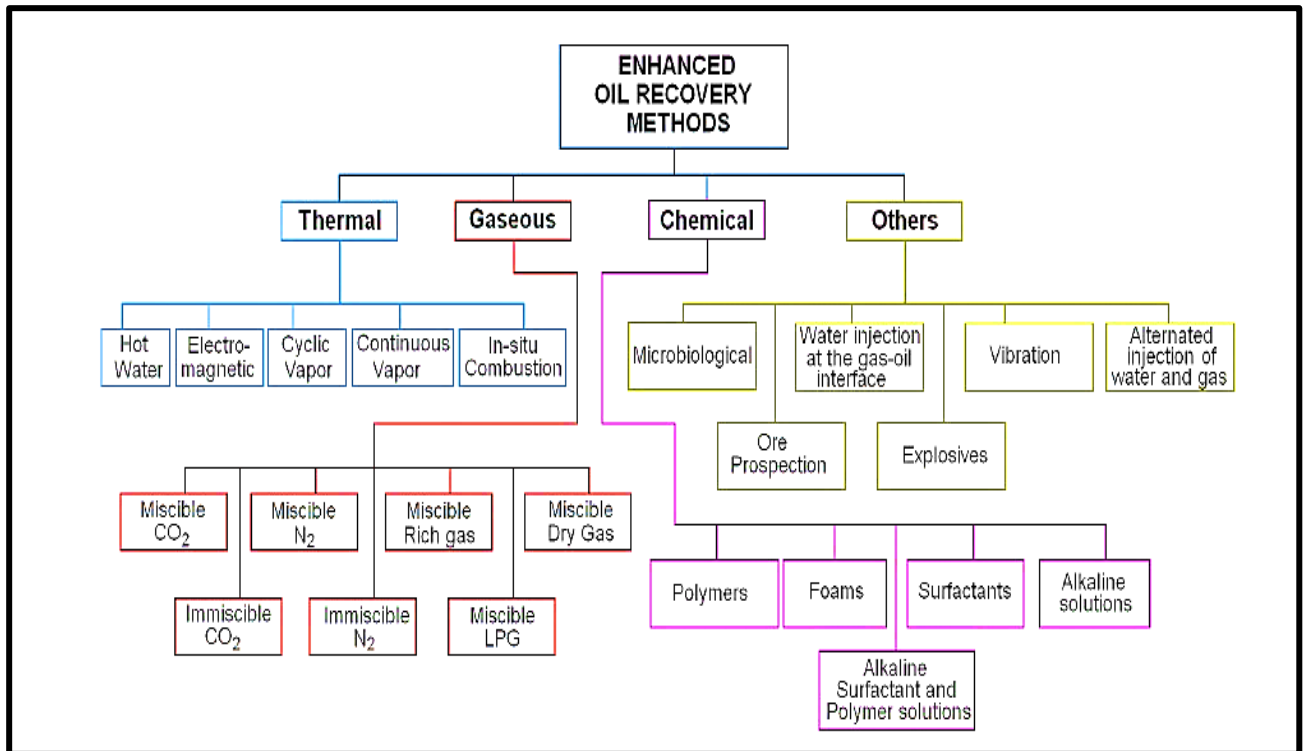


Figure I.6: enhanced oil recovery methods (LPG = liquefied petroleum gas).

I.5 Mechanisms of EOR

Table I -1 mechanisms and challenges of each EOR methods

EOR methods	chemical	thermal	gas	others
mechanisms	<ul style="list-style-type: none"> - Wettability alteration - Reduction of IFT - MOBILITY CONTROL 	<ul style="list-style-type: none"> - Reduction of viscosity and IFT - Gravity drainage 	<ul style="list-style-type: none"> - Expansion of oil - Reduction of viscosity - Maintenance pressure 	<ul style="list-style-type: none"> - Reduction of viscosity - Maintenance pressure
challenges	<ul style="list-style-type: none"> - Viscosity fingering - High cost - Sensitivity to salinity and heat 	<ul style="list-style-type: none"> - High cost - Heat loss 	<ul style="list-style-type: none"> - Gas corrosion - Asphaltene problems 	<ul style="list-style-type: none"> - Low recovery in some cases - Sensitive to reservoir conditions

I.6 factors affecting the efficiency of EOR process

I.7.1 Relative permeability

Relative permeability is defined as the ratio of the effective permeability to a given fluid at a definite saturation to the permeability at 100% saturation. The terminology most widely used is simply k_g/k , k_o/k , k_w/k , meaning the relative permeability to gas, oil, and water, respectively. Since k is a constant for a given porous material, the relative permeability varies with the fluid saturation in the same fashion as does the effective permeability. The relative permeability to a fluid will vary from a value of zero at some low saturation of that fluid to a value of 1.0 at 100% saturation of that fluid. Thus, the relative permeability can be expressed symbolically as follows :

$$k_{rg} = \frac{k_g}{k} \quad (I.2)$$

$$k_{ro} = \frac{k_o}{k} \quad (I.3)$$

$$krw = \frac{k_w}{k} \quad (I.4)$$

where :

k_{ro} = relative permeability to oil

k_{rg} = relative permeability to gas

k_{rw} = relative permeability to water

k = absolute permeability

k_o = effective permeability to oil for a given oil saturation

k_g = effective permeability to gas for a given gas saturation

k_w = effective permeability to water at some given water saturation

I.7.2 Wettability

Wettability is defined as the tendency of one fluid to spread on or adhere to a solid surface in the presence of other immiscible fluids (Ahmed, 2001). The concept of wettability is illustrated in Figure. Small drops of three liquids; mercury, oil, and water are placed on a clean glass plate. The three droplets are then observed from one side as illustrated in Figure. It is noted that the mercury retains a spherical shape, the oil droplet develops an approximately hemispherical shape, but the water tends to spread over the glass surface.

The tendency of a liquid to spread over the surface of a solid is an indication of the wetting characteristics of the liquid for the solid. This spreading tendency can be expressed more conveniently by measuring the angle of contact at the liquid-solid surface. This angle, which is always measured through the liquid to the solid, is called the contact angle θ . The contact angle θ has achieved significance as a measure of wettability. As shown in Figure, as the contact angle decreases, the wetting characteristics of the liquid increase. Complete wettability would be evidenced by a zero-contact angle, and complete nonwetting would be evidenced by a contact angle of 180° .

There have been various definitions of intermediate wettability but, in much of the published literature, contact angles of 60° to 90° will tend to repel the liquid. The wettability of reservoir rocks to the fluids is important in that the distribution of the fluids in the porous media is a function of wettability. Because of the attractive forces, the wetting phase tends to occupy the smaller pores of the rock and the nonwetting phase occupies the more open channels.

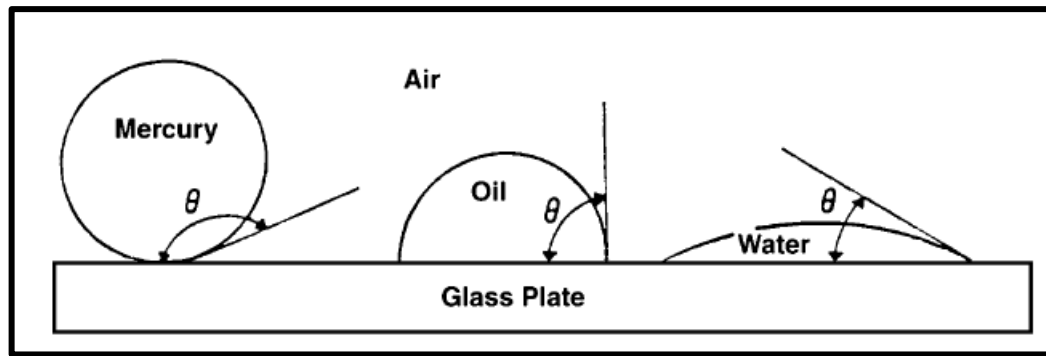


Figure I.7 : Illustration of wettability.

I.7.3 Interfacial tension

The imbalance of molecular forces at the interface between two phases is known as interfacial tension ([properties of petroleum fluids, william D. McCAIN,Jr](#)). In dealing with multiphase systems, it is necessary to consider the effect of the forces at the interface when two immiscible fluids are in contact. When the interface is between two liquids, the acting forces are called interfacial tension ([Ahmed, 2001](#)).

The surfaces of liquids are usually blanketed with what acts as a thin film. Although this apparent film possesses little strength, it nevertheless acts like a thin membrane and resists being broken. This is believed to be caused by attraction between molecules within a given system. All molecules are attracted one to the other in proportion to the product of their masses and inversely as the squares of the distance between them. The surface or interfacial tension has the units of force per unit of length, e.g., dynes/cm, and is usually denoted by the symbol σ .

I.7.4 Capillary pressure

The capillary forces in a petroleum reservoir are the result of the combined effect of the surface and interfacial tensions of the rock and fluids, the pore size and geometry, and the wetting characteristics of the system. Any curved surface between two immiscible fluids has the tendency to contract into the smallest possible area per unit volume. This is true whether the fluids are oil and water, water, and gas (even air), or oil and gas. When two immiscible fluids are in contact, a discontinuity in pressure exists between the two fluids, which depends upon the curvature of the interface separating the fluids. We call this pressure difference the capillary pressure and it is referred to by p_c . The displacement of one fluid by another in the pores of a porous medium is either aided or opposed by the surface forces of capillary

pressure. As a consequence, in order to maintain a porous medium partially saturated with nonwetting fluid and while the medium is also exposed to wetting fluid, it is necessary to maintain the pressure of the nonwetting fluid at a value greater than that in the wetting fluid. Denoting the pressure in the wetting fluid by p_w and that in the nonwetting fluid by p_{nw} , the capillary pressure can be expressed as:

Capillary pressure = (pressure of the nonwetting phase) - (pressure of the wetting phase)

$$p_c = p_{nw} - p_w \quad (I.5)$$

Mobilization of residual oil is influenced by two major factors: Capillary Number (N_c) and Mobility Ratio (M). Capillary Number is defined as

$$N_c = \frac{v\mu}{\sigma} \quad (I.6)$$

where v is the Darcy velocity (m/s), μ is the displacing fluid viscosity (Pa. s) and σ is the interfacial tension (N/m). The most effective and practical way of increasing the Capillary Number is by reducing σ , which can be done by using a suitable surfactant or by the application of heat. An approximation of the effect of Capillary Number on residual oil saturation is shown in Figure I.8. Capillary number at the end of a waterflood is $\sim 10^{-7}$.

A 50% reduction in residual oil saturation requires that the Capillary Number be increased by 3 orders of magnitude. Capillary number in a miscible displacement becomes infinite, and under such conditions, residual oil saturation in the swept zone can be reduced to zero if the mobility ratio is “favorable”. Mobility ratio is defined as

$$M = \lambda_{ing} / \lambda_{ed} \quad (I.7)$$

where λ_{ing} is the mobility of the displacing fluid (e.g. water), and λ_{ed} is the mobility of the displaced fluid (oil).

$$\lambda = \frac{k}{\mu} \quad (I.8)$$

where k is the effective permeability, (m²) and μ is the viscosity (Pa.s) of the fluid concerned). Mobility ratio influences the microscopic (pore level) and macroscopic (areal and vertical sweep) displacement efficiencies. A value of $M > 1$ is considered unfavorable, because it indicates that the displacing fluid flows more readily than the displaced fluid (oil), and it can cause channeling of the displacing fluid, and as a result, bypassing of some of the

residual oil. Under such conditions, and in the absence of viscous instabilities, more displacing fluid is needed to obtain a given residual oil saturation. The effect of mobility ratio on displaceable oil is shown in Figure I.9 . the data for which was obtained from calculations using Buckley-Leverett theory for waterflooding. The three curves represent 1, 2 and 3 pore volumes of total fluid injected, respectively. Displacement efficiency is increased when $M = 1$ and is denoted a “favorable” mobility ratio.

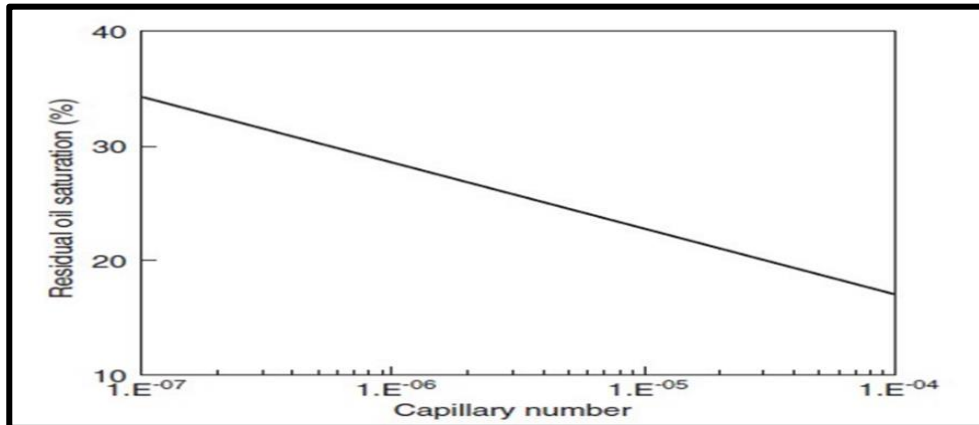


Figure I.8 : Effect of capillary number on residual oil saturation.

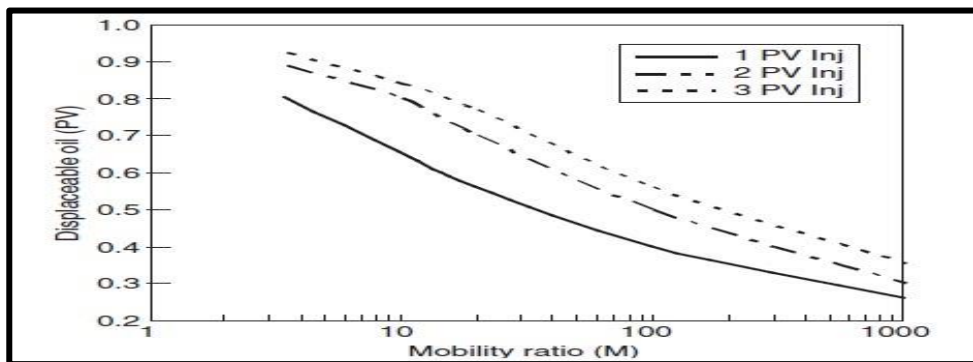
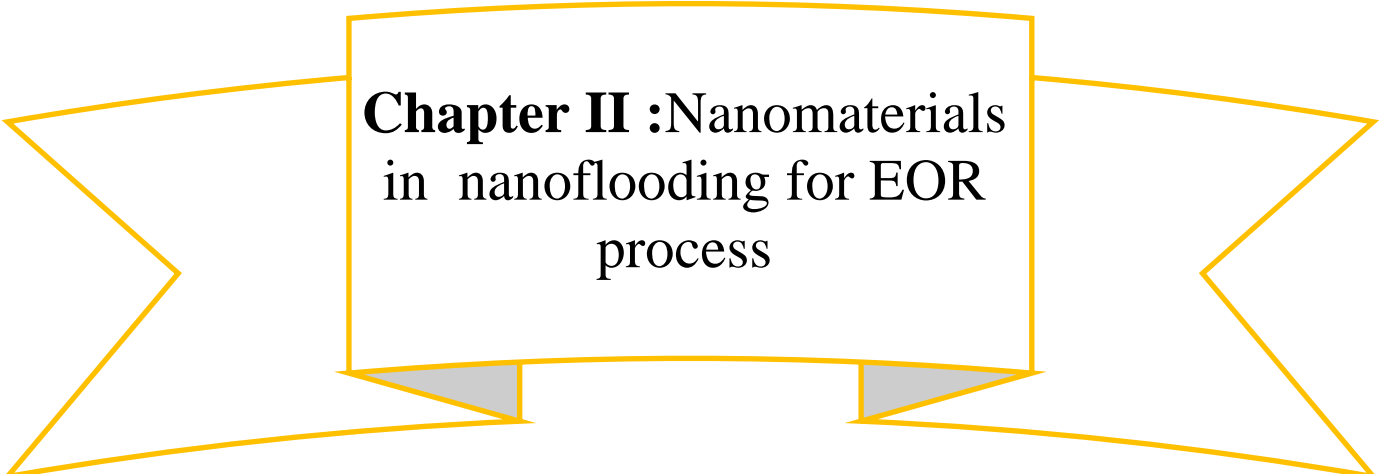


Figure I.19 : Effect of mobility ratio on displaceable oil.

conclusion

In brief, all these EOR methods tend to recover more oil from reservoirs by various mechanisms such as IFT reduction, wettability alteration, mobility control, change of physical properties and gravity drainage. However, all these traditional EOR processes face some important challenges. For example, for gas methods, the injected gas often quickly penetrates through reservoirs from injection wells to producing wells, resulting in a large amount of residual oil remaining uncovered in reservoirs because of the high mobility ratio of injected gas and oil. Moreover, chemical processes are often limited by the high cost of

chemicals, possible formation damages, and losses of chemicals. Therefore, less expensive, more efficient, and environmentally friendly EOR methods are greatly needed. Nanoparticles (NPs) offer novel pathways to address the unsolved challenges.



**Chapter II :Nanomaterials
in nanoflooding for EOR
process**

Introduction

Petroleum engineers working on small scale structure of fluid saturation to increase oil recovery in early stages are very beneficial to these enhanced properties of fluid. Nanomaterials have emerged as effective EOR techniques over the last decade, addressing issues in heavy and semi-heavy oil reservoirs, with nanoparticles (NPs) being used in injection solutions to enhance oil recovery. In this chapter, the effects of NPs on the enhancement of oil recovery is introduced. Besides, mechanisms of NPs and some of the last obtained experimental results are presented with the evaluation methods of nanoparticles and how to enhance the stability of them.

II.1 Nanomaterials

Nanomaterials are structural components with a size smaller than $1\ \mu\text{m}$ with an external dimension in the Nanoscale. They exist in spherical, tubular, and irregular shapes and can be found in a single, fused, aggregated, or agglomerated form.

Nanomaterials, including nanoparticles, nanoclays, and nanoemulsions, this classification is based on their size and composition. Nanoparticles are divided into organic and inorganic, while nanoclays are made of mineral silicate layers, and nanoemulsions are colloidal systems with varying submicron sizes.

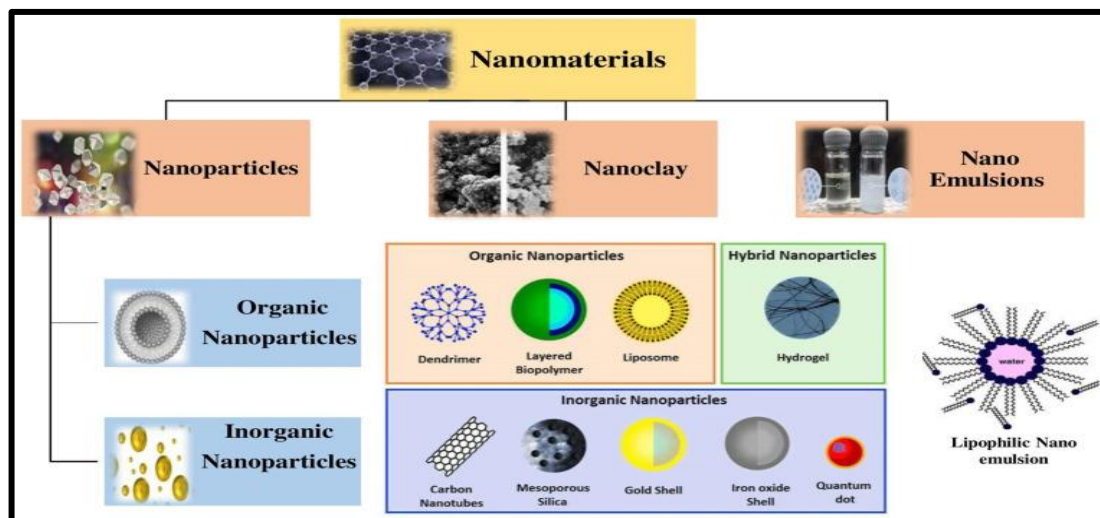


Figure II.1: nanomaterials classes

II.1.1 Nanoparticles

A nanoparticle size ranges between 1 and 100 nm (Mageswarriet al., 2016). Nanoparticles are found in the form of nanocomposites or structures. All nanostructures are

mainly composed of elementary units with low dimensions(blocks). They may be zero-dimension, one dimension, two dimensions, and three dimensions in which the effect of size on the resultant characteristic is visible, also known as quantum dots. As depicted in the next table, nanomaterials are divided into Zero dimensional (quantum dots), one dimensional (quantum wires), two dimensional (thin films) and three-dimensional nanoparticles as building blocks to build nanostructured materials (Strambeanuet al.,2015). In zero-dimensional nanomaterials, electron movement is different in all three directions. Electrons can only move in the X-direction in one dimension; in two dimensions, they can only move on the X-Y plane, and in three dimensions, they can move in the X, Y, and Z directions (Siegel, 1993). Depending on their material type, nanoparticles are classified as organic or inorganic. The inorganic salts precipitation, which is bound to molecules by metallic and covalent interactions produce inorganic nanoparticles (Sun et al., 2017). The organic nanoparticles are self-assembled into a three-dimensional structure. For the preparation of organic nanoparticles synthetic and natural organic compounds such as milk emulsion, protein aggregates, lipid bodies and other complex structures are used to make organic nanoparticles (Mohanraj and Chen, 2006).

Table II.1: Examples of different nanomaterials dimensions

Elementary units	Examples
<ul style="list-style-type: none"> Units of 0D (In the monometric range, there are 3 dimensions) 	<ul style="list-style-type: none"> Fullerenes, Clusters, powders, molecules, rings, grains, metal carbides
<ul style="list-style-type: none"> Units of 1D (In the monometric range, there are 2 dimensions) 	<ul style="list-style-type: none"> Nanotubes, filaments, fibres, whiskers, belts, spirals, columns, springs,
<ul style="list-style-type: none"> Units of 2D (In the monometric range, there are 1 dimension) 	<ul style="list-style-type: none"> Layers

II.1.1.1 Nanoparticles characteristics

Nanoparticles have characteristics like high surface area, surfaces which are active and special optical & chemical responses. The material which have nano particles have large surface areas which increases rapidly with decreases in diameter of particle. The surface energy will increase as result of increase in proportion of particles on the surface of the material as increase in area of material. And this large surface to volume ratio also administers driving force for diffusion at high temperature and pressure. Micrometer scale including wettability, coalescence, mass transfer effects, transient phenomena are the

processes at the nanometer which are related to the EOR. We argue that at this scale & with the use of these phenomena for the EOR process understanding of oil phase distribution, oil drop mobilisation, oil bank formation is required. EOR is dependent on process at the nanoscale and extend to macro & micro scale.

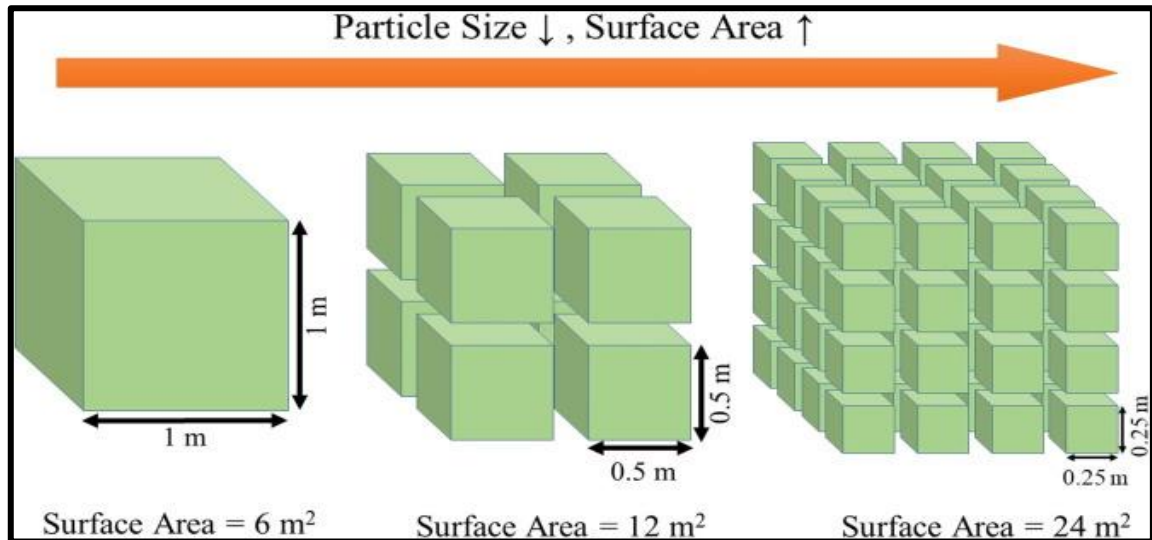


Figure II.2: High surface area relative to volume of nanoparticles

II.1.1.2 Silica Nanoparticles (SiO₂)(SiNPs)

Silica-based nanoparticles are commonly studied for enhanced oil recovery due to their easy production, well-known properties, and ability to be engineered for different characteristics. They are abundant, non-toxic, and cost-effective compared to other nanoparticles. Different types of engineered silica nanoparticles exist, categorized based on wettability behavior. Studies have shown that hydrophilic silica nanoparticles can be adsorbed onto pore walls, changing wettability, and improving oil recovery. Further research has shown that silica nanoparticles dispersed in fluids can alter wettability and reduce oil-water interfacial tension. Coreflood experiments have demonstrated that silica nanoparticles can improve oil recovery, with earlier injection being more effective. In heavy oil recovery, silica nanoparticles dispersed in brine have significantly increased recovery rates.

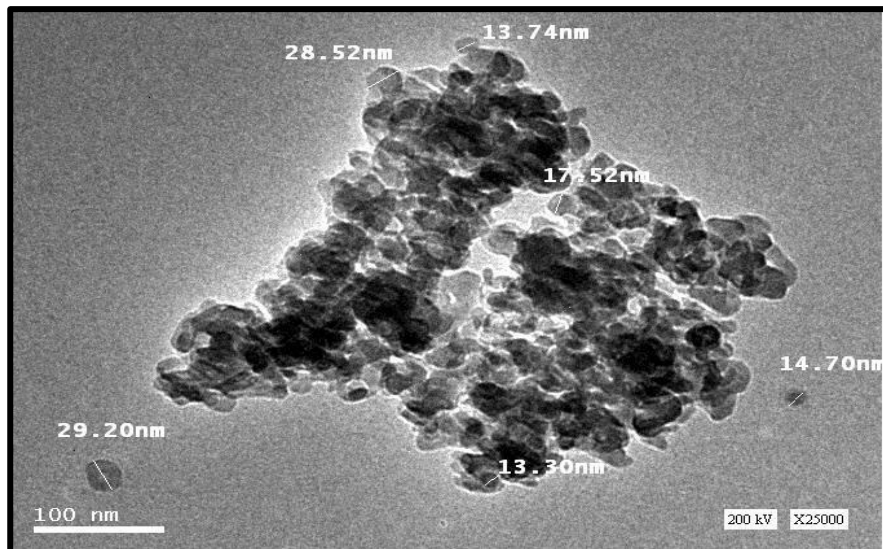


Figure II.3 SEM of nano-silica

Maghazi et al. studied the combination of silica nanoparticles with polyacrylamide for enhanced oil recovery, finding that adding 0.1 wt % of silica NP improved the polymer solution's pseudo-plasticity and overall viscosity, resulting in up to 10% additional oil recovery. Sharma et al. discovered that silica NP dispersed in a polymer and surfactant mixture could lower interfacial tension, leading to 21% extra oil recovery compared to conventional methods. Nanofluid mixtures also exhibited stable behavior at high temperatures for chemical EOR. Attar Hamed et al. showed that hydrophobic silica NP in CO₂-water foam improved stability, with optimal NP size varying based on concentration. Silica NP is cost-effective and eco-friendly, but safety risks should be assessed.

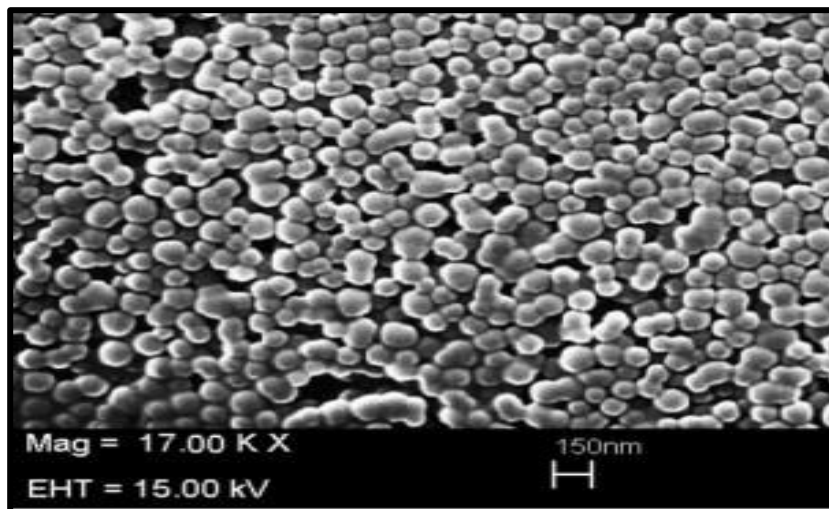


Figure II.4 : silica nanoparticle Dispersion (SiO₂, Purity: 99.9%)

II.1.2 Nanoclays

Nanoclays are nanoparticles made up of mineral silicate layers. Nanoclays are classified into various classes based on their chemical composition and nanoparticle morphology. Commonly found nanoclays are montmorillonite, bentonite, kaolinite, hectorite, and halloysite. For example, montmorillonite is made up of numerous overlapping layers of crystal particles with a diameter of 100-200 nm and an average thickness of 0.96 nm. The chemical composition of nanoclays can be easily determined using inductively coupled plasma, Fourier transforms infrared spectroscopy, X-ray diffraction and gravimetric analysis. Depending on the surface layered charge and the types of interlayer ions there are two forms of nanoclays such as cationic and anionic. Preparation of nanoclays and organoclays in aqueous or solid form employs charged (hydrophilic) molecules such as phosphonium or imidazolium, alkyl, or aryl ammonium. The ion exchange reaction involves two effects: it increases the distance between single sheets, allowing organic cation chains to move between them and it alters each sheet's surface qualities from hydrophilic to hydrophobic or organophilic.

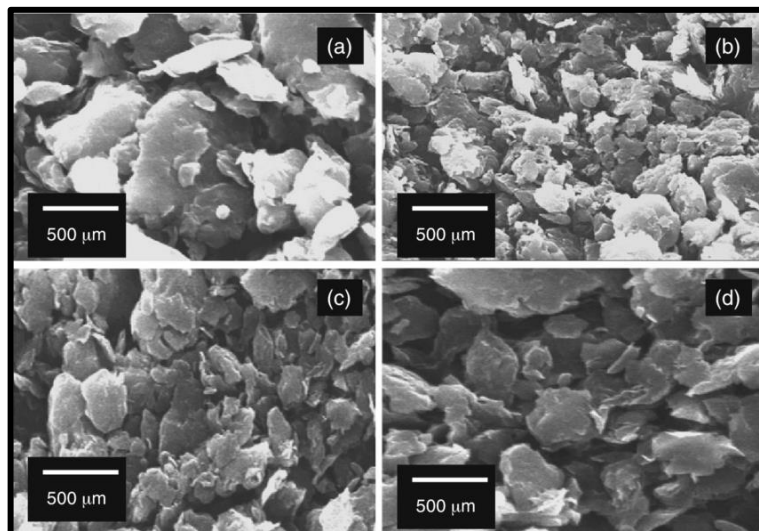


Figure II.5: SEM images for nanoclay

II.2 nanoflooding

Nanofluid flooding (also called nanoflooding) is a new chemical EOR technique whereby nanomaterial or nanocomposite fluids are injected into oil reservoirs to effect oil displacement or to improve injectivity (A. I. El-Diasty and A. M. Aly, 2015). This technique has the potential to produce a greater portion of the 50% of in-place oil reserves, which is

currently not recoverable by conventional primary and secondary recovery methods, nor even by conventional EOR, such as polymer or surfactant flooding

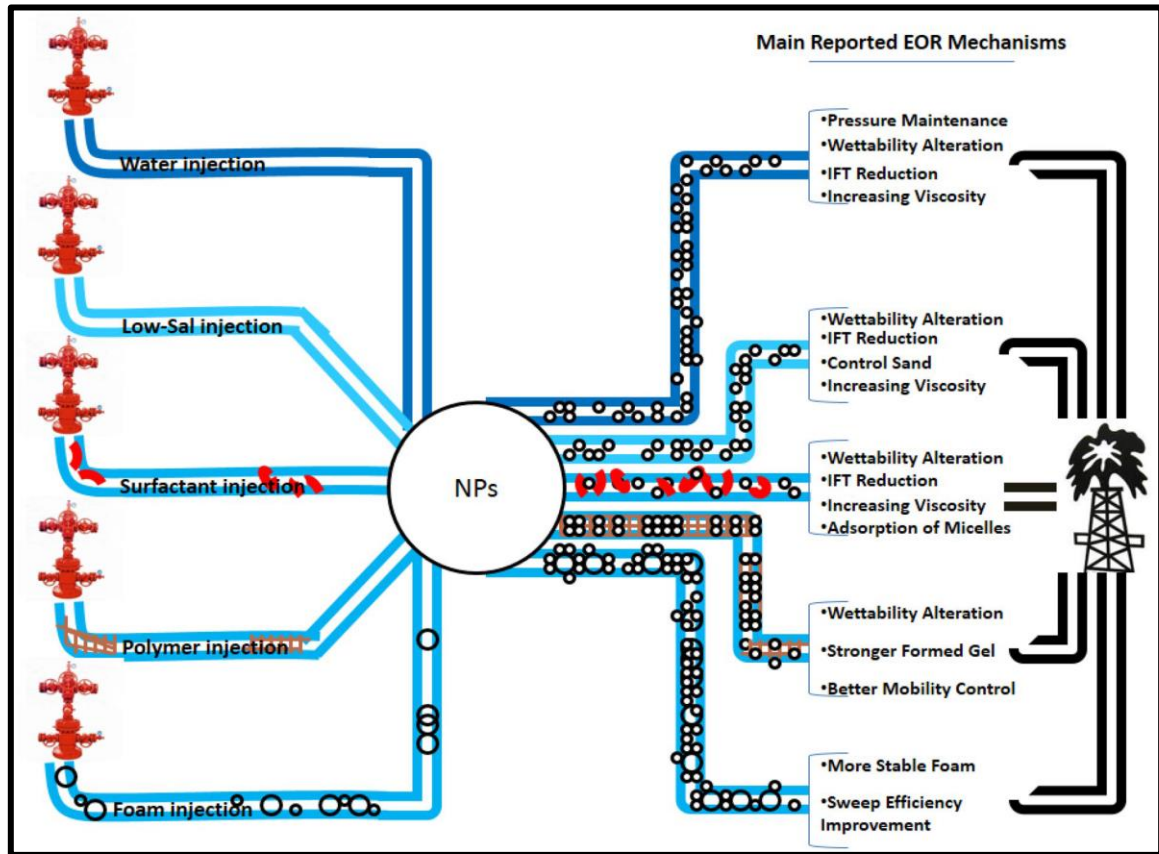


Figure II.6: Schematic illustration of the main reported EOR methods

II.2.1 The Mechanisms of nanoparticles in EOR

When nanoparticles are used as novel EOR agents, it is critical to understand their EOR mechanisms. Some EOR mechanisms have been discovered in recent research of nanofluid, oil, and rock interactions. The EOR processes of nanoparticles (NPs), on the other hand, are still a mystery. Nanofluids, nanocatalysts, and nanoemulsions are three key techniques to using NPs in EOR processes today. The parts that follow go over their respective EOR mechanisms.

II.2.1.1 Nanofluids

A nanofluid is a colloidal suspension of nanoparticles in a base fluid with an average particle size of fewer than 100 nm. The base fluid might be any liquid, including oil, water, or gas. Nanofluids are frequently utilized to aid in flood recovery since they are made by dissolving different NPs in water or brine.

EOR processes of nanofluids have been explored in the literature, including disjoining pressure, pore channel clogging, injection fluid viscosity increase, interfacial tension (IFT) decrease, wettability alteration, and blocking asphaltene precipitation. At a discontinuous phase such as oil, gas, paraffin, or polymers, nanoparticles in an aqueous dispersion will arrange themselves into structured arrays. For nanofluids, three distinct mechanisms have been proposed.

II.2.1.1.1 Difference in Densities

The density differential between water and nanoparticles causes nanoparticles to clump together at the entrance of ultra-small holes' throats. The agglomeration causes the injected fluid to migrate towards neighboring pores and pressurize them. As a result, the oil in nearby pores moves and produces. The displacement of the oil reduces pressure, resulting in the gradual restoration of pore blockages. Under these conditions, the carrier fluid can displace the nanoparticles once more.

II.2.1.1.2 Pore Channels Plugging

The propagation of nanoparticles in the porous medium is affected by some key mechanisms including, physical filtration, solution chemical stability, and adsorption on the rock's surface. For instance, the occurring of physical filtration when the size of NPs is larger than the dimensions of the pore. In addition, the mechanism of the well-dispersed nanoparticles, when injection process is achieved in low permeability rocks. Furthermore, solution chemical stability, states to the solubility of nanoparticles, which the large salinity cause to the low stability of the chemicals that will cause the precipitation of nanoparticles. In the case of adsorption mechanism, may obstacle the transportation of nanoparticles from the porous medium by adsorbing into a solid surface. Decreasing adsorption on the rock to improve the EOR process economically. Obviously, various mechanisms can decrease the concentration of nanoparticles when the nanofluids enter the porous media. As result of that is the pore channel plugging which the pore channels plugged by the mechanical entrapment or log-jamming as shown in the Figure.

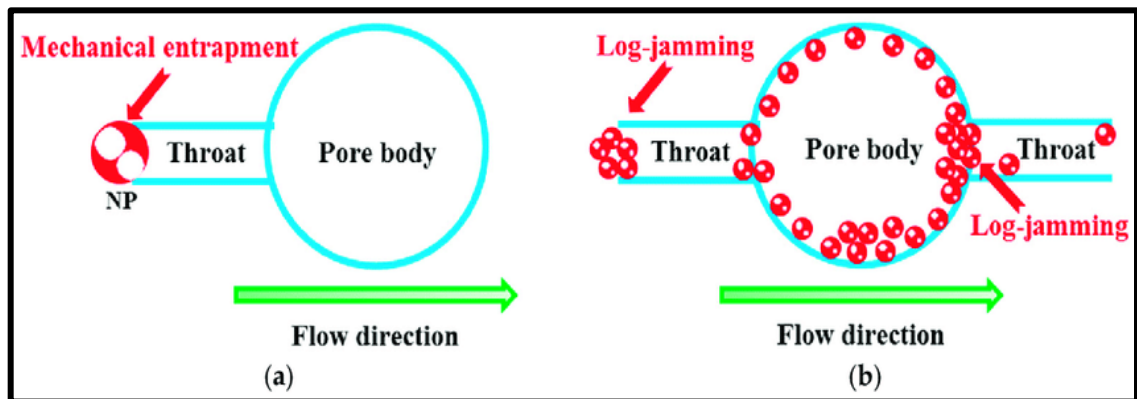


Figure II.7: Mechanisms of pore channels plugging

The first mechanism is mechanical entrapment which has occurred when the size of pore throat of the rock is smaller than size of injected nanoparticle. The pore throats size is in micro-scale, that their size is larger than NPs size thousand times. Hence, nanoparticles are effortlessly capable to cross through the pore throats of the rock without any mechanical entrapment mechanism. However, it is demonstrated that the blocking of the pore throat is because of large size of nanoparticles. To avoid this mechanism effect, the size of the injected nanoparticles should be smaller than the pore throats size. The second mechanism is Log-jamming which has resulted because the movement of the nanoparticles in a very small pore throat of rock, where the variance of density between water and the nanoparticles, making them to accumulate. Consequently, the diameter of pore will decrease, and blockage will happen. Because of this plugging, in the adjacent pores pressure will rises which forces the oil to flow out of pore. When the oil is released, pressure declines in the edges of the pore, blockage resulted by nanoparticles is gradually dissolved and they tend to flow with the flowing water. However, the mechanism of log-jamming mostly depends on the pore throats size, amount, and size of nanoparticles in nanofluids.

II.2.1.1.3 Changes in Wettability

Flooding the system with nanofluids improves the system's wettability quality. Nanoparticles also have an impact on the density of the injecting and reservoir fluids. Silicone nanofluids are frequently utilized to achieve this technique. As previously stated, these nanoparticles can have varying degrees of wettability. For neutral and hydrophobic nanoparticles, alcohol is an appropriate solvent, whereas hydrophilic nanoparticles are properly suspended in watery settings. Changing these nanoparticles' wettability from oily to neutral or watery, and vice versa, is the most common manufacturing procedure.

Adsorbing nanoparticles with the appropriate wettability changes the wettability of the rock surface. Overall, wettability is an important factor affecting displacement efficiency of fluid in porous media that subsequently increases oil recovery. Altering the wettability of rock from strongly oil wet (hydrophobic) to water wet (hydrophilic) is the most efficient method for enhanced oil recovery applications.

measurement of contact angle presented that there was change of rock wettability from oil wet to water wet condition. They also described that the presence of the NPs in the aqueous solutions in the porous media improved EOR through the alteration of wettability from hydrophobic to hydrophilic. However, in the porous media the trapped oil droplets are mobilized through IFT reduction as illustrated in Figure. In addition, through wettability alteration the impact of capillary pressure was altered from being a barrier force to a driving force. The influence of NPs size on the incremental oil recovery through wettability variation was taken through measurement of the contact angle.

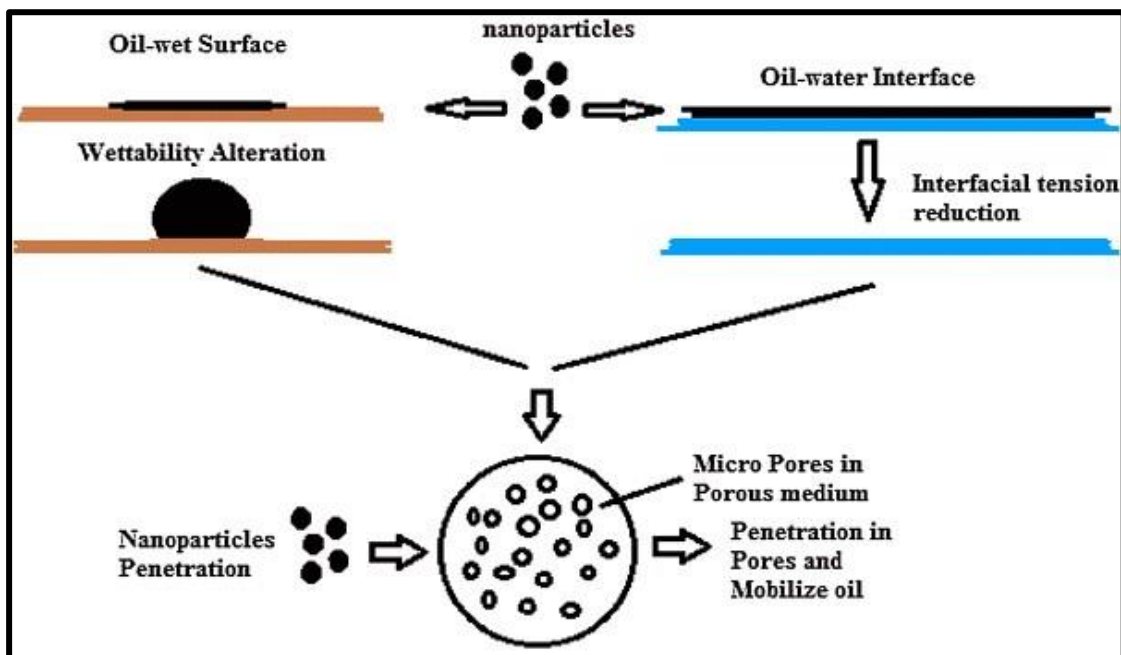


Figure II.8: Wettability-alteration-and-interfacial-tension-reduction-by-nanoparticles

II.2.1.1.4 IFT Reduction

The reduction in the IFT is a vital mechanism for achievement of miscibility and increases the efficacy of water flooding process. IFT is usually affected by some parameters like salinity, pH, asphaltene content of crude oil, etc. (Behrang M, 2021). There are numerous evidence that prove NPs are capable of reducing the interfacial tension (IFT) of oil and water. Hydrophobicity and hydrophilicity of NPs play key roles in attachment of NPs

to the interface of immiscible fluids. The next equation describes the dependence of adhesion energy on contact angle. This equation could be used to investigate the behavior of NPs at the interface of fluids (Mostafa Iravani¹ · Zahra Khalilnezhad² · Ali Khalilnezhad¹, 2023):

$$\Delta E = \pi R^2 \sigma_{12} (1 \pm \cos \theta_{12})^2 \quad (\text{II.1})$$

where E represents adhesion energy, R is the radius of particle (nm), σ_{12} defines the interfacial tension between 2 fluid phases (mNm^{-1}) and θ_{12} is the contact angle of particle at the surface of fluids. In fact, the required energy for detachment of NPs from interface could be calculated by this equation. Obviously, the magnitude of adhesion energy for smaller particles is lower than greater ones. Therefore, the interfacial attachment of smaller particles is less than larger ones.

Hosseini et al. examined the effects of NPs concentration in the range of 0.01–5 wt% on IFT. Finally, they concluded that increasing the concentration of nanoparticles decreases IFT. Also, they expressed that NPs could decrease the value of IFT about 50%. However, this value is not as high to the extent that be considered as a significant EOR mechanism (Hosseini E, 2019) .

Rezvani et al. checked out the potential of ZrO₂ NPs for application in EOR process at reservoir conditions. They observed that the addition of zirconium oxide NPs to the diluted formation water reduces IFT. Also, by observing the behavior of various concentrations they claimed that there is an optimum concentration for zirconium oxide NPs. Further addition of NPs for obtaining nanofluids above the optimum concentration causes an inverse trend, and IFT increases directly with any increase in concentration (Rezvani H, 2018).

The tendency of NPs for attachment to the interface of fluids, on the one hand, and their catalytic effect in asphaltene adsorption, on the other hand, are the main reasons for forming a layer between oil and water. Due to their tendency for adsorption of asphaltenes, mass transfer between fluids increases in the presence of NPs and sequentially IFT decreases.

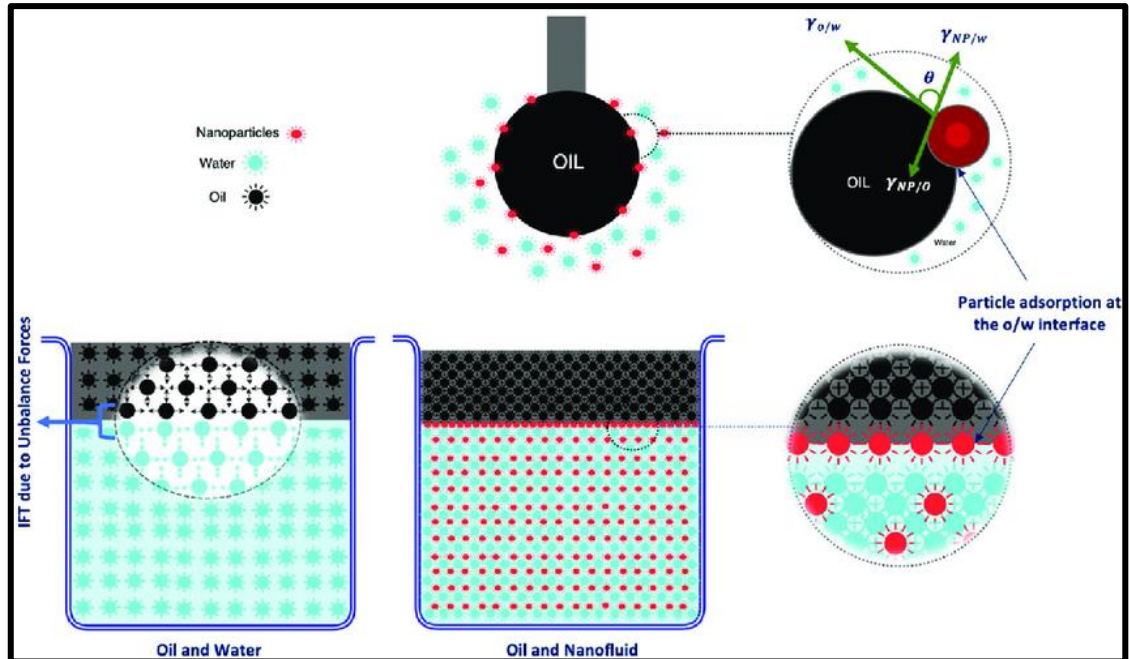


Figure II.9: Mechanism of IFT reduction using NPs showing particle adsorption (contact angle) at the oil-water interface and formation of a monolayer which replaces the existing oil-water interface.

II.2.1.1.5 Disjoined pressure

This is the pressure that allows the fluid to detach from the solid surface by resisting the fluid's adhesion force. The pressure difference between the thin layer of fluid and the bulk of the fluid is called this. Nanoparticles at the interface of a discontinuous fluid form a wedge-like layer as a result of this activity. Brownian motion and the electrostatic repulsion force between nanoparticles contribute in the construction of such devices. The repulsive forces are stronger with smaller nanoparticles. Furthermore, when the concentration of nanoparticles rises, this force becomes stronger. The pressure at the interface of two fluids is increased when nanoparticles are arranged in this way.

The increasing number of particles in the fluid will result in stronger forces at the interface. One of the driving forces for extracting oil from a rock's pore region is structural disjoining pressure. The shape of the nanoparticle raises the disjoining pressure in the nanoparticle wedge film during nanoflooding, as seen in Figure, with higher pressure at the wedge tip than in the remainder of the meniscus.

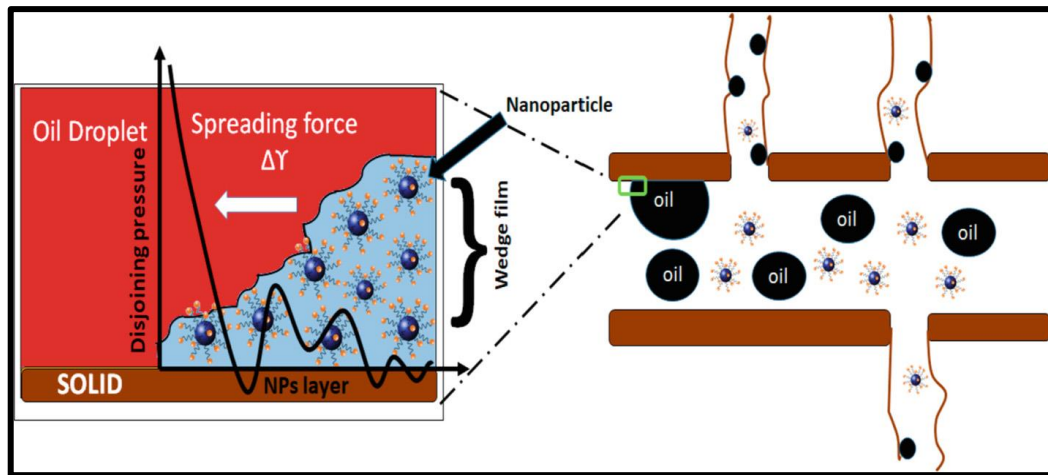


Figure II.10: Disjoining pressure in porous medium for oil extraction mechanism

II.2.1.1.6 Decreasing the Mobility Ratio of Injected Fluids

Another important dimensionless number in EOR is mobility ratio, which is the ratio between the displacing fluid and displaced fluid. A higher mobility ratio is desired for more oil displacement, under which has a higher sweep efficiency and less fingering effect in the reserve (Thomas, *Oil Gas Sci*, 2008). Nanofluids have been reported to be used to reduce oil viscosity and increase displacing fluid viscosity. Both factors will contribute to increase mobility ratio and as a result, boost oil recovery ratio (N. A. Ogolo, 2012.).

viscosity increases with higher NP concentration and brine salinity. Different NPs, such as SiO₂, Al₂O₃, and iron oxide, have varying effects on viscosity, with iron oxide showing potential for improving sweep efficiency. Overall, nanofluids offer a versatile solution for enhancing EOR processes by effectively controlling mobility ratios and improving sweep efficiency.

II.2.1.1.7 Preventing Asphaltene Precipitation

Preventing asphaltene precipitation is crucial for improving oil recovery. Some NPs have the tendency to reduce the viscosity of oil by preventing asphaltene precipitation and cracking the long chains (Mostafa Irvani1 · Zahra Khalilnezhad2 · Ali Khalilnezhad1, 2023).

In fact, asphaltene content was reduced from 28.7% to 12.9%, API gravity increased by approximately a 50%, and the viscosity reduction was around 78%. All these results are explained by two main mechanisms, where viscosity reduction is caused by a re-organization of the crude oil viscoelastic network by the strong interactions between asphaltene and

nanoparticles that are generated and by the catalytic activity of the nanoparticles (Oscar E. Medina 1, 2019).

Researchers have found that nanoparticles (NPs) can effectively solve asphaltene issues without causing environmental harm. Studies have shown that NPs can stabilize asphaltene precipitation, with SiO₂-Al₂O₃ nanofluids delaying precipitation as concentration rises. Experiments with SiO₂, NiO, and Fe₃O₄ NPs demonstrated that NPs adsorbed onto asphaltene molecules' surfaces, reducing flocculation in porous media. Factors like asphaltene content, water content, temperature, and contact time influence asphaltene adsorption onto NP surfaces, with more asphaltene adsorbed over time, at higher concentrations, lower temperatures, and less existing water. Overall, NPs show promise in preventing asphaltene precipitation and enhancing EOR techniques.

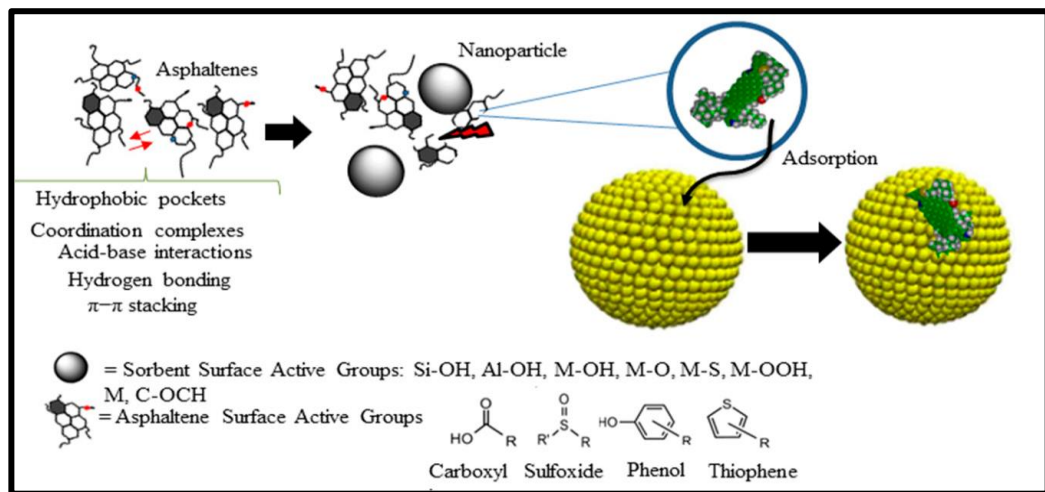


Figure II.11: Asphaltene adsorption mechanism on nanoparticles

Note: The interactions between the nanoparticles and the asphaltenes are favored by the functional groups present in the molecular structure of each one, depending on the nature of the nanoparticle, this will have active groups such as Si-OH, Al-OH, M-OH among others.

II.2.2 Factors controlling success of nanoflooding

II.2.2.1 NP size

The existence of tight and tortuous paths in porous media is a challenging factor for application of the nanoparticles. Mean free path and pore size distribution are two vital properties which should be considered before selection of any nanoparticles for EOR procedure.

Nanoparticle size and charge concentration impact disjoining pressure intensity. Small nanoparticles increase particle density and reduce fluid-rock contact angle. Higher particle density enhances structural disjoining pressure. Smaller particles spread better on less hydrophilic surfaces and exhibit stronger electrostatic repulsion. Small particles enhance oil recovery and displacement efficiency. Reducing particle size boosts oil extraction rates and increases disjoining pressure.

II.2.2.2 NP concentration

High nanoparticle concentration caused blocking of the pore network, significantly in low-permeability rocks, which led to no additional oil recovery. Thus, nanoparticle concentration was found to be a critical parameter for nano-EOR (Akram Al-Asadi, 2022)

II.2.2.3 Salinity

The salinity of nanofluids and reservoir fluids affects dispersion stability. High salinity reduces particle zeta potential, leading to agglomeration. Ionic strength from salt decreases electrical repulsion, favoring van der Waals forces. High salinity requires NP modification for stability, achieved through surface modification or ionic control with a surfactant. Adsorption of NPs increases at high salinity, altering rock wettability and improving oil recovery. However, high salinity reduces NP stability, emphasizing the need for optimal salinity levels and surface modifications to prevent agglomeration.

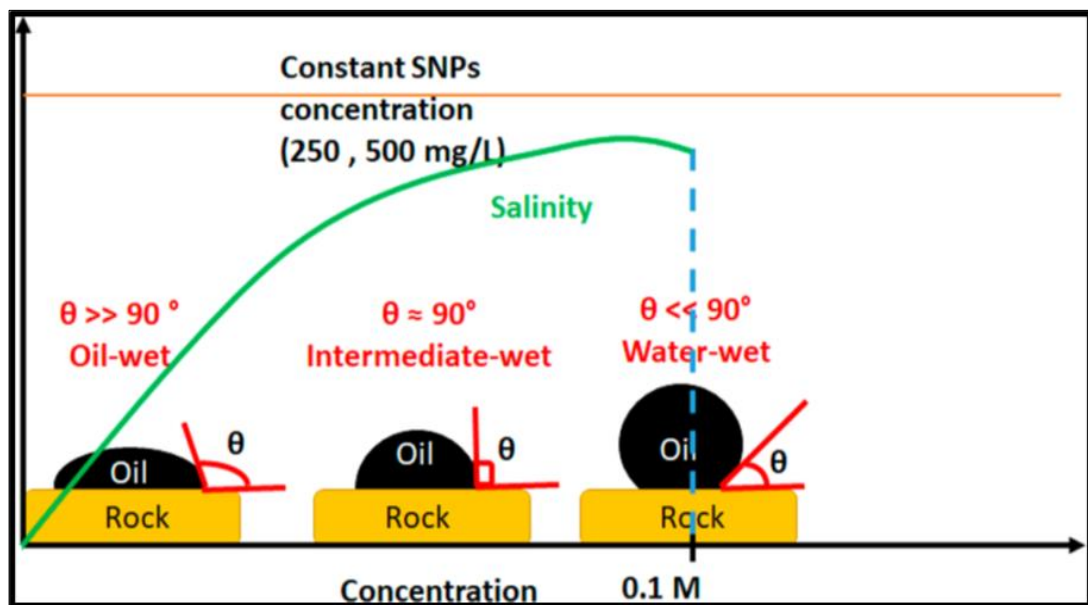


Figure II.12: Effect of increasing salinity at constant silica NPs concentration on the wettability change of carbonate rocks.

II.2.2.4 Reservoir temperature

Nanofluids can operate effectively at elevated temperatures in nano-EOR applications. Temperature has a minimal impact on NP retention, but significantly influences oil recovery by altering reservoir fluids at a molecular level. Further research is needed.

II.2.2.5 Rock wettability

Enhancing rock water-wettability boosts oil recovery while the opposite reduces it. Morrow explains how strong water wetness aids efficient oil displacement, but there are exceptions. Oil-wet and neutrally wet reservoirs can also increase oil recovery. Wettability's crucial in hydrocarbon mobility, affecting distribution and displacement within the matrix. During nano-EOR, initial wettability determines the success of wettability alteration. Studies show that intermediate-wet conditions yield the highest oil recovery through nano-EOR. Research into factors influencing nano-EOR is vital for its successful real-world application.

II.2.2.6 The rock grain size

The rock grain size is expected to be a factor that may impact the holding of nanoparticles. The area of the surface of the porous medium is related to the grain size. If rock grains are larger than it results in decrease in the surface area per unit bulk volume. The porosity of larger grain size is greater than the smaller one. When reduction in surface area per unit bulk volume decreases, then the retention of the nanoparticles on the rock also decrease. Also, mechanisms like naturally occurring fines entrainment and redeposition can cause abnormal productivity decline.

II.2.2.7 Clay content

Nanoparticles retention on the rock can be affected by the clay content. As the clay occupies empty space between grains, there will be great reduction in porosity as the clay amount increases. Also, with increasing content of the clay, retention of nanoparticles increases on the reservoir rock. This happens due to greater surface area per unit volume of bulk of clay particles, as it allow more sites with more surface area at which particles can be retained and attached.

II.2.2.8 Reservoir permeability effect

Some Berea cores of sandstone with permeability ranging from 7 to 223 mD have been conducted flooding of nanofluid about 7 nm and 0.05 wt % to notice the effect of rock permeability on oil recovery increment (Luky, 2013). But results show that there is no

proportion relationship of oil recovery increment with increasing permeability. Also, the results show that even in low permeability, the nanofluid can work. Thus, nanofluid is effectively applicable in a variety range of reservoir permeability.

II.2.2.9 Rate of injection

Nanoparticles flowing through porous medium have been classified into two types of particles retention in pores: pore surface deposition and pore throat blocking. Mechanical entrapment and log-jamming (accumulation) are two main reasons for pore throat blocking. It occurs because a single particle is greater in size than the size of pore throat. Bridging of pore throat takes place if two or higher numbers of particles are trapped at pore throat. Blocking and bridging plugging of throat is stochastic in nature and causes some of throat for close of flow. As injection rate increases, smaller molecules of water will accelerate faster than nanoparticles, so it will assemblage and block pore throat, and thus recovery of oil is reduced. So, it is expected that as the injection rate increases, the nanofluid injection effect on oil recovery will be reduced as the nanoparticles will assemblage at pore throat. Thus, further reduction happens in absolute permeability and thus recovery factor decreases (Luky, 2013).

II.3 Enhancing the Stability of NPs

The widely used technique to enhance the stability of nanoparticles is to use polymers or surfactants as dispersants or sometimes to coat the nanoparticles with a polymer (Shamsijazeyi, Miller, Wong, Tour, & Verduzco, 2014). However, it is important to mention that the stability of most nanoparticles in the presence of surfactants usually depends on the charges of each of them as well the concentration of the nanoparticles suspended (Allam, 2019).

On one hand, if the suspension of the NPs is supplied with high concentration of surfactant followed by polymers, the surfactant particles are adsorbed on the NPs while micelles are formed in the solution surrounded by the polymer. On the other hand, adding the polymer followed by the surfactant polymer mixture causes the adsorption of polymer chains around the NPs surface. Previously formed micelles surrounded by polymers attach to one another to cause the compaction of the polymer capsule that is initially adsorbed on the NPs' surface as shown in Figure

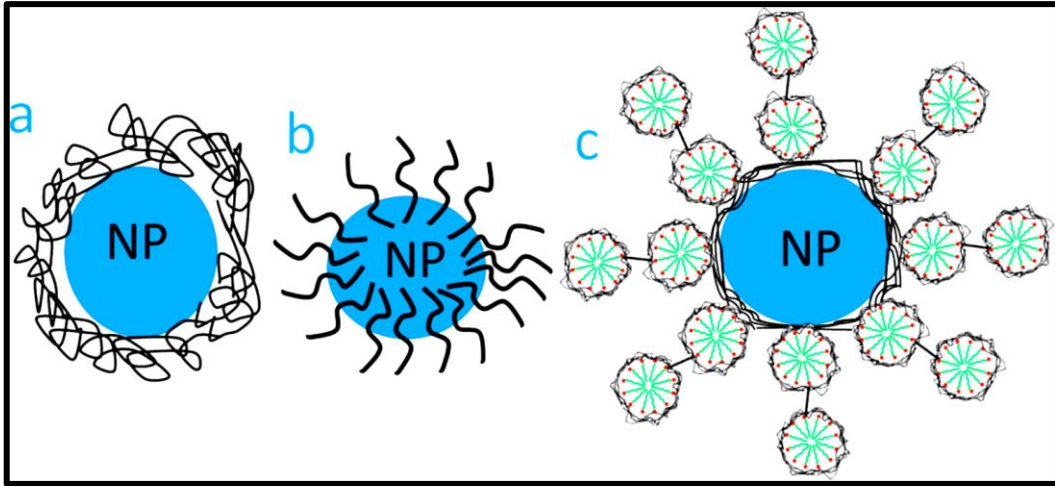


Figure II.13: Steric stabilization of nanoparticles using (a) polymer, (b) surfactant, and (c) polymer followed by a mixture of surfactant and polymer (Fiedot, Rac, Suchorska-Woźniak, Karbownik, & Teterycz, 2014).

There are some methods recommended for stabilization of NPs in various ranges of salinity. Jafari et al. stabilized hydrophilic silica in seawater by using H⁺ protection. This method refers to adding some amounts of HCl to nanofluid. The generated H⁺ ions protect the NPs from free ions in the bulk and increase the stability of nanofluids (Sofla SJD, 2018).



**Chapter III : Analyses and
experimental strategies**

Introduction

This study explores the potential of silica nanoparticles and nanoclay in nanoflooding to enhance oil recovery. Silica nanoparticles and nanoclay were selected for their distinctive properties, including the ability to modify interfacial tension, alter reservoir rock wettability, and enhance fluid mobility within pore spaces. By dispersing these nanoparticles in suitable base fluids, nanofluids are engineered to optimize oil displacement and recovery. The primary objective is to experimentally investigate how nanofluids interact with reservoir conditions, focusing on their efficacy in displacing trapped oil. This involves measuring saturation levels, porosity, permeability, oil recovery rates, recovery factors, and interfacial tension for each case using two types of micromodels: one based on pure sand and another incorporating sand with asphaltene. The experiments are conducted under ambient laboratory conditions at a temperature of 29°C.

III.1 Experimental Project

In this section, we present the materials, nanofluids, and porous media selected for this study, along with the experimental procedures employed.

III.2 Materials

III.2.1 Sand

Despite the fact that the majority of producing wells in Algeria are drilled in siliciclastic reservoirs and that most of the recent discoveries have been in unconsolidated sandy formations or poorly consolidated and cemented sandstones, we have therefore undertaken the reconstruction of identified sand samples. The sand sampling was carried out in the Sidi Khouiled Ouargla region, with a golden yellow hue.

III.2.2 Brine

It is a mixture of distilled water with sodium chloride NaCl (34g of NaCl / 100 ml). This brine is used for the liquid/liquid displacement of samples during all drainage and imbibition experiments.

III.2.3 Diesel fuel

Diesel fuel has been used in all single-phase and two-phase flow experiments and imbibition tests; therefore, it is used as the base fluid in formulating the micro emulsion. The diesel fuel used is commercialized by the company NAFTAL.

Table III.1: Properties of diesel fuel

Final boiling point	Initial boiling point	Pour point	Flash point	Dynamic viscosity	Density	Surface tension
320°C	152 °C	-14°C	88°C	5.6 mPa s	0.828g/cm ³	30mN/m

III.2.4 Silica powder

Table III.2: The Physical properties of silica fume (powder)

Physical state	Micronized powder
Odour	odorless
Appearance	White color powder
Color	white
Pack density	0.76 gm/cc
pH of 5% solution	6.90
Specific gravity	2.63
Moisture	0.058%
Oil absorption	55ml/100gms
Melting point	1710°C
Boiling point	2230°C

III.2.5 Clay powder

Bentonite is a type of clay composed primarily of the mineral montmorillonite. It's a very absorbent clay. Its chemical and physical properties are shown in table III.3

Table III.3: The Physical and chemical properties of clay (bentonite powder)

color	Light gray
texture	Soft, fine texture
density	2,7
Swelling	Bentonite can absorb several times its weight in water, causing it to swell and become gelatinous.
Cation exchange capacity (CEC)	high CEC

pH	8,9
----	-----

III.3 Samples characterization

III.3.1 Grain size analysis

The method of granulometric analysis allows us to identify the type of sediment of various sands by studying the distribution of grains in a sample based on their physical properties such as weight and size. Granulometry involves measuring the proportion of the total mass that corresponds to each particle size. All tests were conducted on sand samples.

Before starting the test, wash the sand with distilled water, then let it dry.

After drying, we begin the analysis by sieving using the HAVER BOEKHER sieve type D-59302 OELDE (shown in figure). The operation of this sieve is based on :

1. The location of superimposed sieves of decreasing sizes (0.250mm/0.200mm/0.160mm/0.100mm/0.080 mm) in the sieve.
2. Turn on the device.
3. Set the following Parameters : agitation mode (continuous agitation), and agitation time (10 min).
4. Place the sample in the sieve column.
5. Start the device by pressing the on/off button.

The sieves can only support 200g of weight, so we split this quantity each time.



Figure III.1: The sieve machine used in granulometric analysis.

III.3.2 X-ray diffraction image (XRD)

The degree of crystallinity of the samples was determined by X-ray diffraction analysis (XRD). The analysis was conducted using an Olympus Diffractometer (Sahara Geology Laboratory, University of Ouargla) with Cu-K α radiation ($\lambda = 1.5418 \text{ \AA}$) over a 2θ range from 0 to 50° , with a step size of 0.0131° and a dwell time of 122.145 seconds.

III.3.3 X-ray fluorescence (XRF)

Micro X-ray fluorescence (μ XRF) is a non-destructive elemental analysis technique, applicable to solid, liquid, or gaseous samples, either qualitatively or quantitatively. However, the analytical limitation of XRF lies in its inability to detect light elements (low atomic number): measurements of Hydrogen (H), Lithium (Li), and Beryllium (Be) are not possible, while those of Boron (B), Carbon (C), Nitrogen (N), Oxygen (O), and Fluorine (F) are very challenging.

III.3.4 Scanning Electron Microscopy (SEM) / X-ray microanalysis (EDS)

The SEM equipped with EDS used is a FEI model QUANTA 600 from CRAPC-Ouargla. The SEM analysis allows high-resolution observation under environmental conditions with a gas pressure in the chamber of up to 26 mbar. The analyses were conducted using energies ranging from 1 keV to 5 keV.

III.4 Characteristics of Chemical product

III.4.1 Extraction of nanoparticles

The extraction of silica nanoparticles begins with the precise preparation of the mixture, where five grams of silica are accurately weighed and introduced into 100 milliliters of brine solution. To ensure a uniform dispersion of the silica particles within the brine, an agitator is employed to homogenize the mixture for 10 minutes. This mechanical stirring is crucial for creating a consistent suspension.

Subsequently, a minimal quantity of hydrochloric acid (HCl) is added to the mixture. The purpose of this addition is to maintain the dispersion stability of the silica particles, preventing them from agglomerating and thus ensuring a more effective formation of nanoparticles. The mixture is then allowed to rest undisturbed for 45 minutes. This step is essential for the stabilization and precipitation of the particles. During this period, the interaction between the silica and the brine solution facilitates the formation of silica nanoparticles.

Once the stabilization period is complete, a syringe is used to carefully extract the suspended silica nanoparticles from the solution. This extraction must be done meticulously to avoid

disturbing the settled particles and to ensure that only the suspended nanoparticles are collected.

The next step involves passing the extracted solution through filter paper. This filtration process separates the solid nanoparticles from the liquid phase, capturing the silica nanoparticles on the filter medium.

Finally, the nanoparticles retained on the filter paper are left to dry completely. After drying, the weight of the nanoparticles is measured with precision, providing an accurate assessment of the yield from the extraction process.

Through these methodical steps, the extraction process efficiently isolates silica nanoparticles using brine as the medium, demonstrating a practical approach to nanoparticle production that is both scalable and cost-effective.

III.4.2 Preparation of Nanofluid

The preparation of nanofluids involves a systematic approach to disperse nanoparticles effectively within a base fluid, typically brine in this study, supplemented with a surfactant for stabilization. Initially, nanoparticles previously extracted are carefully measured to achieve desired concentrations. These nanoparticles are then introduced into 100 mL of brine, followed by the addition of 1.5 mL of surfactant to facilitate uniform dispersion. The mixture undergoes rigorous stirring for 12 cycles to ensure thorough mixing and even distribution of nanoparticles throughout the brine.

Furthermore, silica nanofluids are prepared across a range of concentrations including 0.01, 0.05%, 0.1%, and 0.5%, employing the same methodology of mixing with brine and surfactant, followed by agitation. Similarly, clay nanofluids are prepared at varying concentrations of 0.001%, 0.005%, and 0.01%, following identical steps for uniform dispersion.

III.4.3 Addition of polymer

To further enhance the properties of the prepared nanofluid, we incorporated 0.1 grams of biopolymer into 100 mL of the previously prepared nanofluid. This mixture was subjected to heating and thorough stirring to ensure complete dissolution and uniform dispersion of the biopolymer within the nanofluid. The heating process aids in reducing the viscosity and promoting better interaction between the biopolymer and the nanoparticles, thereby enhancing the overall stability and performance of the nanofluid. This method aims to

optimize the rheological properties and thermal conductivity of the nanofluid, making it more effective for various industrial and scientific applications.

III.5 Experimental apparatus and measurements

III.5.1 Experimental apparatus description and flow behavior in a porous medium

The installation of fluid displacement in a porous medium is represented in the figure (III. 2)

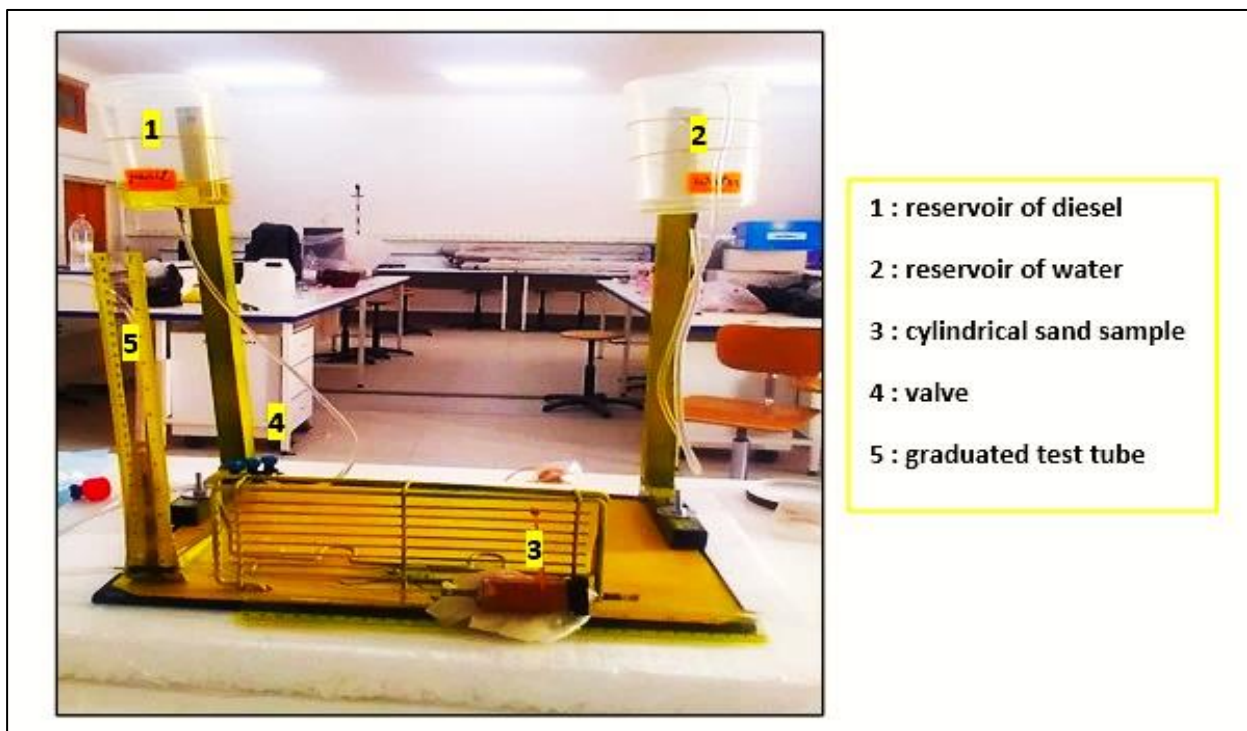


Figure III.2: The installation of fluid displacement in a porous medium

It consists of:

1. A cylindrical sample holder containing a porous medium.
2. Two feeding tanks (tank of diesel and the other one used to inject brine, silica nanofluid, clay nanofluid and polymer).
3. A graduated test tube allowing to measure the flow rate at the outlet of the porous medium using a stopwatch.
4. Valve to control the flow of injection

III.5.2 Porous media micromodels

➤ Sand micromodels

The cylindrical sand micromodel is shown in figure III.3



Figure III.3: cylindrical sand micromodel

➤ Sand and asphaltene micromodels

The sand was mixed with 7% asphaltene dissolved in oil and then left to dry for 24 hours to ensure the asphaltene adhered to the sand the micromodel is shown in figure (III.4)



Figure III.4: asphaltenic sand micromodel

III.6 Experimental procedure

The tests performed on the porous medium are carried out in four steps:

Step 01:

- 1- Saturate the porous medium with brine (Initial conditions of a porous medium with a water saturation of 100%).
- 2- Inject the diesel to displace the brine until the first drop of oil is recovered. In this case, the goal is to reach the irreducible water saturation (S_{wi}).
- 3- Determine the oil saturation volume (Amount in place in the system).
- 4- System imbibition by reinjection of brine.
- 5- Stop brine injection as soon as the first drop of brine is recovered.
- 6- Observe capillary rises in both types of capillaries (Determine the heights of the aqueous and oily phases).
- 7- Measure the volume of recovered oil (Oil recovered in the graduated cylinder).
- 8- Measure the oil recovery efficiency

$$R = \frac{V_r}{V_T} \quad (\text{III.1})$$

With, R is the oil recovery yield (%), V_r is the volume of oil recovered, V_T is the total volume of the micromodel corresponding only to the oil phase.

Step 02:

- 1- Injection of the prepared Nanofluid formulation into the micromodel.
- 2- Ensuring liquid/liquid displacement.
- 3- Measuring the volume of recovered oil (Oil recovered in the graduated cylinder).
- 4- Measuring the oil recovery efficiency.
- 5- Calculating the residual oil saturation.

Step 03:

1. Injection of the Nanofluid formulation prepared with a polymer into the micromodel.
2. Ensuring liquid/liquid displacement.
3. Measuring the volume of recovered oil (Oil recovered in the graduated cylinder).
4. Measuring the oil recovery efficiency.
5. Calculating the residual oil saturation.

Note:

The three previous steps are repeated using each type of Nanofluid and with different concentrations.

III.7 Petrophysical properties Measurements**III.7.1 Porosity measurement**

The measurement of porosity is done by:

1. Putting a quantity of sand (or sand with asphaltene) into a sample holder and weighing it.
2. Saturating the sample from bottom to top with brine.
3. Weighing the sample again.
4. Calculating the porosity by applying the following law:

$$\phi = \frac{m_{sat} - m_{dry}}{m_t} \quad (III.2)$$



Figure III.5: weighing the wet sand sample, saturated sand sample and asphaltene sand sample respectively

III.7.2 Permeability measurement

The absolute permeability of both the water phase and the oil phase is calculated following the preparation of the samples. Using Darcy's, we calculate the absolute permeability of both phases:

$$Q = K \cdot \frac{A}{\mu} \cdot \frac{dP}{dx} \quad (III.3)$$

Here,

Q represents the flow rate of the phase through the sample (cm³/s),

K is the absolute permeability of the flowing phase (Darcy),

A is the fluid passage area (cm²), μ is the fluid viscosity (cP),

dP is the pressure difference (atm), and dx is the sample length.

The process takes place in the subsequent stages:

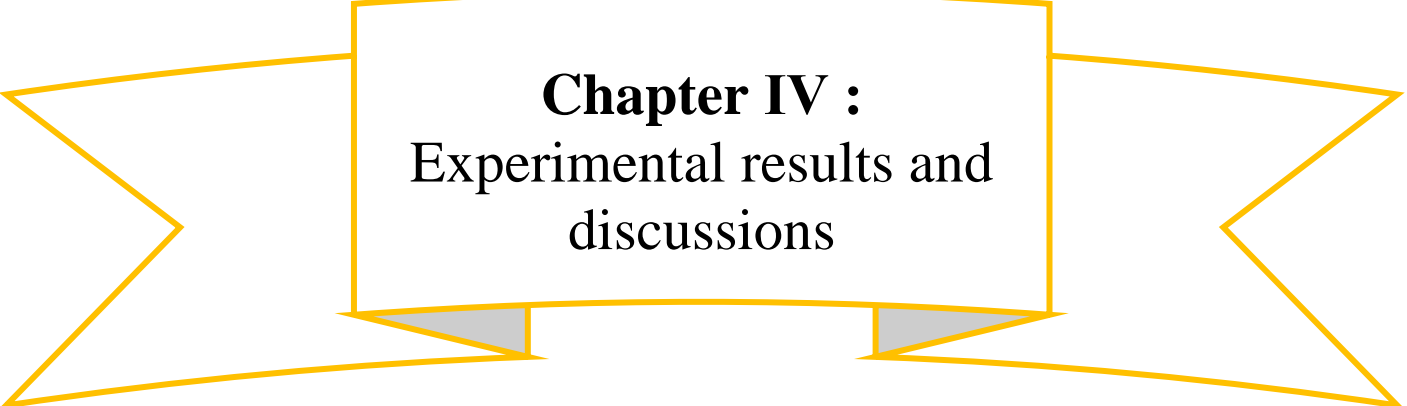
- 1- Sample placement in the fluid displacement setup
- 2- Injection of brine at constant flow rate (ensuring a regime of laminar axial flow).
- 3- A duration of one hour (stabilization time) is important to meet the conditions for applying Darcy's law (one-dimensional flow, laminar flow in an isotropic and homogeneous medium).
- 4- Once the stabilization state is reached, the values of flow rate, inlet and outlet pressure are recorded.
- 5- Calculate the absolute permeability of the brine.
- 6- The same procedure is carried out to determine the absolute permeability of diesel fuel.

conclusion

In this chapter, we have described in detail the experimental processes of Applying silica nanoparticles and nanoclay in nanoflooding to improve the efficiency of enhanced oil recovery.

The work is based on the characterization of sand and asphaltene.

The evaluation of both phenomena was based on the determination of the volumes of recovered oil for each system designed.



Chapter IV :
Experimental results and
discussions

IV.1 Samples characterization results

IV.1.1 Grain size analysis results

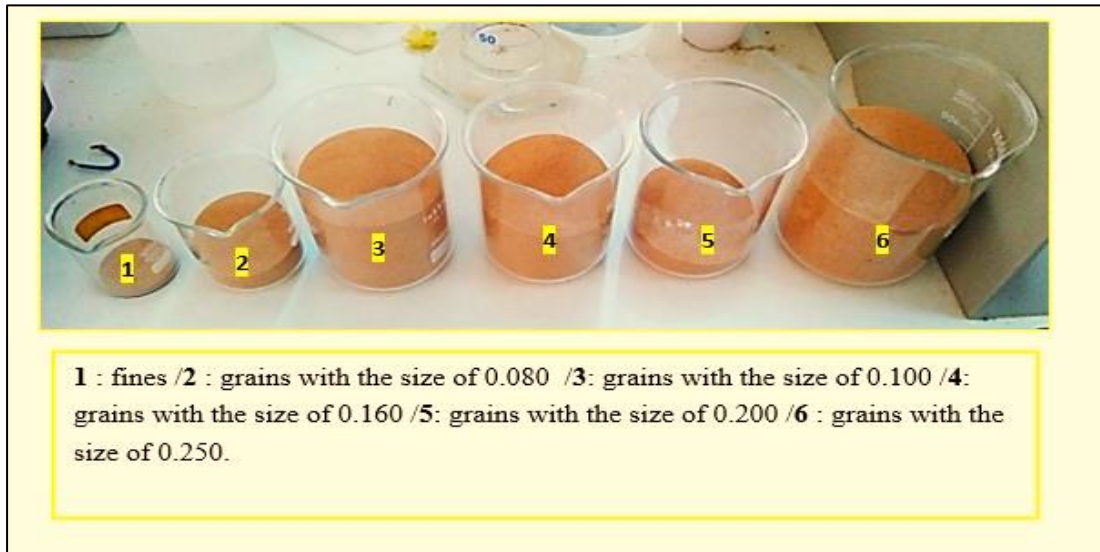


Figure IV.1: distribution of grain size (mm) in the weighted sand sample (10,865kg)

Table IV.1: The quantities and percentages of sand in each sieve in relation to the diameter of the sieves.

Sieve mesh in mm	Weight of sand (kg)	Percentages (%)
0.800	0	00%
0.500	0.075	0.70%
0.250	3.941	36.88%
0.200	0.611	5.71%
0.160	1.831	17.13%
0.100	3.210	30.04%
0.08	0.915	8.56%
<0.08	0.102	0.95%
Total	10.685	100%

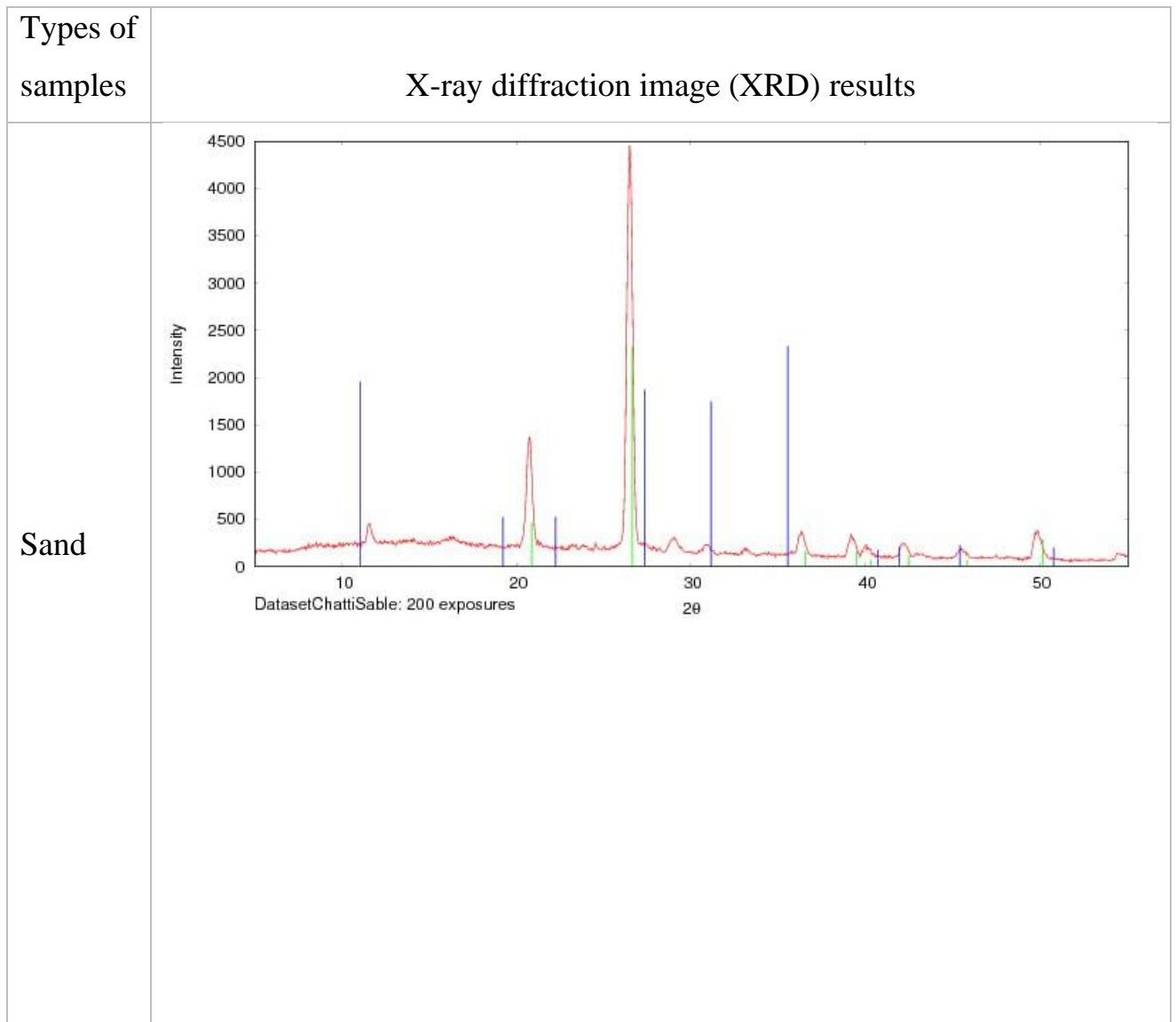
➤ Interpretation of the result

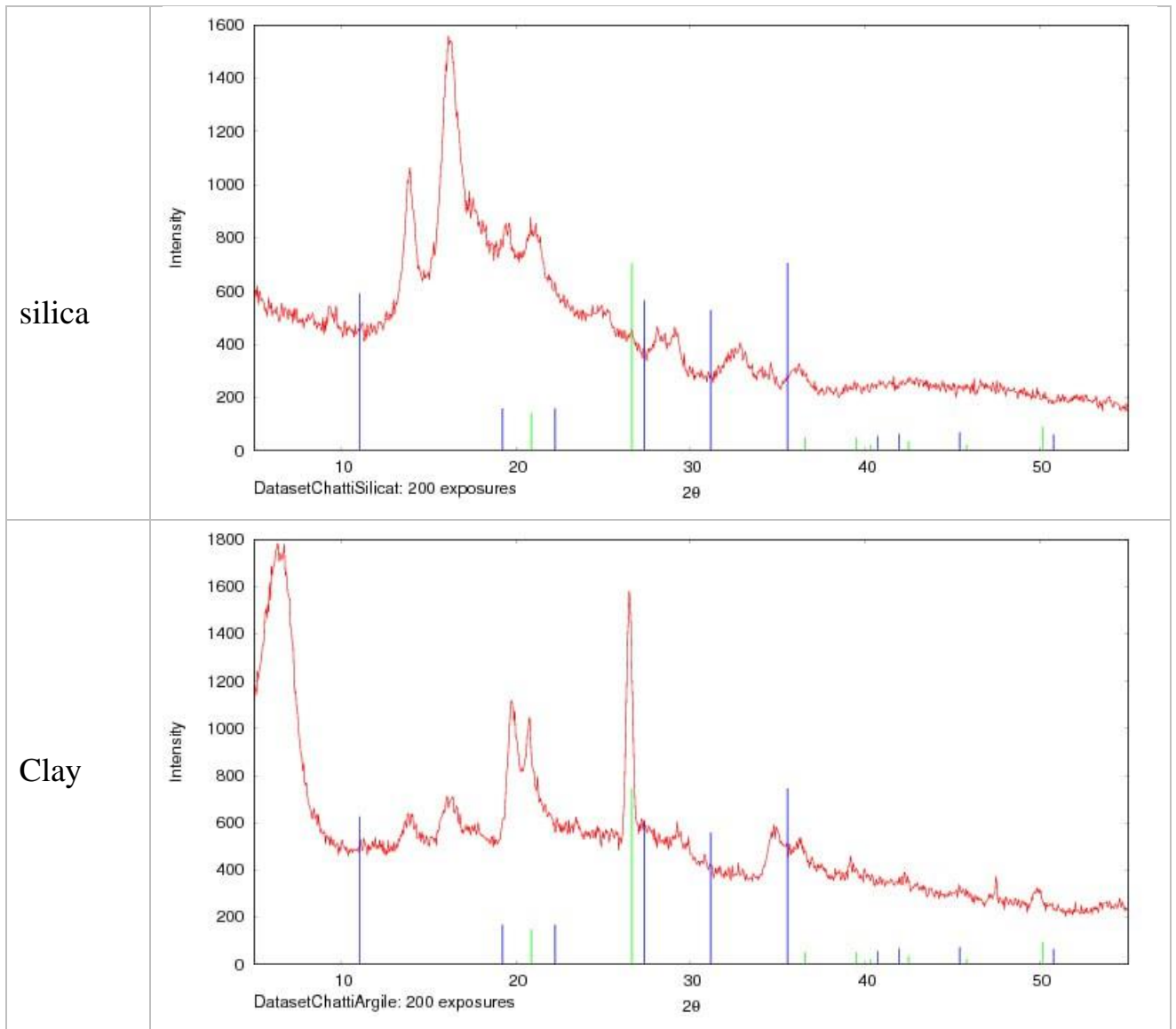
According to the results obtained, and the geological classification of the materials, we see that the sand used is sand with a majority of fine grains (0.160,0.100,0.250). For our study we did use the sample of the size 0.250 mm. we eliminate the use of grains <0.250 mm to avoid the phenomenon of fine migration.

IV.1.2 X-ray diffraction (XRD) results

The XRD results of the samples are shown in table number IV.2

Table IV.2: X-ray diffraction (XRD) results



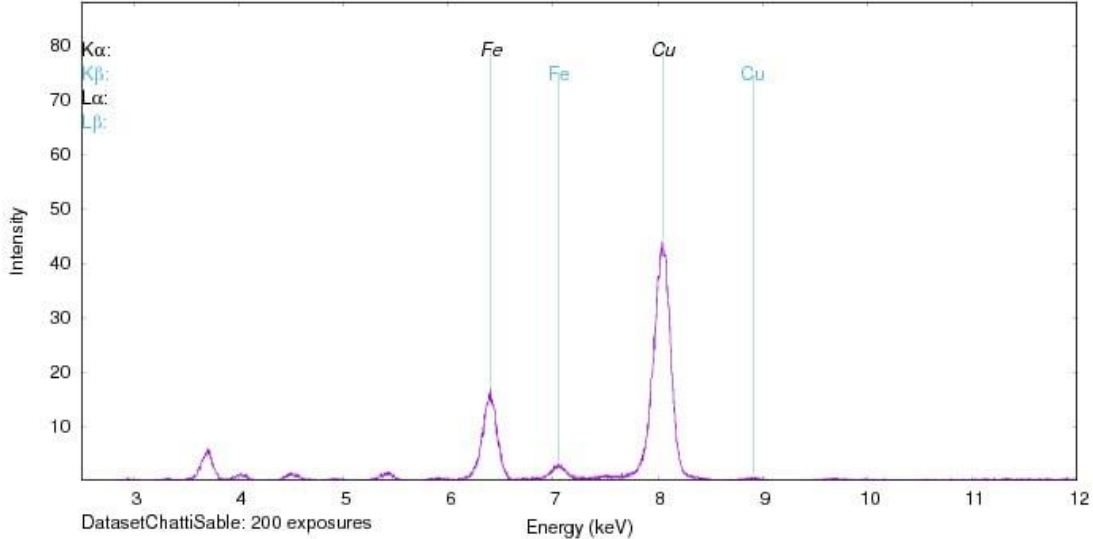


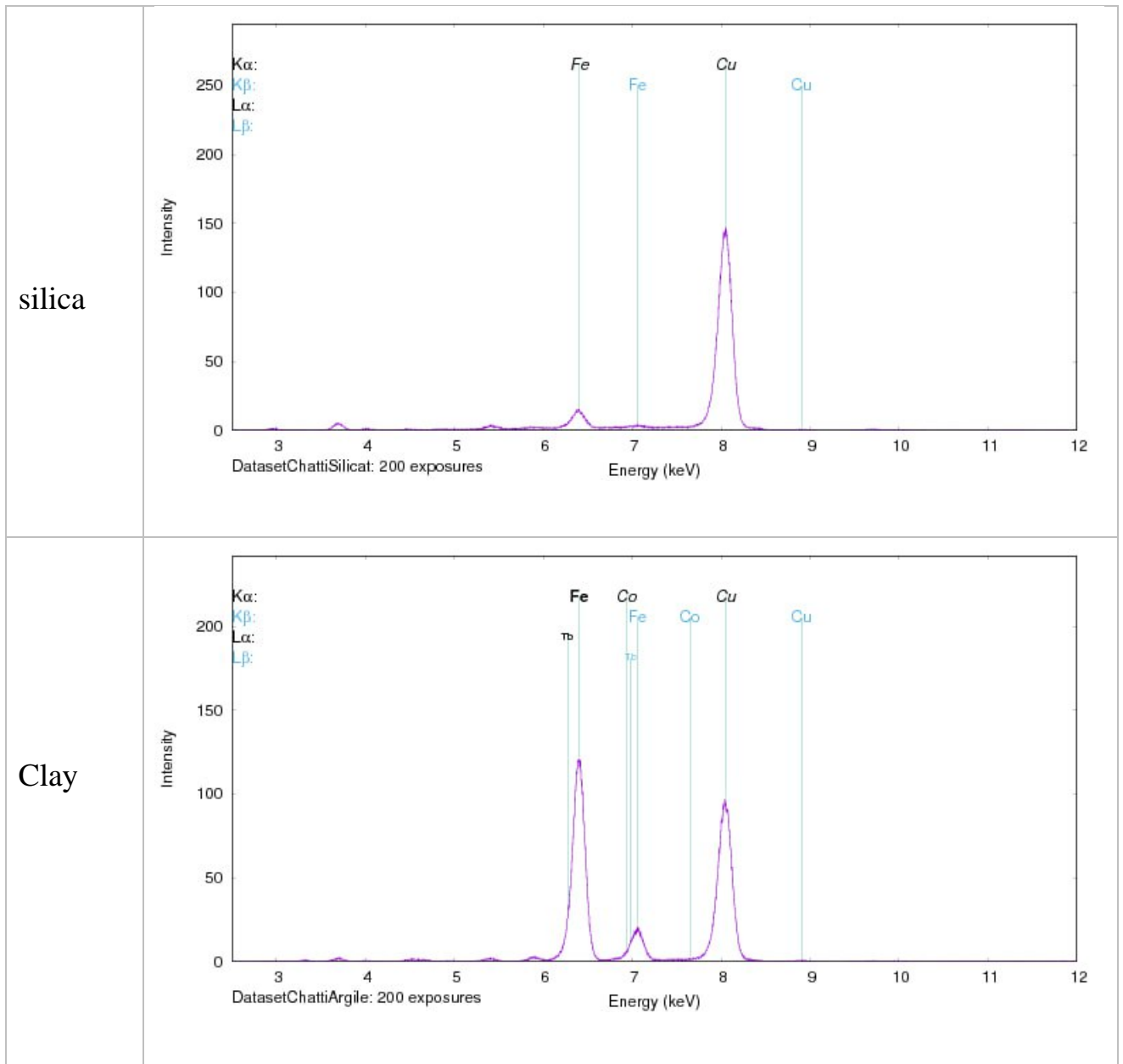
From the X-ray diffraction patterns of the samples, it can be observed that the XRD profiles of sand and clay exhibit a strong peak reflection at 26° , indicating a high degree of crystallinity. The broadening of the peak may suggest a lower degree of crystallinity or graphitization in the samples, as seen in the profiles of silica and clay.

IV.1.3 X-ray fluorescence (XRF) results

The X-ray micro fluorescence (table) shows that the samples (sand, silica) contain impurities such as Fe and Cu. It is noted that clay contains a large quantity of Fe and Cu, and a small amount of Tb and Co.

Table VI.3: Result of X-ray fluorescence (XRF)

Types of samples	X-ray fluorescence (XRF) results
Sand	 <p>Dataset: ChattiSable: 200 exposures</p>



IV.1.4 Scanning Electron Microscopy (SEM) / X-ray microanalysis (EDS) results

IV.1.4.1 Silica sample

In **Figure (IV.2.a)** the typical morphology of silica was shown, composed of crystals with sizes less than 10 μm . These particles contain a high content of carbon (16%), oxygen (45%), silica (15%), and traces of Mg, Al, Ca, etc.

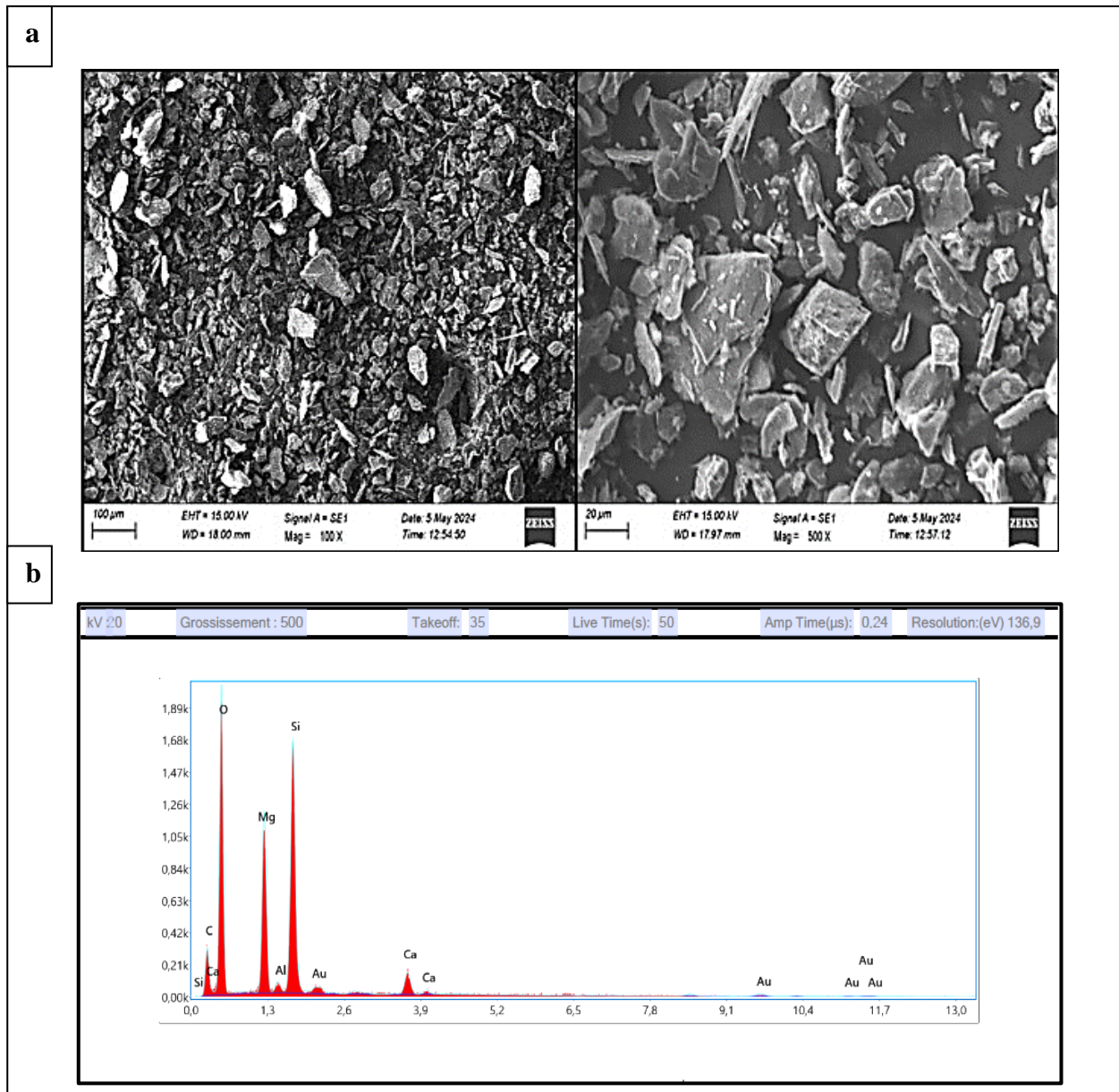


Figure IV.2: SEM/EDS image of Silica powder.

IV.1.4.2 Clay sample

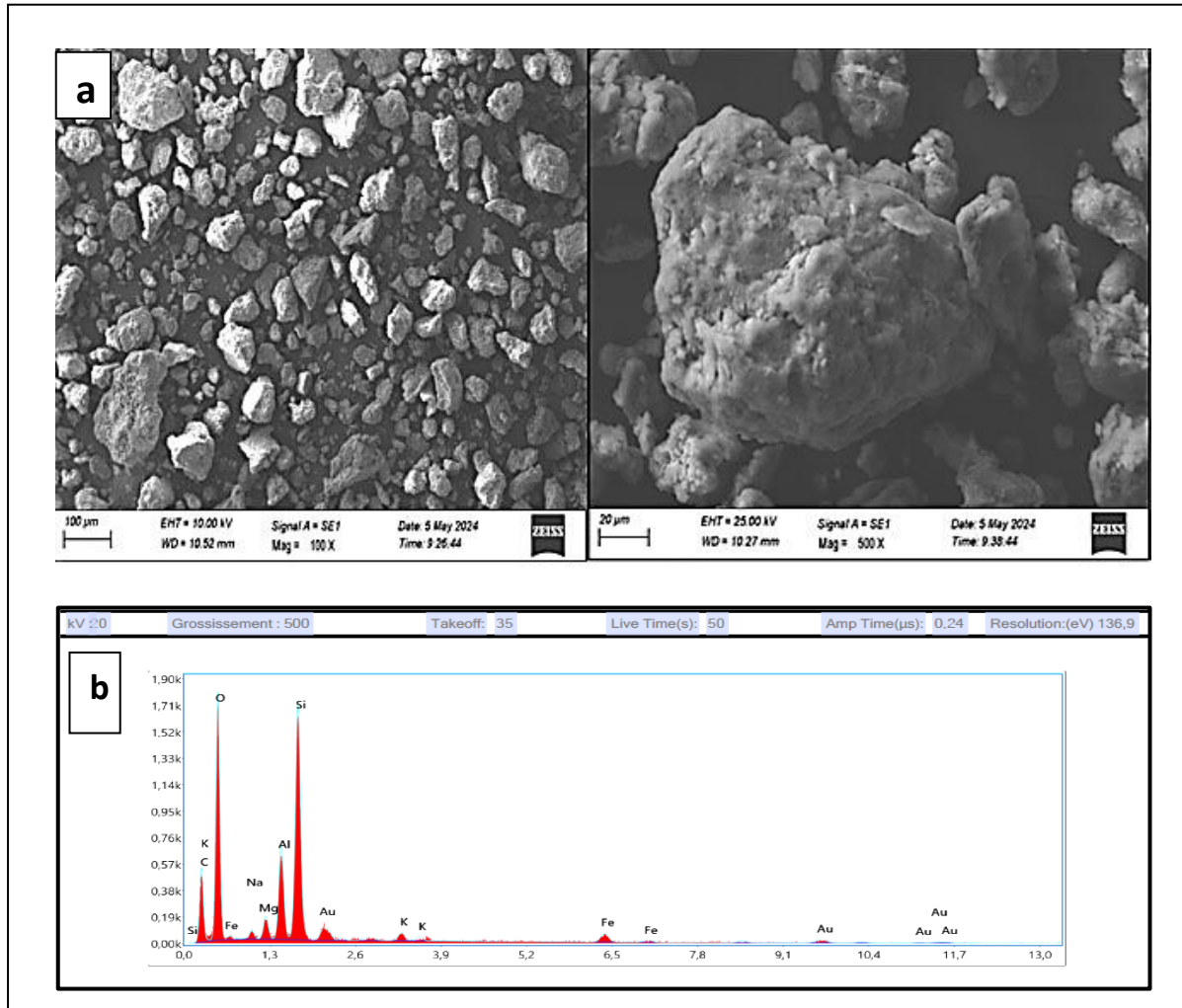


Figure IV.3: SEM/EDS image of clay powder

Regarding the structure and morphology of clay (**Figure IV.3.a**), the SEM showed low porosity and a uniform particle size distribution with smaller sizes. According to the EDS spectrum depicted in the **figure(IV.3.b)**, the sample contains a high percentage of carbon, silicon, and oxygen, with low concentrations of Mg, Al, etc., also detected.

IV.1.4.3 Biopolymer sample

The **figure(IV.4.a)** displays the SEM image of the typical morphology of biopolymer structures. The particles appear to aggregate together in a spherical form with a diameter of less than 500 nm and well-defined pores. Chemical analysis of the product using EDX, as shown in the **figure(IV.4.b)**, confirms a high content of carbon (24%) and oxygen (40%), along with the presence of impurities such as Na, Mg, Fe, K, etc

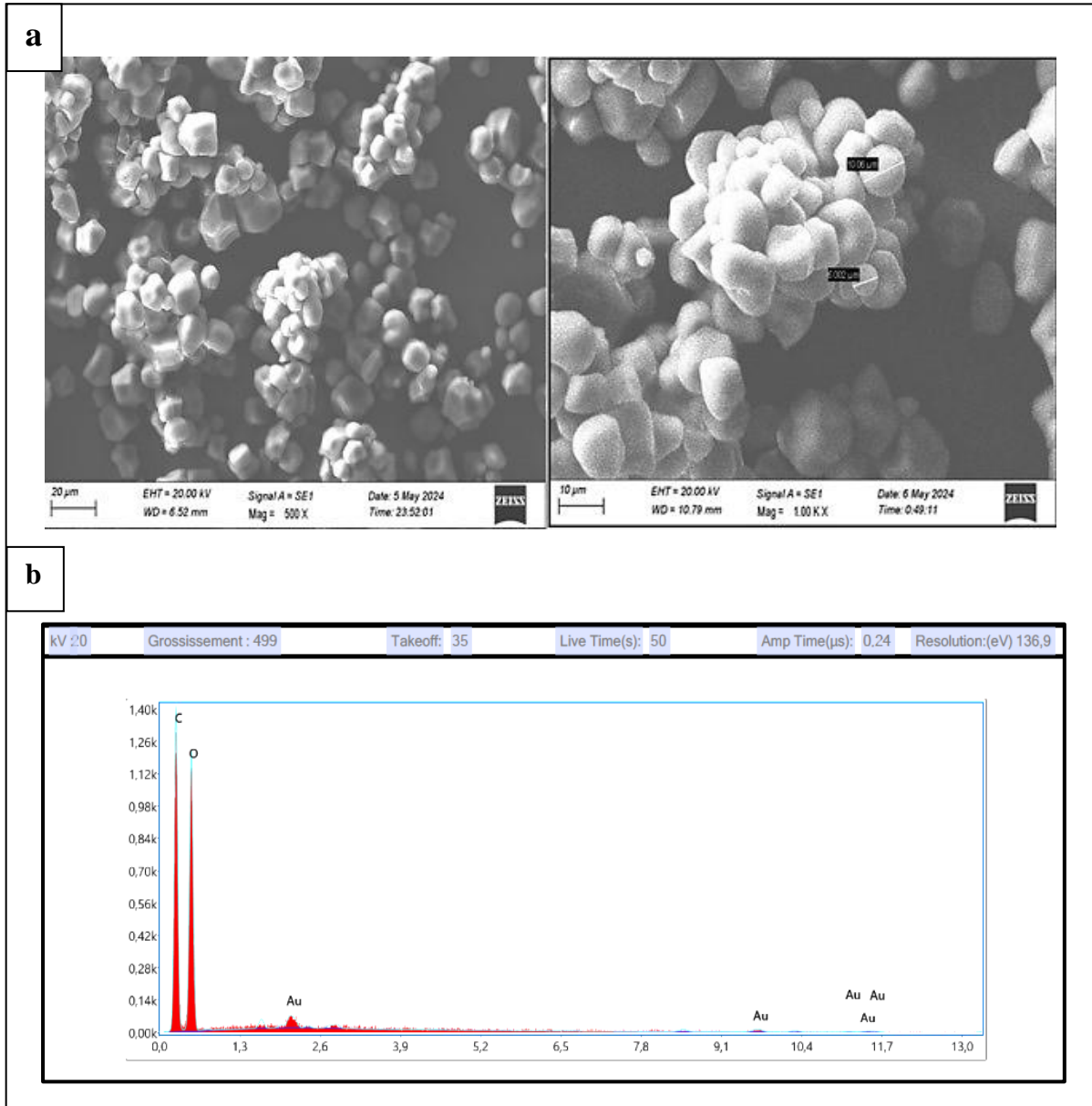


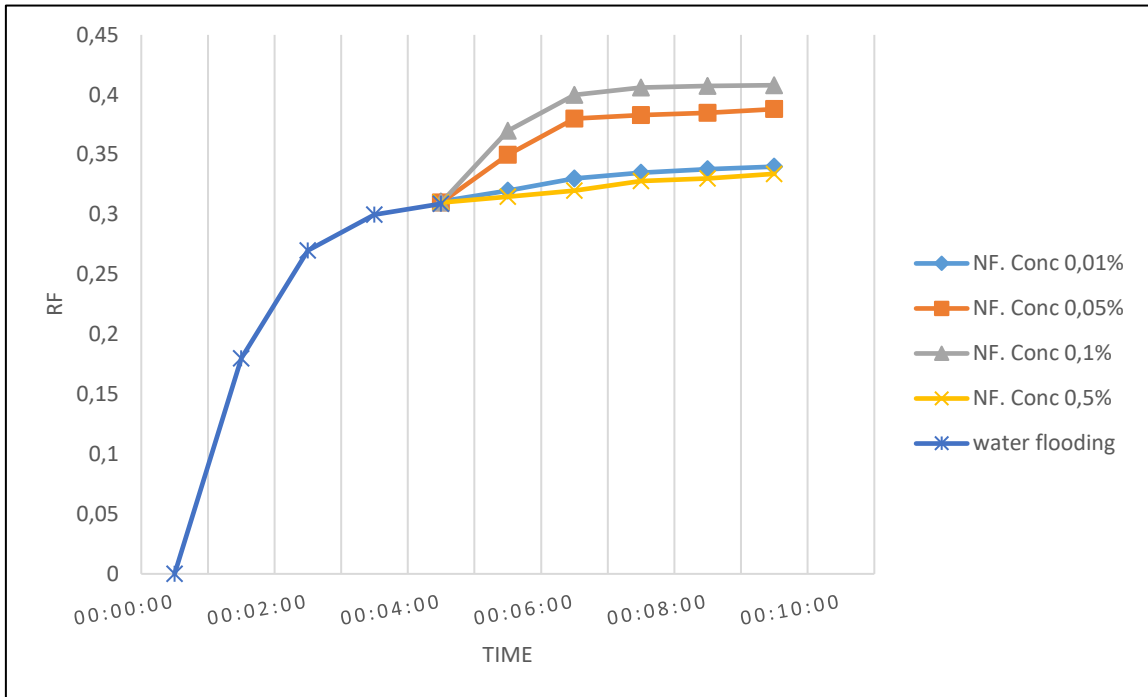
Figure IV.4: SEM/EDS image of biopolymer

IV.2 Effect of nanomaterials concentration in oil recovery

It was observed that the injection of silica nanofluid in the core enhances oil production, especially as the silica concentration increases. The higher the silica concentration, the higher the amount of recovered oil up to an optimum silica nanofluid concentration after which the oil recovery decreases. And we can observe the same thing in the nanoclay concentration.

IV.2.1 Effect of Nanosilica concentration in recovery factor

Figure IV.5: diagrams represented the effect of nanosilica concentration in recovery factor



IV.2.2 Effect of nanoclay concentration in recovery factor

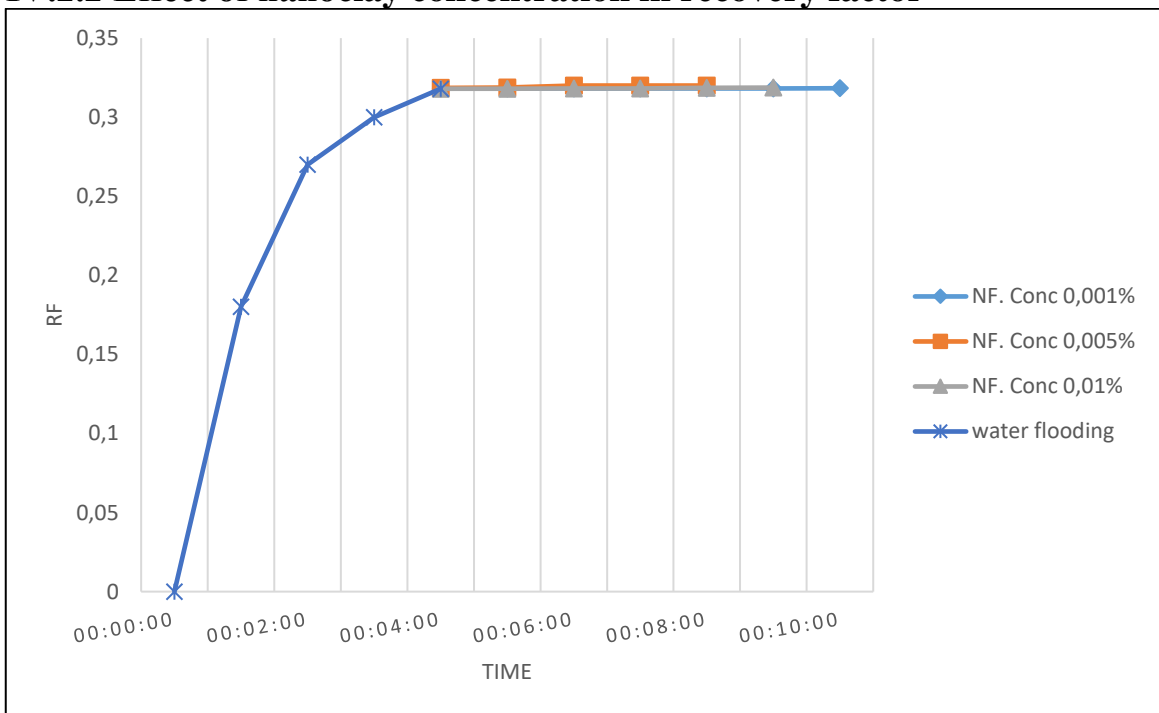


Figure IV.6: diagrams represented effect of nanoclay concentration in recovery factor

IV.3 Displacements tests results and discussion

IV.3.1 Case 01: sand micromodel

➤ **Porosity measurement**

The porous samples were prepared, with a diameter of 2.5 cm and a length of 6 cm. The sample was then saturated with brine. The porosity measurement was repeated to demonstrate the accuracy of the data determination. The results of the porosity measurements are represented in the table:

Table IV.4: results of porosity measurements.

Test	Dry mass (g)	Saturated mass (g)	Porosity %
1	64.354	78.689	18.21
2	63.952	78.358	18.38
3	64.523	78.869	18.18
Average porosity	18.25		

The average porosity of the sample was 18.25 %.

➤ Permeability measurement

the permeability results shown in this table.

Table IV.5: result of Absolute permeability measurement.

	pressure (atm)	Flow(cm ³ /s)	Permeability(md)
Brine	0,016422	0.20	14,91260
diesel fuel	0,016422	0.038	2,83339

➤ Oil recovery measurement

- Saturate the capillary micromodel with brine:
- Brine Saturation volume = 13 ml.
- Inject the diesel to displace the brine until the first drop of oil is recovered:
- Diesel saturation volume = 11 ml
- Irreducible water saturation (S_{wi}) = 2 ml

IV.3.1.1 Silica Nanoflooding

a) Brine flooding:

Table IV.6: results of brine flooding.

Test	Pressure(atm)	Duration (min)	Oil in place (ml)	Oil recovery (ml)	Recovery factor%

Brine drainage	0,016422	03:11	11	3,4	30,9

b) Silica nanofluid flooding:

Table IV.7: results of silica nanoflooding

Test	Pressure(atm)	Duration (min)	Oil in place (ml)	Oil recovery (ml)	Recovery factor %
Silica Nanofluid	0,016422	05:19	7,6	3,1	40,8

c) silica nanofluid flooding and polymer injection.

Table IV.8: results of silica nanofluid flooding and polymer injection.

Test	Pressure(atm)	Duration (min)	Oil in place (ml)	Oil recovery (ml)	Recovery factor %
Silica and polymer nanofluid	0,016422	15:00	4,5	4	88,9

The histogram in Figure IV.7 represent comparison between oil recovery for brine, silica nanofluid, silica nanofluid and polymer.

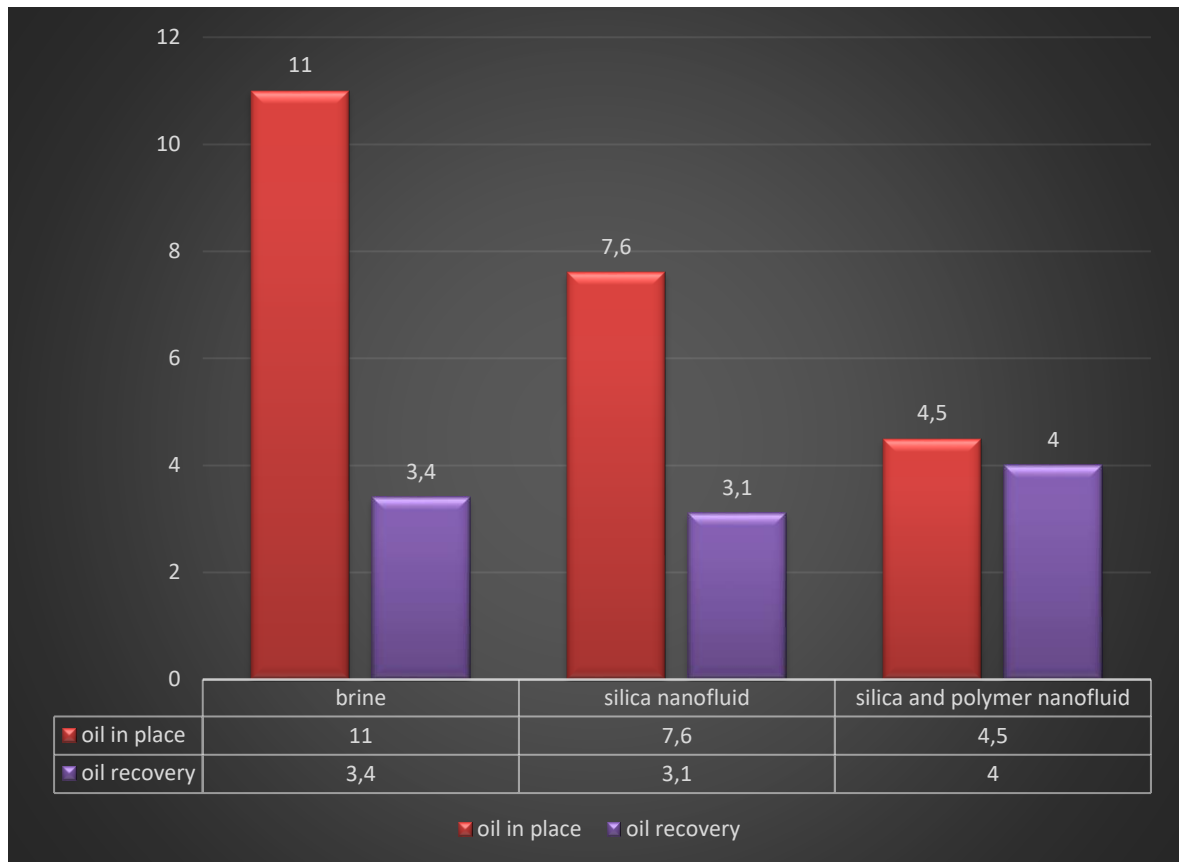


Figure IV.7: Histogram represented the oil in place and the recoverd oil after brine flooding, nanosilica flooding and nanosilica flooding with polymer injection.

We observe that the initial amount of oil in the porous medium is 11 ml. After brine flooding, we recovered 3.4 mL of the total amount. Following this, 7.6 mL of oil remained. Injecting silica nanofluid resulted in the extraction of 3.1 ml from the remaining 7.6 ml. Finally, injecting silica nanofluid with polymer recovered 4 ml from the remaining 4.5 mL. Consequently, the residual oil is only 0.5 ml, indicating the high efficiency of silica nanofluid in enhanced oil recovery.

The graph shown in Figure IV.8 illustrates the changes in the recovery factor as a function of time during different stages of fluid injection.

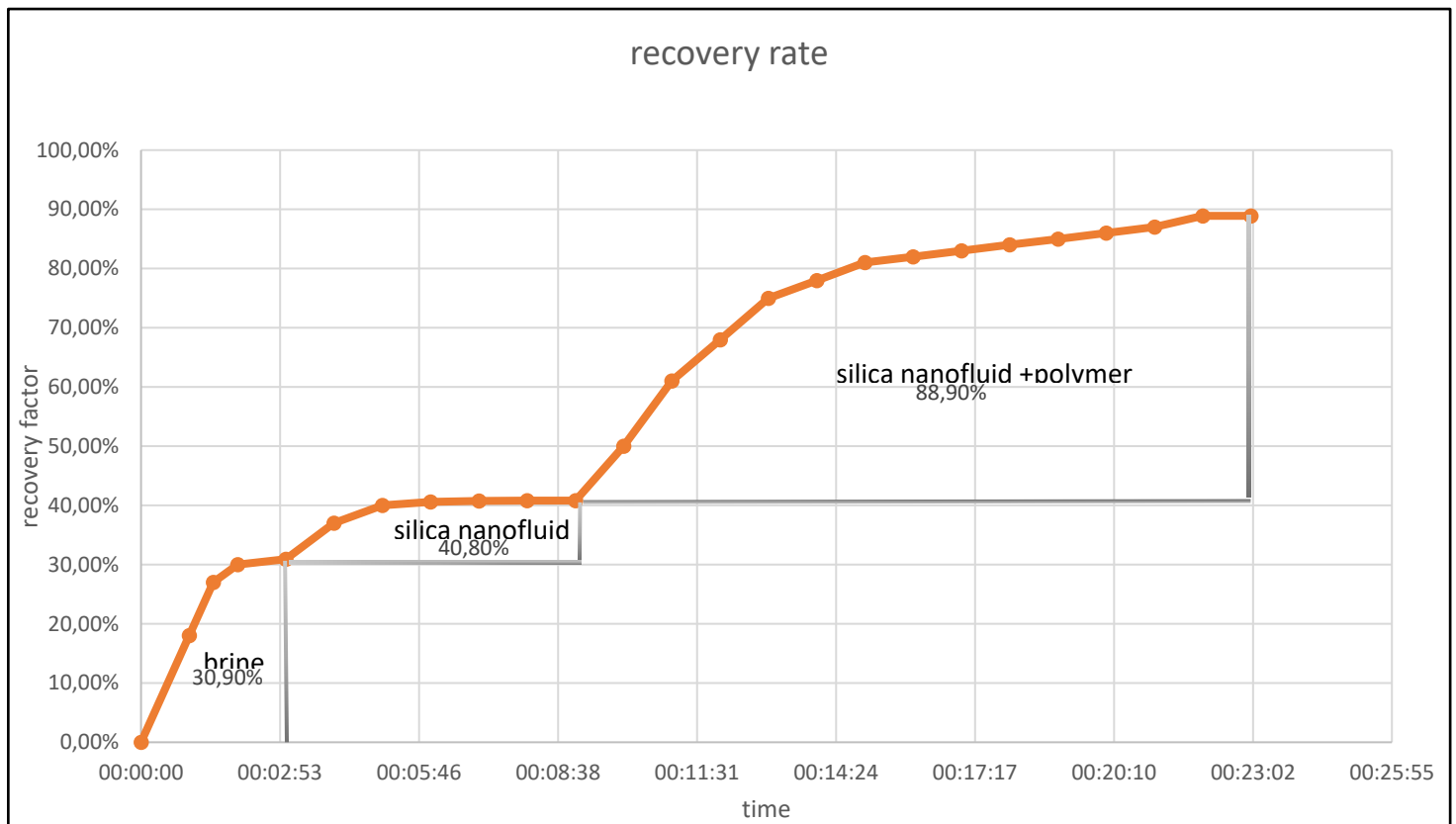


Figure IV.8: diagram represented the results of RF after brine flooding, nanosilica flooding and nanosilica flooding with polymer injection.

a) Brine Injection:

Initially, the recovery factor increases sharply to 30.9% within a short period. This indicates that brine injection effectively mobilizes and recovers oil initially. However, after reaching 30.9%, the recovery factor plateaus, suggesting that the effectiveness of brine in enhancing recovery diminishes as the process progresses.

b) Silica Nanofluid Injection:

Following the plateau with brine injection, the introduction of silica nanofluid results in a renewed increase in the recovery factor, reaching 40.8%. This suggests that silica nanoparticles significantly improve oil recovery by reducing the interfacial tension between the oil and water phases, thus enhancing the mobilization of the remaining oil.

c) Silica Nanofluid + Polymer Injection:

When the extraction with silica nanofluid alone is halted, silica nanofluid combined with polymer is injected. This combination leads to a substantial increase in the recovery

factor, reaching 88.9%. However, this increase occurs over a longer period of approximately 15 minutes. The addition of polymer increases the viscosity of the displacing fluid, which helps stabilize the displacement front and prevents viscous fingering, thereby improving the sweep efficiency and overall oil recovery.

IV.3.1.2 Nanoclay flooding

a) Brine flooding:

Table IV.9: results of brine flooding.

Test	Pressure(atm)	Duration (min)	Oil in place (ml)	Oil recovery (ml)	Recovery factor %
Brine flooding	0,016422	04:31	11	3,5	31,8

b) Clay nanofluid flooding:

Table IV.10: results of nanoclay flooding.

Test	Pressure(atm)	Duration (min)	Oil in place (ml)	Oil recovery (ml)	Recovery factor%
Nanoclay fluid	0,016422	05:10	7,5	2,4	32,0

c) clay nanofluid flooding and polymer injection

Table IV.11: results of clay nanofluid and polymer injection.

Test	Pressure (atm)	Duration (min)	Oil in place (ml)	Oil recovery (ml)	Recovery factor %
Nanoclay and polymer fluid	0,016422	00:16:25	5,1	3,9	76,5

The histogram in Figure IV.9 represent comparison between oil recovery for brine, clay nanofluid, clay nanofluid and polymer.

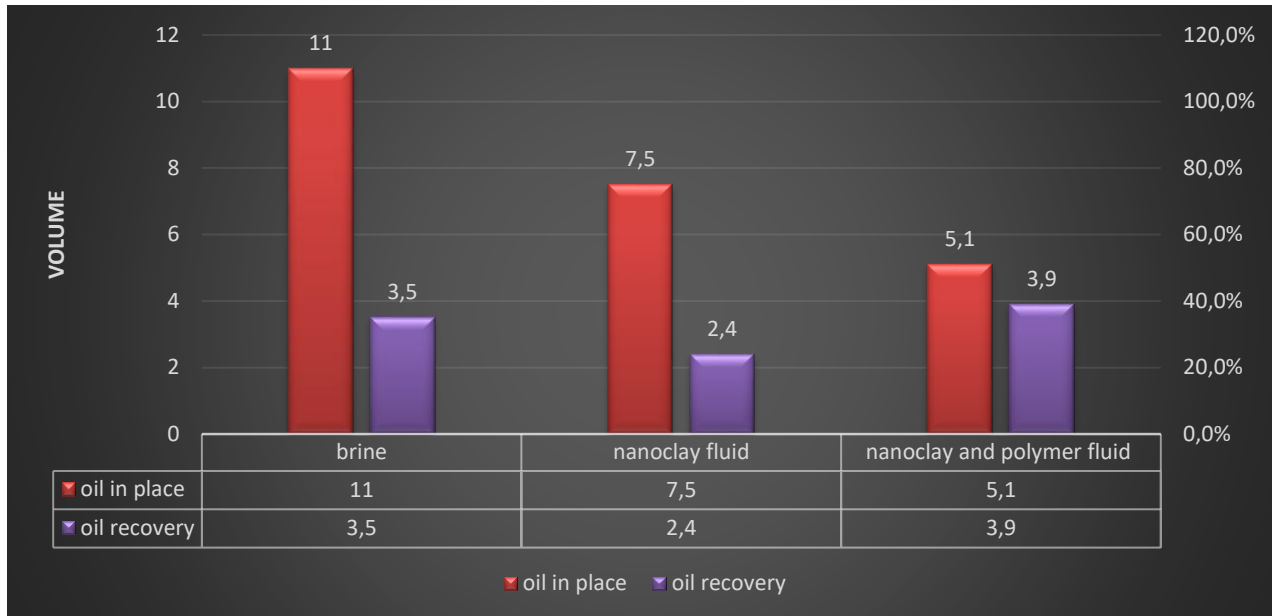


Figure IV.9: Histogram represented the oil in place and the recovered oil after brine flooding, nanoclay flooding and nanoclay flooding with polymer injection.

Brine flooding has the lowest recovery factor (32.22%).

Nanoclay fluid flooding has a slightly higher recovery factor (34.43%) than brine flooding.

Nanoclay and polymer fluid flooding shows the highest recovery factor (60%), indicating it is the most effective method among the three for enhancing oil recovery.

The data suggests that adding polymer to nanoclay fluid significantly improves oil recovery efficiency compared to using brine or nanoclay fluid alone.

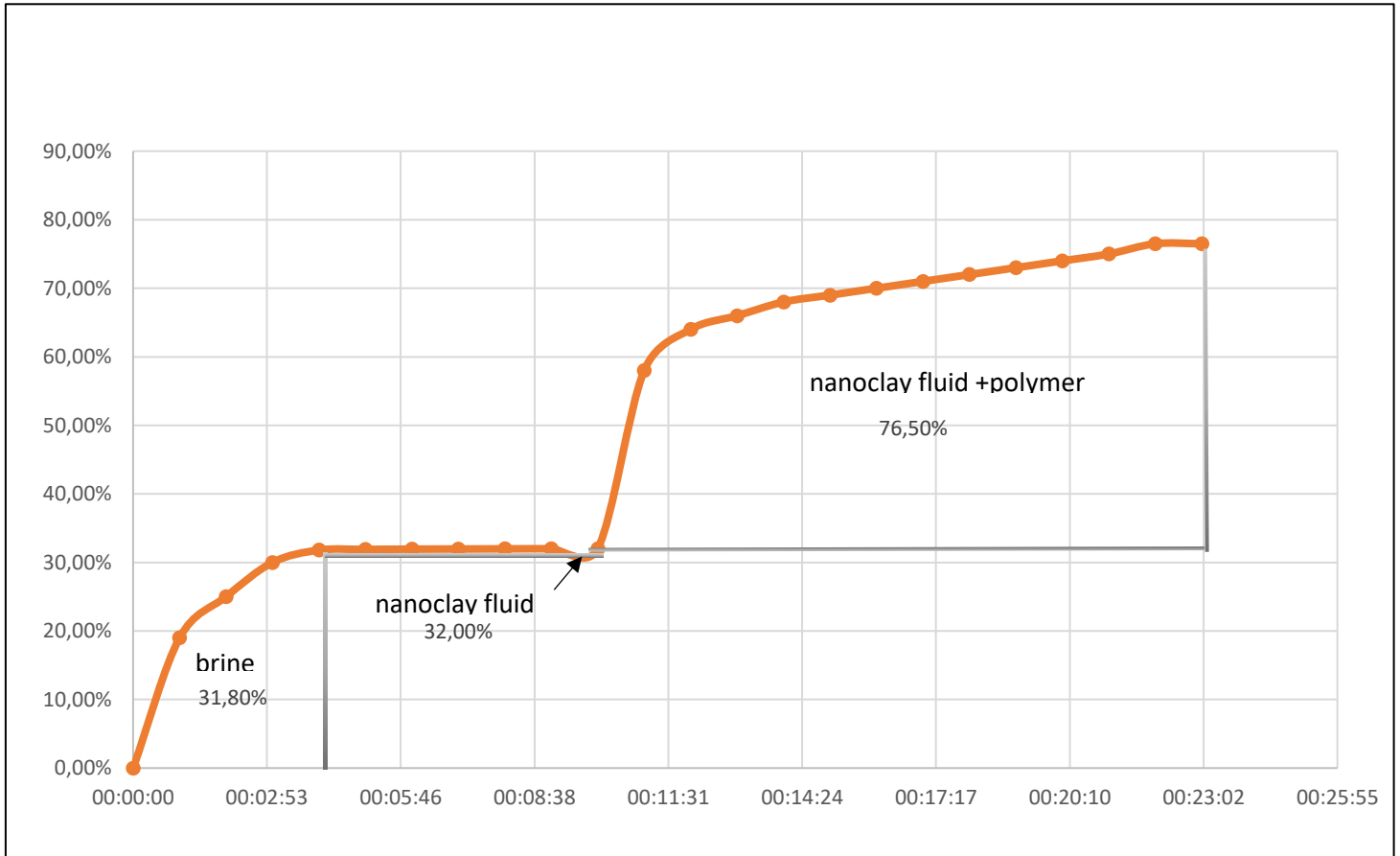


Figure IV.10: diagram represented the results of RF after brine flooding, nanoclay flooding and nanoclay flooding with polymer injection.

IV.3.1.3 silica+ clay nanofluid flooding:

a) Brine flooding

Table IV.12: results of brine flooding.

Test	Pressure(atm)	Duration (min)	Oil in place (ml)	Oil recovery (ml)	Recovery factor %
Brine flooding	0,016422	00:04:19	11	3,5	31,8

b) Silica+ clay nanofluid flooding

Table IV.13: result of silica+ clay flooding.

Test	Pressure(atm)	Duration (min)	Oil in place (ml)	Oil recovery (ml)	Recovery factor%
Silica+ clay Nanofluid	0,016422	00:04:52	7,5	4	53.3

c) Silica+ clay nanofluid flooding and polymer injection

Table IV.14: results of Silica+ clay nanofluid flooding and polymer injection.

Test	Pressure(atm)	Duration (hh:min:ss)	Oil in place (ml)	Oil recovery (ml)	Recovery rate %
Silica+ clay nanofluid and polymer	0,016422	00:13:31	3.5	3.2	91.4

The histogram in Figure IV.11 represent comparison between oil recovery for brine, clay nanofluid, clay nanofluid and polymer.

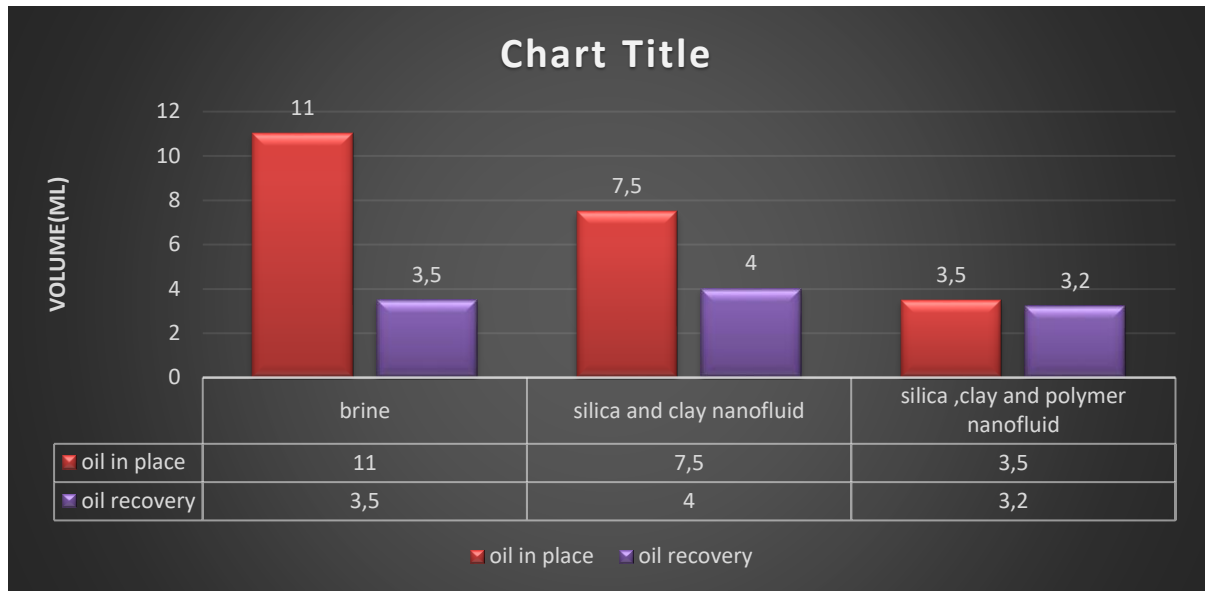


Figure IV.11: Histogram represented the oil in place and the recovered oil after brine flooding, nanocomposite flooding and nanocomposite flooding with polymer injection.

Brine flooding has the lowest recovery factor (33.33%).

Silica and clay nanofluid flooding has a higher recovery factor (51.67%) than brine flooding.

Silica, clay, and polymer nanofluid flooding shows the highest recovery factor (86.21%), indicating it is the most effective method among the three for enhancing oil recovery.

The data indicates that adding silica, clay, and polymer nanofluid significantly improves oil recovery efficiency compared to using brine or silica and clay nanofluid alone. This combination maximizes the recovery factor, making it the most effective method tested.

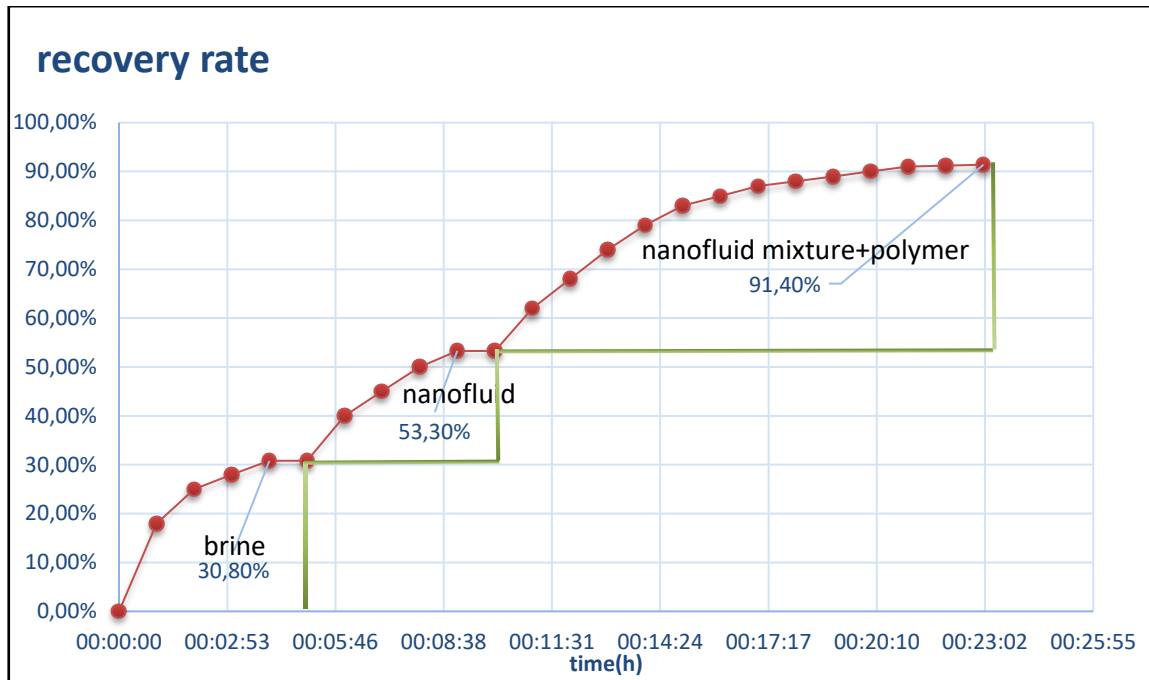


Figure IV.12: diagram represented the results of RF after brine flooding, nanocomposite flooding and nanocomposite flooding with polymer injection.

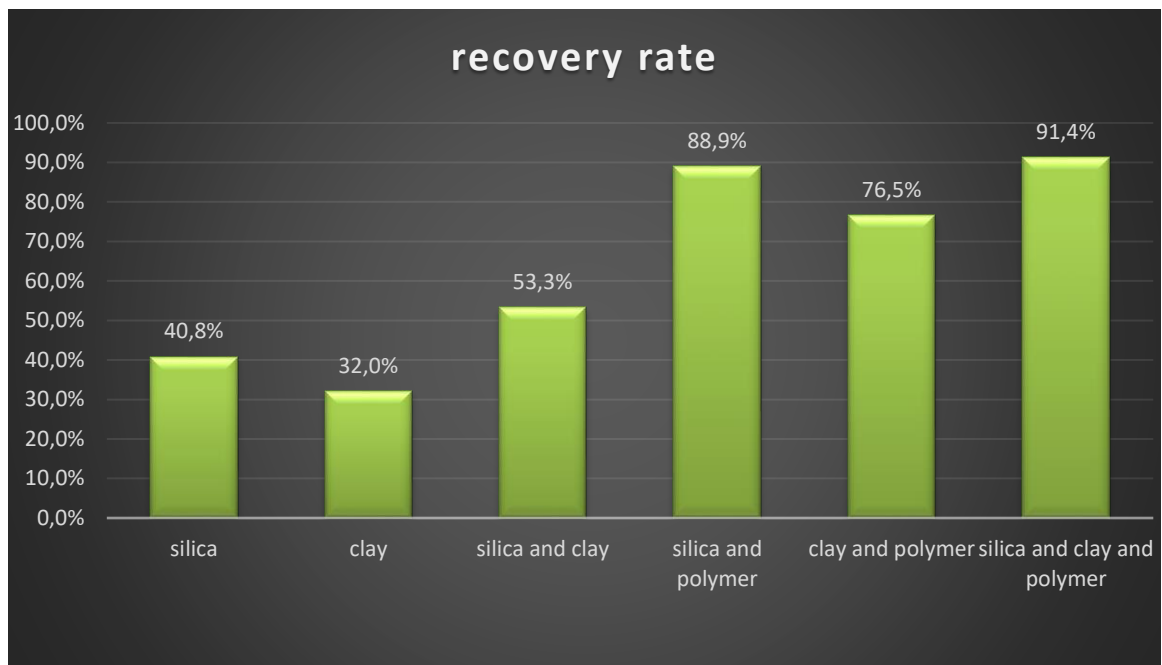


Figure IV.13: Histograms represented the results of recovery factors in the case of sand micromodel.

Discussion:

Silica alone has a better recovery rate (40.8%) compared to clay alone (32.0%).

- Combining silica and clay improves the recovery rate to 53.3%.
- Combining silica with polymer results in a substantial increase in recovery rate to 88.9%.
- Combining clay with polymer achieves a recovery rate of 76.5%.
- The combination of silica, clay, and polymer achieves the highest recovery rate of 91.4%, suggesting that the synergistic effect of all three components maximizes the recovery efficiency.

This data indicates that using polymers in combination with either silica or clay, and especially with both, significantly enhances the oil recovery rate, with the combination of all three (silica, clay, and polymer) being the most effective.

IV.3.2 Case 02: sand and asphaltene micromodel:

➤ Porosity measurement

The porous samples were prepared, with a diameter of 2.5 cm and a length of 6 cm. The sample was then saturated with brine. The porosity measurement was repeated to demonstrate the accuracy of the data determination.

The results of the porosity measurements are represented in the table IV.15:

Table IV.15: The results of the porosity measurements.

Test	Dry mass (g)	Saturated mass (g)	Porosity %
1	74.179	81.968	09.50
2	74.010	81.812	09.53
3	74.893	82.541	09.26
Average porosity	09.43		

The average porosity of the sample was 09.43 %.

➤ Permeability measurement

the permeability results in case of sand and asphaltene micromodel shown in this table.

Table IV.16: results of permeability measurement.

	pressure (atm)	Flow(cm ³ /s)	Permeability(md)
Brine	0,016422	0.11	8,20193
diesel fuel	0,016422	0.021	1,565823

➤ Oil recovery measurement:

Saturate the capillary micromodel with brine:

Brine Saturation volume = 5 ml in 3:40 min

Inject the diesel to displace the brine until the first drop of oil is recovered:

Diesel saturation volume = 4 ml in 4:30 min

Irreducible water saturation (S_{wi}) = 1 ml

IV.3.2.1 Silica Nanoflooding

a) Brine flooding:

Table IV.17: results of brine flooding.

Test	Pressure (atm)	Duration (min)	Oil in place (ml)	Oil recovery (ml)	Recovery factor %
Brine flooding	0,016422	03:08	9	3	33.33

b) Silica nanofluid flooding:

Table IV.18: results of silica nanofluid flooding.

Test	Pressure (atm)	Duration (min)	Oil in place (ml)	Oil recovery (ml)	Recovery factor%
Silica Nanofluid	0,016422	02:48	6	2.4	40.00

c) Silica nanofluid flooding and polymer injection:

Table IV. 19:results of silica nanofluid flooding and polymer injection.

Test	Pressure (atm)	Duration (min)	Oil in place (ml)	Oil recovery (ml)	Recovery factor %
Silica nanofluid and polymer	0,016422	09:00	3.6	2.5	69.44



Figure IV.14: samples of the recovered oil after brine flooding, nanosilica flooding and nanosilica flooding with polymer injection respectively from right to left.

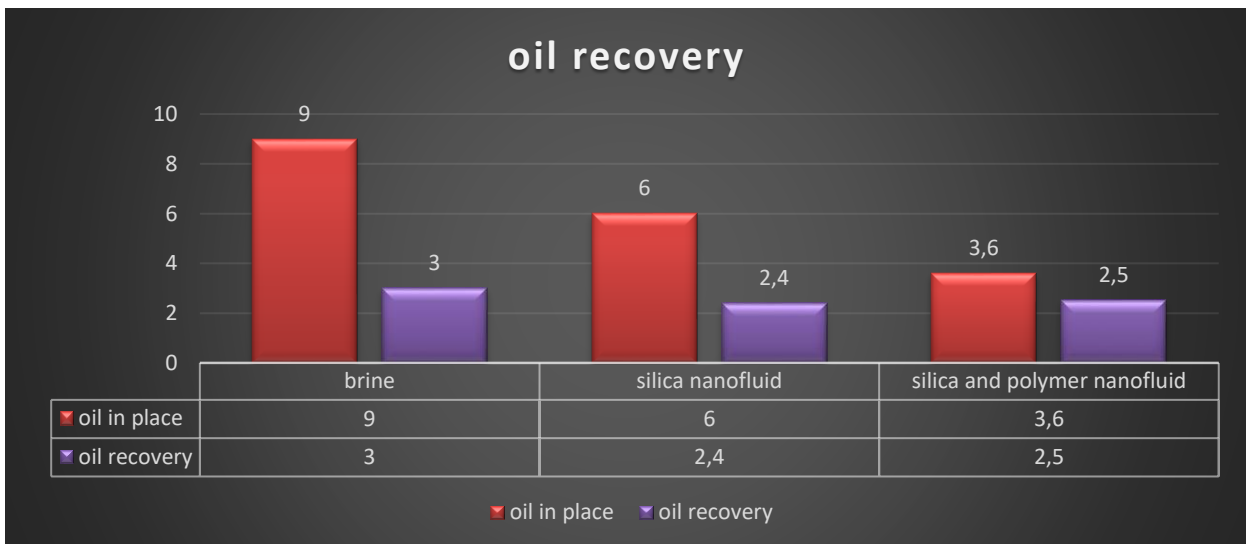


Figure IV.15: Histogram represented the oil in place and the recoverd oil after brine flooding, nanosilica flooding and nanosilica flooding with polymer injection.

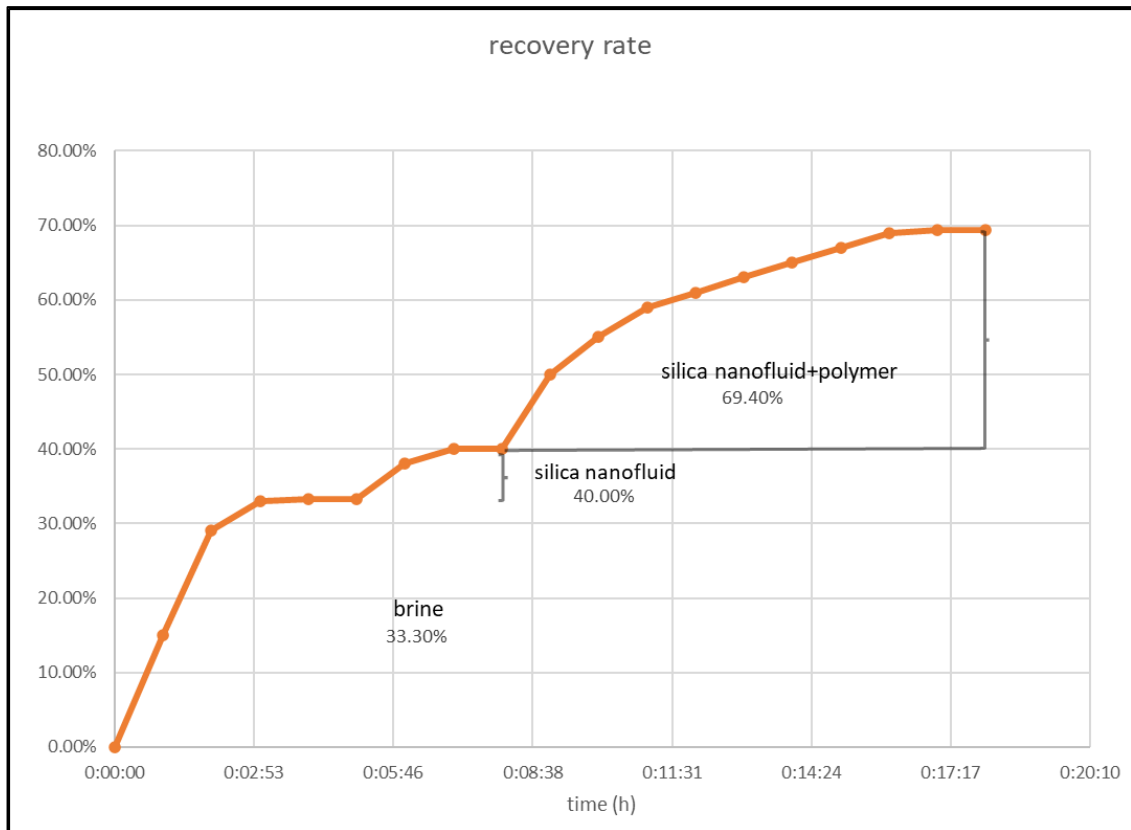


Figure IV.16: diagram represented the results of RF after brine flooding, nanosilica flooding and nanosilica flooding with polymer injection.

IV.3.2.2 Nanoclay flooding

a) Brine flooding:

Table IV.20: results of brine flooding.

Test	Pressure (atm)	Duration (min)	Oil in place (ml)	Oil recovery (ml)	Recovery factor%
Brine drainage	0,016422	03:26	9	2.9	32.22

b) Drainage after injection of the nanoclay fluid formulation:

Table IV.21: result of nanoclay flooding.

Test	Pressure (atm)	Duration (min)	Oil in place (ml)	Oil recovery (ml)	Recovery factor%
Nanoclay fluid	0,016422216	00:04:15	6.1	2.1	34.43

c) Drainage after injection of the nanoclay and polymer fluid formulation:

Table IV.22: result of nanoclay flooding and polymer injection.

Test	Pressure (atm)	Duration (min)	Oil in place (ml)	Oil recovery (ml)	Recovery factor%
Nanoclay and polymer fluid	0,016422216	10:27	4	2.4	60.00

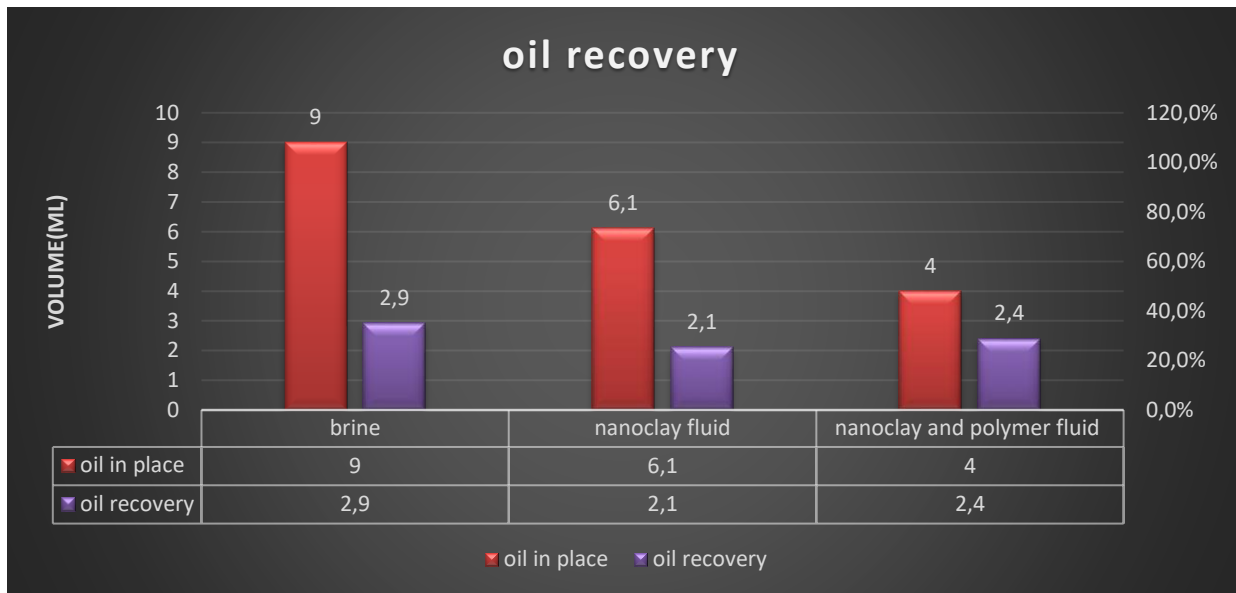


Figure IV.17: Histogram represented the oil in place and the recoverd oil after brine flooding, nanoclay flooding and nanoclay flooding with polymer injection.

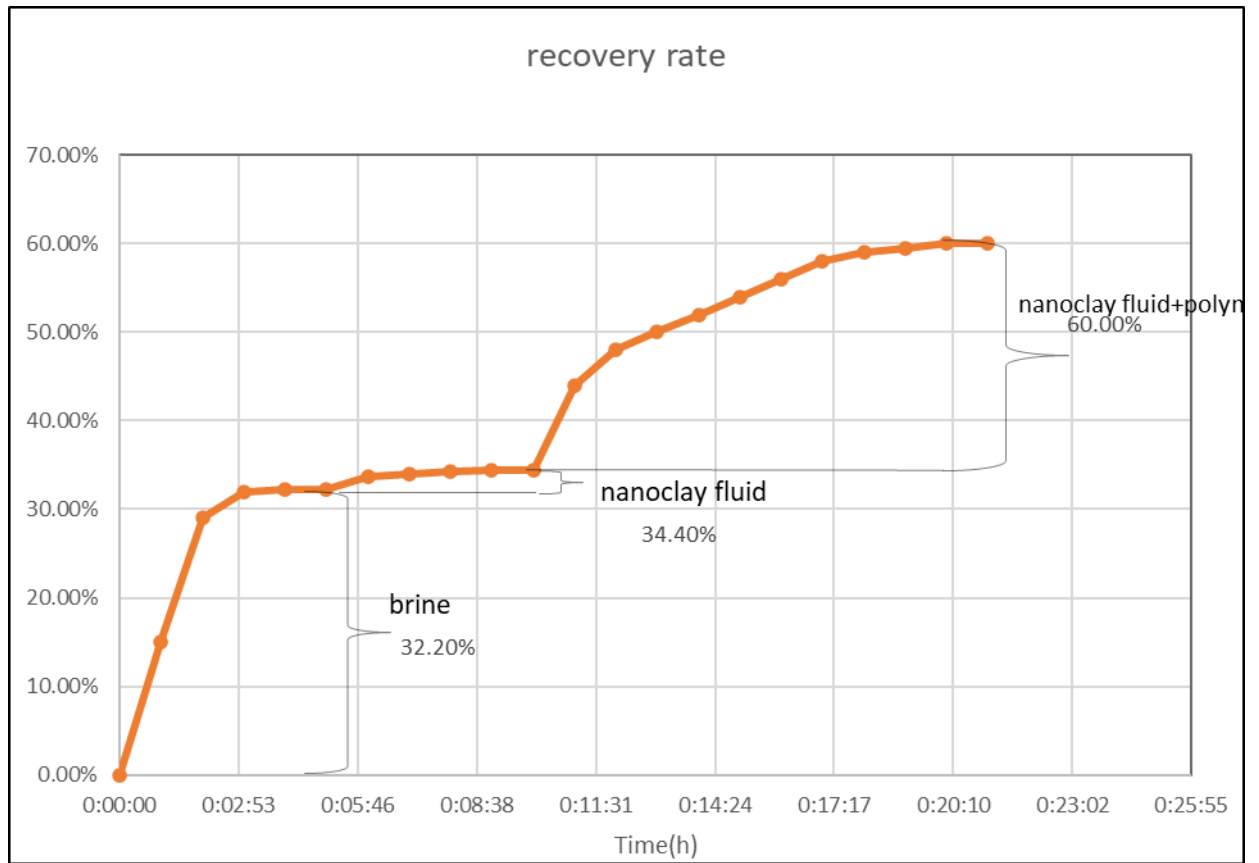


Figure IV.18: diagram represented the results of RF after brine flooding, nanoclay flooding and nanoclay flooding with polymer injection.

IV.3.2.3 Silica +clay nanofluid flooding

a) Brine flooding

Table IV. 23: results of brine flooding.

Test	Pressure (atm)	Duration (min)	Oil in place (ml)	Oil recovery (ml)	Recovery factor%
Brine flooding	0,016422216	00:04:02	9	3	33.33

b) Silica+ clay flooding

Table IV. 24: results of silica+ clay flooding.

Test	Pressure(atm)	Duration (min)	Oil in place (ml)	Oil recovery (ml)	Recovery factor %
Silica+ clay nanofluid	0,016422216	00:03:22	6	3.1	51.67

c) Silica+ clay nanofluid and polymer injection

Table IV.25: results of Silica+ clay nanofluid and polymer injection.

Test	Pressure(atm)	Duration (hh:min:ss)	Oil in place (ml)	Oil recovery (ml)	Recovery rate %
nanofluid Mixture and polymer	0,016422	00:08:30	2.9	2.5	86.20

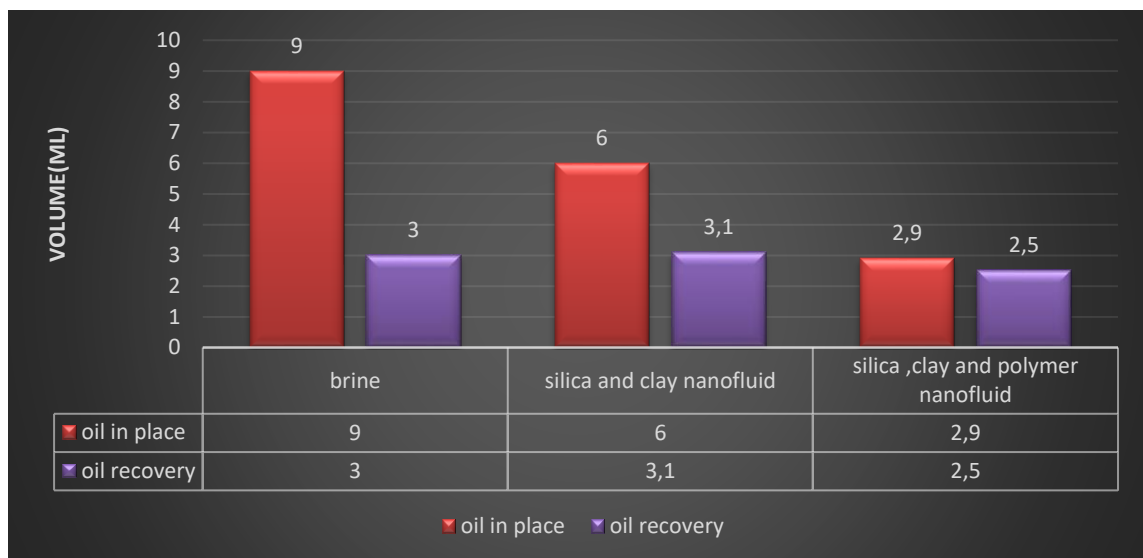


Figure IV.19: Histogram represented the oil in place and the recovered oil after brine flooding, nanocomposite flooding and nanocomposite flooding with polymer injection.

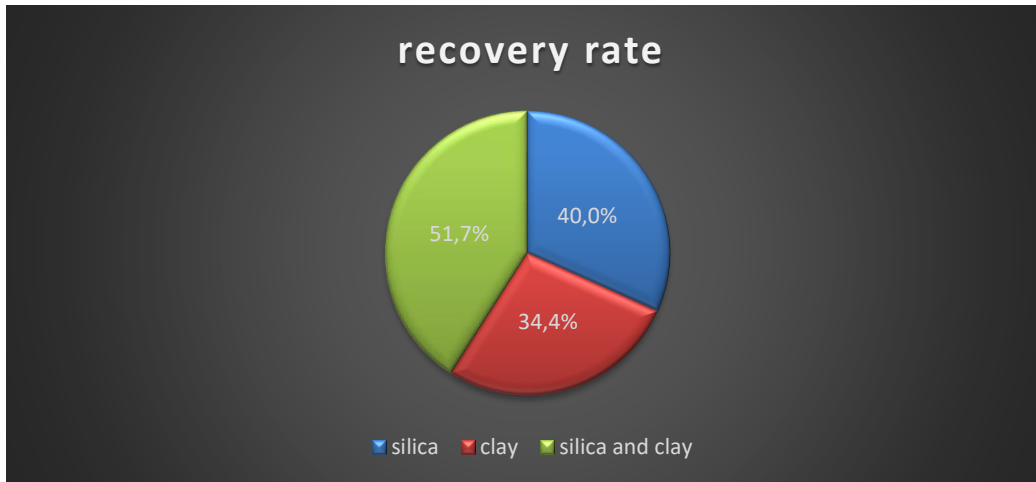


Figure IV.20: relative circle represented the result of RF after nanoflooding without injecting the polymer

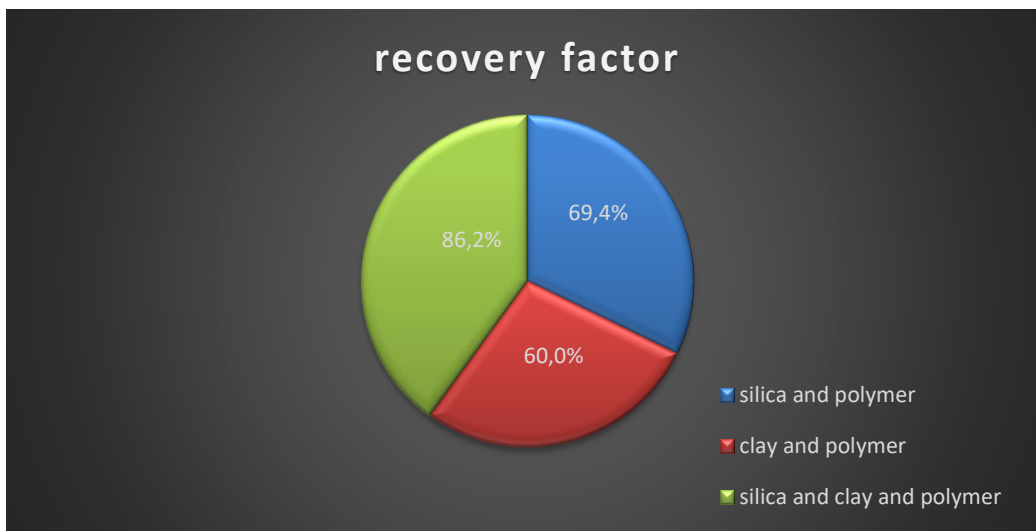


Figure IV.21 : relative circle represented the result of RF after nanoflooding with the polymer injection

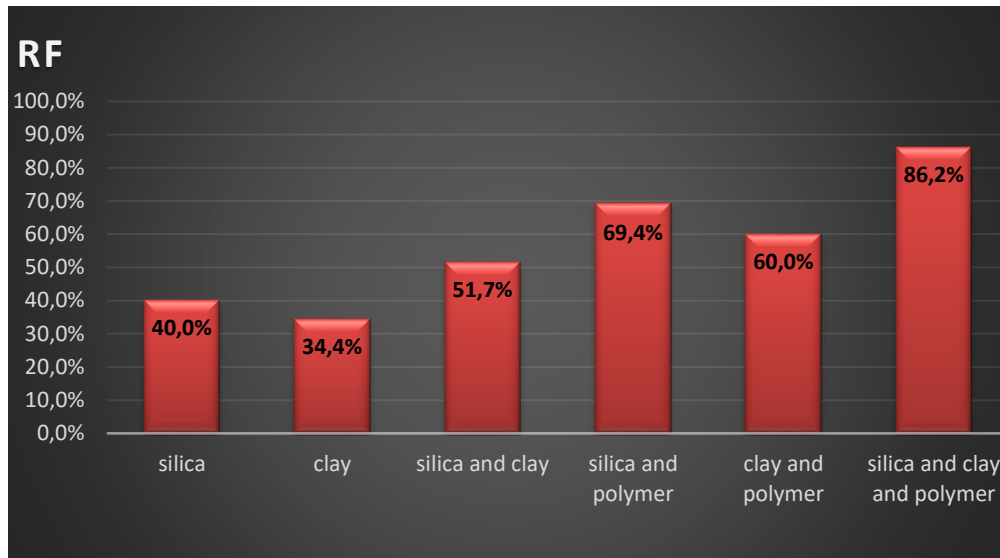


Figure IV.22: Histograms represented the results of recovery factors in the case of asphaltenic sand micromodel.

Discussion

Silica alone has a better recovery rate (40.0%) compared to clay alone (34.4%).

- Combining silica and clay improves the recovery rate to 51.7%.
- Combining silica with polymer results in a substantial increase in recovery rate to 69.4%.
- Combining clay with polymer achieves a recovery rate of 60.0%.
- The combination of silica, clay, and polymer achieves the highest recovery rate of 86.2%, suggesting that the synergistic effect of all three components maximizes the recovery efficiency.

This data indicates that using polymers in combination with either silica or clay, and especially with both, significantly enhances the oil recovery rate, with the combination of all three (silica, clay, and polymer) being the most effective.

IV.4 Results of IFT measurement:

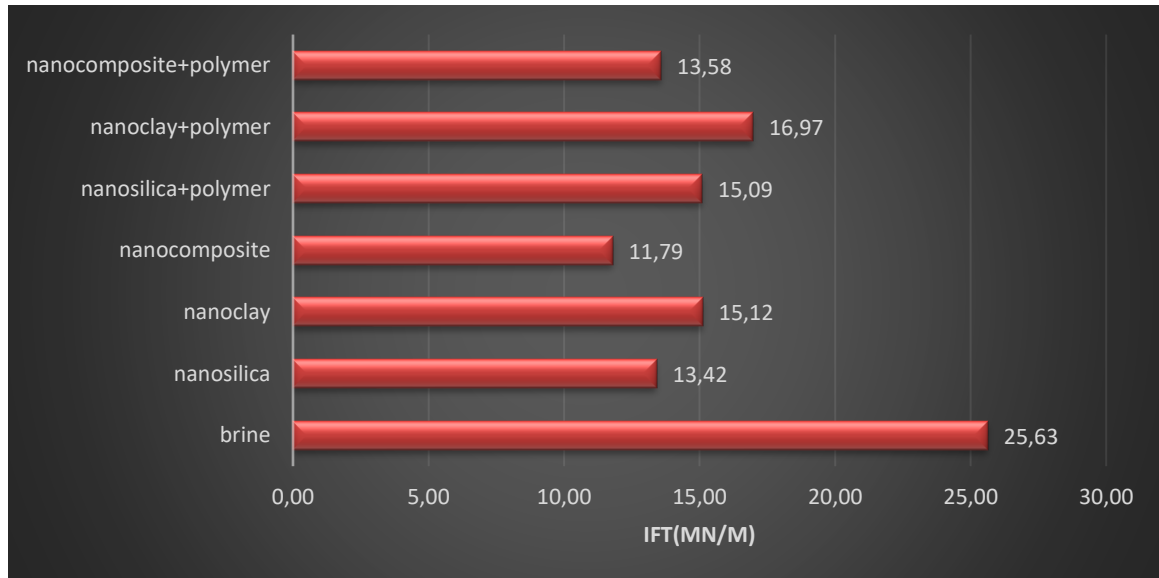


Figure IV.23: IFT between diesel fuel and different fluid

Discussion

The results presented in Figure IV.23 highlight the impact of various fluids on the interfacial tension (IFT) with diesel fuel. The IFT values provide insight into the efficiency of these fluids in reducing the tension at the interface, which is crucial for enhanced oil recovery processes.

Nanocomposite + Polymer: The IFT for the nanocomposite combined with polymer is 13.58 mN/m. This value indicates a moderate reduction in interfacial tension, suggesting that the combination is effective in improving the interaction between diesel and the fluid.

Nanoclay + Polymer: The combination of nanoclay and polymer shows a higher IFT value of 16.97 mN/m. While this combination does reduce the IFT compared to brine (25.63 mN/m), it is less effective than the nanocomposite + polymer and nanosilica + polymer combinations.

Nanosilica + Polymer: With an IFT of 15.09 mN/m, nanosilica combined with polymer exhibits a significant reduction in interfacial tension, although it is not the lowest among the tested fluids. This indicates its potential effectiveness in reducing the IFT, albeit slightly less so than the nanocomposite + polymer combination.

Nanocomposite: The nanocomposite alone achieves an IFT of 11.79 mN/m, the lowest among all the tested fluids. This result suggests that the nanocomposite on its own is highly effective in reducing the interfacial tension with diesel fuel, making it a promising candidate for enhanced oil recovery applications.

Nanoclay: The nanoclay alone has an IFT of 15.12 mN/m, which is higher than the nanocomposite but like the nanosilica + polymer combination. This indicates that while nanoclay is effective in reducing IFT, it is not as efficient as the nanocomposite.

Nanosilica: The IFT for nanosilica alone is 13.42 mN/m, demonstrating its effectiveness in reducing interfacial tension. This value is comparable to the nanocomposite + polymer combination, suggesting that nanosilica can be effective both on its own and when combined with polymers.

Brine: Serving as a control, brine exhibits the highest IFT value of 25.63 mN/m. This baseline indicates the significant reduction in IFT achieved by all tested fluids, underscoring their potential for enhanced oil recovery.

Overall, the results suggest that nanocomposites, both alone and in combination with polymers, are highly effective in reducing the interfacial tension between diesel and the fluid. This reduction in IFT is critical for improving the efficiency of oil recovery processes. Further research could explore the mechanisms behind the superior performance of nanocomposites and investigate the potential for optimizing their formulations for industrial applications



**General conclusion and
recommendations**

General Conclusion:

In this study, we investigated the application of silica nanoparticles and nanoclay in nanoflooding to improve the efficiency of enhanced oil recovery (EOR). Through experimental simulations using a micromodel of reservoirs, which mimics porous media, we conducted sequential injections of silica nanofluid and nanoclay fluid combined with surfactants and biopolymers. The main objectives were to assess the recovery rate and interfacial tension during each stage of injection.

Our findings demonstrate several key insights:

Enhanced Recovery Efficiency: The use of silica nanoparticles and nanoclay in nanoflooding showed promising results in enhancing oil recovery rates. The sequential injections of nanofluids combined with surfactants and biopolymers led to improved displacement of oil from the porous media compared to traditional methods.

Interfacial Tension Reduction: The addition of surfactants effectively lowered interfacial tension between oil and injected fluids, facilitating better oil displacement and recovery.

Impact of Biopolymers: The inclusion of biopolymers further enhanced the mobility control of injected fluids, optimizing the sweep efficiency and contributing to increased oil recovery.

Experimental Validation: The experimental setup using the micromodel provided valuable insights into the dynamics of fluid displacement at a small scale, which can be extrapolated to understand field-scale applications better.

Recommendations for Future Research:

Building on the findings of this study, several recommendations for future research and application include:

Field-Scale Validation: Conducting field-scale trials to validate the effectiveness of silica nanoparticles and nanoclay in actual reservoir conditions. This would provide a more realistic assessment of their impact on enhancing oil recovery.

Optimization of Nanofluid Formulations: Further optimization of nanofluid formulations, including variations in nanoparticle concentration, surfactant types, and biopolymer

compositions, to maximize recovery efficiency while minimizing costs and environmental impact.

Long-Term Stability Studies: Investigating the long-term stability of nanofluids under reservoir conditions to ensure sustained performance over extended injection periods.

Economic Viability Analysis: Conducting cost-benefit analyses to evaluate the economic viability of implementing nanoflooding technologies compared to conventional EOR methods.

Environmental Impact Assessment: Assessing the environmental implications of using silica nanoparticles and nanoclay in oil recovery processes, focusing on potential risks and mitigation strategies.

In conclusion, our study demonstrates the promising potential of nanoparticle-enhanced nanoflooding for advancing EOR practices, even under controlled ambient laboratory conditions. By integrating innovative nanotechnologies with traditional EOR methods, we aim to contribute to sustainable energy production and address global energy challenges effectively.



References

References

1. A. I. El-Diasty and A. M. Aly. (2015). Presented in part at the SPE North Africa technical conference and exhibition. Cairo, Egypt .
2. Adil, M., Zaid, H. M., Chuan, L. K., & Latiff, N. R. (2016). Effect of Dispersion Stability on Electrorheology of Water-Based ZnONanofluids. *Energy Fuels*, 6169–6177.
3. Ahmed, T. (2001). *reservoir engineering handbook*. Boston • London • Auckland • Johannesburg • Melbourne • New Delhi: Gulf Professional Publishing.
4. Akram Al-Asadi, E. R. (2022). Nanoparticles in Chemical EOR: A Review on Flooding Tests. *MDP*, 3.
5. AL-KAABI, S. K. (2010). *Enhanced oil recovery:challenges & opportunities*. SAUDI: ADVANCED RESEARCH CENTRE, SAUDI ARAMCO(World Petroleum Council EXPEC).
6. Allam, M. Y. (2019). Impact of Nanotechnology on Enhanced Oil Recovery: A Mini-Review. *industrial&Engineering chemistry research*, 16288.
7. Aminzadeh, B. D. (2012). Effect of nanoparticles on flowalteration during CO2 injection. *In: SPE 1600* .
8. Behrang M, H. S. (2021). Effect of pH on interfacial tension reduction of oil (Heavy acidic crude oil, resinous and asphaltenic synthetic oil)/low salinity solution prepared by chloride-based salts. . *J Pet Sci Eng 205.*, 108840.
9. Das R, A. M. ((2014)). Current applications of X-ray powder diffraction-a 345 review. . *Rev Adv Mater Sci*, 109.
10. Davis, A. F. (2010). Presented in part at the SPE Improved Oil Recovery. Symposium, Tulsa, Oklahoma, USA,.
11. Espinosa, D. C. (2010). Nanoparticle-stabilized supercritical CO2 foams for potential mobility control applications. *SPE 129925*, , pp. 1–13.
12. Fiedot, M., Rac, O., Suchorska-Woźniak, P., Karbownik, I., & Teterycz, H. (2014). Polymer surfactant interactions and their influence on zinc oxide nanoparticles morphology In Manufacturing Nanostructures. *One Central Press*, pp 108–128.
13. Giraldo, J. B. (2013). Wettability alteration of sandstone cores by alumina-based nano fluids. *Energy Fuels 27(7)*,, 3659–3665.
14. Himanshu Panchal, H. P. (2021). A systematic review on nanotechnology in enhanced oil recovery. *KeAI*, 205.
15. Hosseini E, H. F. (2019). Experimental investigation of the effect of dispersed silica and alumina nanoparticles on oil-aqueous phase interfacial tension. *Pet Sci Technol 37*, 1485–1494.

16. Li, X., Zhu, D., & Wang, X. (2007). Evaluation on dispersion behavior of the aqueous copper nano-Suspensions. *J. Colloid Interface Sci*, 456–463.
17. Luky, H. (2013). Effect of Some Parameters Influencing Enhanced. <https://doi.org/10.2118/165955-MS>. *SPE 165955*.
18. M.Prasad, P. a. (2011). Recovery factor and reserves estimation in the Bakken petroleum system (Analysis of the Antelope, Sanish and Parshall fields).
19. Magda I. Youssif a, R. M.-M. (2017). Silica nanofluid flooding for enhanced oil recovery in sandstone rocks. *Egyptian Journal of Petroleum*, 108-110.
20. Malozyomov, B., Martyushev, N., Kukartsev, V., Tynchenko, V., Bukhtoyarov, V., Wu, X., . . . Kukartsev, V. (2023). Overview of Methods for Enhanced Oil Recovery from Conventional and Unconventional Reservoirs. *MDPI*, 9.
21. Marsalek, R. (2014). Particle Size and Zeta Potential of ZnO. *APCBEE Proc.*, 9, 13–17.
22. Mikolajczyk, A., Gajewicz, A., Rasulev, B., Schaeublin, N., Maurer-Gardner, E., Hussain, S., . . . Puzyn, T. (2015,). Zeta Potential for Metal Oxide Nanoparticles: A Predictive Model Developed by a Nano-Quantitative Structure–Property Relationship Approach. *Chem. Mater.* , 27, 2400–2407.
23. Mostafa Iravani1 · Zahra Khalilnezhad2 · Ali Khalilnezhad1, 3. (2023). A review on application of nanoparticles for EOR purposes: history and current challenges. *Petroleum Exploration and Production Technology*, 963.
24. N. A. Ogolo, O. A. (2012.). Presented in part at the SPE Saudi Arabia section technical symposium and exhibition, . Saudi Arabia; Al-Khobar.
25. Nabipour, M. (2007). *An Introduction to Enhanced Oil Recovery (EOR)*. Marvdasht : Marvdasht Azad University.
26. Oscar E. Medina 1, C. O. (2019). Nanotechnology Applied to Thermal Enhanced Oil Recovery Processes: A Review. *MDPI*, 1.
27. Pandya, H. P. (2019). Comprehensive review on application of various nanoparticles for the production of biodiesel. *Energy Sources*, 1-14.
28. *properties of petroleum fluids*. (william D. McCain,Jr). tulsa,Oklahoma: pennwell publishing company.
29. RE, C. (1976). Flow of fluids through porous materials .
30. Recovery factor and reserves estimation in the Bakken petroleum system (Analysis of the Antelope, Sanish and Parshall fields). (n.d.).
31. Rezvani H, K. A.-B. (2018). Comparative experimental study of various metal oxide nanoparticles for the wettability alteration of carbonate rocks in EOR processes. *In: 80th EAGE conference and exhibition 2018a* , (pp. pp 1–5). European association of geoscientists and engineers.

32. Roustaei, A. M. (2012). An experimental investigation of polysiliconnanoparticles' recovery efficiencies through changes in interfacial tension and wettability alteration. . *In: SPE 156976* .
33. Shamsijazeyi, H., Miller, C. A., Wong, M. S., Tour, J. M., & Verduzco, R. (2014). Polymer-Coated nanoparticles for enhanced oil recovery. *J. Appl. Polym. Sci*, 131, 40576.
34. Sofla SJD, J. L. (2018). Insight into the stability of hydrophilic silica nanoparticles in seawater for enhanced oil recovery implications. *Fuel* 216, 559–571.
35. Thomas, S. (2008). *Oil Gas Sci. Technol* 63, 9–19.
36. Thomas, S. (2007). Enhanced Oil Recovery – An Overview. *Oil & Gas Science and Technology – Rev. IFP, Vol. 63 (2008), No. 1* (p. 11). Canada: Institut français du pétrole.



Appendices

Appendices

Appendix A

Table II.2: nanoparticle types and their mechanism for EOR

Types of nanoparticles	Nanoparticles	Main mechanism for EOR
Metal Oxide nanoparticles	Aluminum oxide (Al_2O_3)	Reduction of oil viscosity Reduction of interfacial tension
	Copper oxide (CuO) Iron oxide (Fe_2O_3/Fe_3O_4) Nickel oxide (Ni_2O_3) Magnesium oxide (MgO)	Reduction of oil viscosity
	Magnetic nanoparticles	ferrofluids Reduction of interfacial tension
	Organic nanoparticles	carbon nanotubes More research is required
Inorganic nanoparticles	SiO ₂ Nanoparticles	Reduction of oil viscosity Reduction of interfacial tension Modification of wettability (depends on the degree of hydrophobicity) Oil/water emulsion stabilizer Greater recovery factor

Appendix B

Properties of silica gel particles

Properties	values
Density	0.7gm/cm ³
Molecular formula	SiO ₂
Melting point	3110°F

Boiling point	4046°F
appearance	Transparent beads
odor	odorless